
**Structure, Function and Regulation of
the CCaMK/CYCLOPS Complex
During Root Symbioses**

**Dissertation zur Erlangung des Doktorgrades der
Naturwissenschaften an der Fakultät für Biologie der
Ludwig-Maximilians-Universität München**

vorgelegt von

Katja Katzer

München, Juni 2017

Erstgutachter:	Prof. Dr. Martin Parniske
Zweitgutachter:	Prof. Dr. Heinrich Leonhardt
Tag der Abgabe:	14.06.2017
Tag der mündlichen Prüfung:	27.09.2017

Eidesstattliche Erklärung

Ich versichere hiermit an Eides statt, dass die vorgelegte Dissertation von mir selbständig und ohne unerlaubte Hilfe angefertigt ist.

München, den 14.06.2017

Katja Katzer

Erklärung

Hiermit erkläre ich, dass die Dissertation nicht ganz oder in wesentlichen Teilen einer anderen Prüfungskommission vorgelegt worden ist. Ich habe mich nicht anderweitig einer Doktorprüfung ohne Erfolg unterzogen.

München, den 14.06.2017

Katja Katzer

Table of Contents

I.	Abbreviation Index	9
II.	List of Publications	11
III.	Summary	13
III.	Zusammenfassung	14
IV.	Introduction	17
1.	Root Endosymbioses	17
1.1.	Nitrogen and Phosphorus Limitation in the Soil.....	17
1.2.	Arbuscular Mycorrhiza	18
1.3.	Root Nodule Symbiosis.....	19
2.	Signaling in Root Endosymbioses	21
2.1.	Early Symbiotic Crosstalk.....	21
2.2.	The Common Symbiotic Genes	23
2.3.	Symbiotic Calcium Responses	26
3.	The CCaMK/CYCLOPS Complex	27
3.1	CCaMK	27
3.2	CYCLOPS	28
3.3	Structure, Mechanism and Conformational Dynamics	29
4.	Transcriptional Regulation during Root Symbioses	32
5.	Aim of the Thesis	35
V.	Results	37
1.	CYCLOPS is a Modular Transcriptional Regulator	37
2.	The N-terminal Half of CYCLOPS has a Negatively Regulatory Function	40
3.	CYCLOPS Binds to Target Genes in a Sequence-Specific and Phosphorylation-Dependent Manner	41
4.	The C-terminal DNA-binding Domain of CYCLOPS Contains a Coiled-Coil Region	44
5.	The Coiled-Coil Domain of CYCLOPS Homodimerizes <i>in planta</i>	49
6.	CYCLOPS Dimerization is Required for DNA-Binding	51
7.	Homo- and Heterodimerization of the CYCLOPS Zipper Determine Root Symbiotic Development	53
8.	CYCLOPS Interacts with Plant bZIP Transcriptional Regulators	54
9.	CCaMK/CYCLOPS Form a Preassembled Complex with bZIP110 on the <i>CYC-RE_{NIN}</i>	56
10.	Heterodimerization with bZIP110 Specifically Anchors CYCLOPS to <i>CYC-REs</i> of Nodulation Promoters	60
11.	CYCLOPS-Mediated Transactivation is Inhibited by Heterodimerization with bZIP110	61
12.	Fine-tuned Expression Pattern of CYCLOPS and bZIP110 Contribute to Cell-Type-Specific Development during RNS	63
13.	bZIP110 is a Negative Regulator and Specifically Inhibits Root Nodule Development, but not Arbuscular Mycorrhiza	65

VI. Material and Methods	69
1. Experimental Model and Subject Details	69
1.1. Plant Lines.....	69
1.2. Microbial and Yeast Strains	69
2. Method Details	69
2.1. Cross-linking	69
2.2. Crystallization and Structural Determination.....	70
2.3. Domain Analyses	70
2.4. Electrophoretic Mobility Shift Assay.....	70
2.5. Fluorimetric Assays and Histochemical Staining	71
2.6. Interaction Studies <i>in planta</i>	71
2.7. <i>In vitro</i> Kinase Assay	71
2.8. Microscale Thermophoresis	71
2.9. Microscopy.....	72
2.10. Plant Growth, Transformation and Inoculation	72
2.11. Protein Blot Analysis	73
2.12. Protein Expression and Purification.....	73
2.13. Root Growth Analysis.....	74
2.14. Sequence Alignment and Structure Prediction	74
3. Quantification and Statistical Analysis.....	74
4. Plant Seed Bag Numbers.....	74
5. Key Resources Table	75
6. Plasmid Construction	77
7. Oligonucleotides.....	83
VI. General Discussion.....	85
1. CYCLOPS is a Novel Type of Transcriptional Regulator.....	85
2. The CCaMK/CYCLOPS Complex is a Central Regulator of Symbiote	
 Development.....	87
3. Regulation of the CCaMK/CYCLOPS Complex.....	92
3.1. Phosphorylation.....	93
3.2. Additional Complex Components.....	95
3.3. Heterodimerization of the CYCLOPS Zipper.....	97
4. Summary and Outlook.....	97
VII. References.....	99
VIII. List of Figures	117
IX. List of Tables	117
X. Acknowledgements	119
XI. Curriculum Vitae.....	121
XII. Republish Permissions.....	126

I. Abbreviation Index

ABA	Abscisic Acid
AD	transcriptional Activation Domain
AM	Arbuscular Mycorrhiza
AON	Autoregulation Of Nodulation
ARID	AT-rich Interaction Domain
BD	DNA-Binding Domain
BiFC	Bimolecular Fluorescence Complementation
BR	Basic Region
bZIP	basic leucine ZIPper transcriptional regulator
CaM	CalModulin
CaMB	CalModulin-Binding domain
CAMK	CAIModulin-dependent Kinase
CC	Coiled-Coil
CCaMK	Calcium- and CalModulin-dependent Kinase
ChIP-seq	Chromatin ImmunoPrecipitation DNA-sequencing
CIP73	CCaMK Interacting Protein 73
CNGC	Cyclic Nucleotide-Gated Channel
CO	Chitin Oligomer
co-IP	co-ImmunoPurification
CSP	Common Symbiosis Pathway
EMSA	Electrophoretic Mobility Shift Assay
ENOD	Early NODulin
ER	Endoplasmatic Reticulum
ERN1	ERF Required for Nodulation 1
GA	Gibberellic Acid
GTPase	Guanosine TriPhosphatase
HMGR1	3-Hydroxy-3-Methyl-Glutaryl CoA Reductase 1
IT	Infection Thread
LCO	LipoChito-Oligosaccharide
LHK1	Lotus Histidine Kinase 1
LNP	Lectine Nucleotide Phosphohydrolase
LysM	Lysin Motif
MAPK	Mitogen-Activated Protein Kinase
MLD	Malectin-Like Domain

MST	MicroScale Thermophoresis
N	Nitrogen
NF	Nod Factor
NF-Y	Nuclear Factor Y
NFR	Nod Factor Receptor
NIN	Nodule INception
NLS	Nuclear Localization Signal
NPL	Nodulation Pectate Lyase
NSP	Nodulation Signaling Pathway
NUP	NucleoPorin
P	Phosphorus
PCR	Polymerase Chain Reaction
PPA	PrePenetration Apparatus
R	heptad sequence Repeats
RAM1	Reduced Arbuscular Mycorrhiza 1
RLK	Receptor-like Kinase
RNS	Root Nodule Symbiosis
SIE3	SYMRK-Interacting E3 ubiquitin ligase 3
SINA	Seven In Absentia
SIP	SYMRK-Interacting Protein
SYMREM	Symbiotic Remorin
SYMRK	SYMBiosis Receptor Kinase
WT	WildType

II. List of Publications

Singh, S., **Katzer, K.**, Lambert, J., Cerri, M., and Parniske, M. (2014). CYCLOPS, a DNA-binding transcriptional activator, orchestrates symbiotic root nodule development. *Cell Host & Microbe* 15, 139-152.

Katzer, K., Basquin, J., Cathebras, C., Fussbroich, B., Cerri, M.R., Heermann, R., Jung, K., Gimenez Oya, V., Andrade, R.E., and Parniske, M. Combinatorial zipper assemblies of CYCLOPS specify root symbiotic development. Unpublished.

Pimprikar, P., Carbonnel, S., Paries, M., **Katzer, K.**, Klingl, V., Bohmer, M.J., Karl, L., Floss, D.S., Harrison, M.J., Parniske, M., and Gutjahr, C. (2016). A CCaMK-CYCLOPS-DELLA complex activates transcription of *RAMI* to regulate arbuscule branching. *Current Biology* 26, 1126.

Cerri, M.R., Wang, Q., Stolz, P., Folgmann, J., Frances, L., **Katzer, K.**, Li, X., Heckmann, A.B., Wang, T.L., Downie, J.A., et al. (2017). The *ERN1* transcription factor gene is a target of the CCaMK/CYCLOPS complex and controls rhizobial infection in *Lotus japonicus*. *New Phytologist* 215, 323-337.

Andrade, R.E., Lambert, J., **Katzer, K.**, Cathebras, C., Heermann, R., and Parniske, M. Role of NIN during root nodule symbiosis. Unpublished.

III. Summary

Legumes form agriculturally and ecologically important plant root symbioses with phosphate-acquiring arbuscular mycorrhiza (AM) fungi and nitrogen-fixing rhizobia (Gutjahr and Parniske, 2013; Oldroyd, 2013; Parniske, 2008). Early signal transduction events of both symbioses are characterized by calcium spiking in the nucleoplasm, which likely activates a nuclear-localized calcium- and calmodulin-dependent protein kinase (CCaMK) (Ehrhardt et al., 1996; Miwa et al., 2006b; Sieberer et al., 2012). CCaMK emerged as central regulator of the genetically separable symbiotic programs: nodule organogenesis and rhizobial or AM fungal infection (Singh et al., 2014; Takeda et al., 2012; Tirichine et al., 2006; Yano et al., 2008). However, the connection between CCaMK activation and transcriptional reprogramming remained unknown. During this study, the interacting protein and phosphorylation substrate of CCaMK, CYCLOPS, was identified as DNA-binding transcriptional activator containing a central transactivation domain (AD), a C-terminal DNA-binding domain (BD) and an N-terminal regulatory domain (Singh et al., 2014). A model was established in which phosphorylation of CYCLOPS by CCaMK induces conformational changes that release CYCLOPS from inhibition and enable sequence-specific binding to target promoters and interaction with the transcriptional machinery (Singh et al., 2014). The nodulation-specific *Nodule Inception (NIN)* and *ERF Required for Nodulation 1 (ERN1)* and the AM-specific *Reduced Arbuscular Mycorrhiza 1 (RAM1)* promoters were identified to be bound by CYCLOPS via *cis*-regulatory elements of GC-rich content and palindromic nature, the *CYC-REs* (Cerri et al., 2017; Pimprikar et al., 2016; Singh et al., 2014). X-ray crystallography provided structural indications for the combinatorial recruitment of various transcriptional regulators to the CCaMK/CYCLOPS complex. Part of the CYCLOPS-BD was structurally solved, revealing a dimeric coiled-coil (CC) arrangement with a long zipper of nine heptad tandem repeats. Based on the structure, the CCaMK interactor and basic leucine zipper transcriptional regulator 110 (bZIP110) was identified as novel complex component and heterodimeric partner of CYCLOPS. bZIP110 acts as a transcriptional repressor and preferentially binds to the nodulation-specific *CYC-RE_{NIN}*. Since rapid and dynamic changes in heterodimer compositions are characteristic for zipper arrangements, a model was established in which recruitment of specific interactors to the CYCLOPS zipper controls the spatio-temporal gene expression during root symbiotic development.

III. Zusammenfassung

Leguminosen können landwirtschaftlich und ökologisch wichtige Wurzelsymbiosen mit arbuskulären Mykorrhiza (AM)-pilzen, die Phosphate liefern, und stickstofffixierenden Rhizobien eingehen (Gutjahr and Parniske, 2013; Oldroyd, 2013; Parniske, 2008). Frühe Entwicklungsstadien beider Symbiosen sind charakterisiert durch Kalziumoszillationen im Zellkern, welche von der kalzium- und calmodulin-abhängigen Proteinkinase (CCaMK) dekodiert werden (Ehrhardt et al., 1996; Miwa et al., 2006b; Sieberer et al., 2012). CCaMK löst das gesamte Entwicklungsprogramm aus und ist in die Spezifitätsdeterminierung der wesentlichen Symbioseereignisse involviert: Knöllchenorganogenese und Infektion mit Rhizobien oder AM-Pilzen (Singh et al., 2014; Takeda et al., 2012; Tirichine et al., 2006; Yano et al., 2008). Allerdings war der Zusammenhang zwischen CCaMK-Aktivierung und der transkriptionellen Umprogrammierung nicht bekannt. In dieser Arbeit wurde der von CCaMK phosphorylierte Interaktionspartner CYCLOPS als DNA-bindender Transkriptionsaktivator identifiziert, der die Expression symbiontischer Gene auslöst (Singh et al., 2014). Deletionsanalysen von CYCLOPS konnten eine zentrale Transaktivierungsdomäne (AD), eine C-terminale DNA-bindedomäne (BD) und eine N-terminale regulatorische Domäne aufzeigen. Ein Modell wurde etabliert, in dem CYCLOPS während der symbiontischen Kalziumoszillationen von CCaMK phosphoryliert wird, was eine Konformationsänderung auslöst, die CYCLOPS aus einem inhibierenden Zustand löst und dazu befähigt, sequenzspezifisch an Zielpromotoren zu binden und mit der Transkriptionsmaschinerie zu interagieren (Singh et al., 2014). Mehrere nodulierungs- und AM-spezifische Promotoren wurden identifiziert, die von CYCLOPS mittels *cis*-regulatorischer Elemente mit hohem GC-Gehalt und palindromischem Aufbau, die *CYC-REs*, gebunden werden (Cerri et al., 2017; Pimprikar et al., 2016; Singh et al., 2014), was CCaMK und CYCLOPS als wichtigsten regulatorischen Komplex in der Unterscheidung zwischen Knöllchensymbiosen- und AM-Entwicklung bestätigte. Mittels Röntgenkristallografie wurden strukturelle Beweise für die kombinatorische Integration von verschiedenen Transkriptionsregulatoren zum CCaMK/CYCLOPS-Komplex erhalten (Katzer et al., unpubliziert). Die Struktur eines Teiles der BD von CYCLOPS wurde aufgelöst und zeigte eine dimere Coiled-coil (CC)-Anordnung mit einem langen Zipper bestehend aus neun Wiederholungen von sieben Tandemreihen (Katzer et al., unpubliziert). Mittels der Struktur wurde der basische Leucinzipper 110 (bZIP110) als neuer Bestandteil des Komplexes und als Heterodimer-

Partner von CYCLOPS identifiziert (Katzer et al., unpubliziert). bZIP110 funktioniert als transkriptioneller Repressor und vermittelt eine höhere Bindungsaffinität von CYCLOPS für nodulierungsspezifische *CYC-REs*. Da schnelle und dynamische Änderungen in der Heterodimer-Komposition charakteristisch für Zipper-Formationen ist, wurde ein Modell etabliert, in dem Rekrutierung von spezifischen Interaktoren zum CYCLOPS-Zipper die örtliche und zeitliche Genexpression während der Entwicklung von Wurzelsymbiosen kontrolliert (Katzer et al., unpubliziert).

IV. Introduction

1. Root Endosymbioses

1.1. Nitrogen and Phosphorus Limitation in the Soil

Plant productivity and growth relies on the availability of nutrients in the soil. Phosphorus (P) and nitrogen (N) are two of the most limiting elements in terrestrial ecosystems (Maathuis, 2009; Menge et al., 2012). The N and P availability depends on climatic and edaphic factors including soil drainage, texture, temperature, aeration and the rate of mineralization from organic matter decomposition (Masclaux-Daubresse et al., 2010). Within the N and P circuit, the elements cycle through the lithos-, pedos-, atmos- and biosphere and are converted into forms, which plants can use. N is present in many vital organic compounds such as amino acids, proteins, nucleic acids and secondary plant molecules and gets taken up predominantly as nitrate into the plant root where it is subsequently reduced to ammonium, the major assimilation form in plants (Maathuis, 2009; Masclaux-Daubresse et al., 2010). While the gaseous N, which makes up 78 % of the atmosphere, can not be absorbed by plants itself, the rock incorporated N is slowly mineralized and can easily be drained away below the root zone due to its water-solubility (Maathuis, 2009; Masclaux-Daubresse et al., 2010; Menge et al., 2012). P is incorporated into nucleotides, phosphatides and utilized for metabolic processes e.g. phosphorylation events (Schachtman et al., 1998). Declining P inputs are caused by out-washing P from rocks and subsequent run-off into ground water and oceans where it is deposited as sediments on the sea floor and slowly extracted into water again (Schoumans et al., 2015). Plants have evolved a variety of mechanisms to overcome deficient nutrient concentrations in the soil such as expansion of the root surface or the production of root exudates that solubilize and mobilize chemical bound elements from mineral surfaces (Vance et al., 2003). However, humans have accelerated the natural circuits by an unsustainable N and P management. Over-use of N fertilizers, facilitated by the synthetic production of the Haber-Bosch process, resulted in a run-off into ground water and oceans causing water pollution and eutrophy (Howarth and Marino, 2006; Howarth et al., 2006). P mining, excessive fertilizer application and effluent losses in cities caused a “terminal steady state” of P deficiency (Menge et al., 2012). Besides recycling and identifying new fertilizer production ways, researchers and farmers try to reduce the fertilizer input by breeding more effective crop varieties with reduced need for fertilizers and by finding ways to manage N and P application in a most efficient manner (Bonvin et al., 2015;

Schoumans et al., 2015). Another strategy implements a specialized biological process: root endosymbiosis. Plants can associate with a variety of beneficial fungi or bacteria in their roots which facilitate plant mineral uptake in exchange for organic metabolites (Zuccaro et al., 2014). These symbiotic interactions contribute to a significant portion to plant growth in P and N depleted environments (Gutjahr and Parniske, 2013; Oldroyd, 2013; Parniske, 2008) and thus may serve as a natural “bio-fertilizer“.

1.2. Arbuscular Mycorrhiza

AM, the most ancient plant root endosymbiosis, is a mutualistic interaction between plants and obligate biotrophic fungi of the phylum Glomeromycota (Parniske, 2008; Schüßler et al., 2001). Fossil records indicate that AM evolved at least 400 Million years ago and it is believed to have promoted the evolution of land plants (Remy et al., 1994; Zuccaro et al., 2014). Approximately 70-90 % of land plant species engage in AM symbiosis, making it probably the most widespread symbiosis in terrestrial ecosystems (Fitter et al., 2005). The symbiotic interaction is characterized by the formation of spezialized structures, which are formed inside of root cells. These tree-shaped structures, so-called arbuscules, are the main site of nutrient exchange between both partners: AM fungi supply water and nutrients to the plant and receive plant-fixed carbon and β -monoacylglycerols derivatives in return (Bago et al., 2003; Bravo et al., 2017; Keymer et al., 2017; Parniske, 2008). Beside nutritional benefits, plants also profit from an enhanced biotic and abiotic tolerance, increased pathogen resistance and improved soil structure (Gianinazzi et al., 2010).

Upon contact with a host root, AM fungal hyphae differentiate into a hyphopodium at the root surface and penetrate the rhizodermis (Gutjahr and Parniske, 2013; Parniske, 2008). In anticipation of a fungal infection, the plant forms an accommodation structure comprised of microtubules, microfilaments and endoplasmatic reticulum (ER), termed prepenetration apparatus (PPA), which guides the fungus through the root cells towards the inner cortical tissue (Genre et al., 2008). PPA formation is strictly controlled by the host plant and involves relocation of the cell nucleus right below the position of the appressorium (Takemoto and Hardham, 2004). The nucleus determines the fungal pathway through the cell by moving ahead the growing PPA. In the inner cortex, fungal hyphae expand longitudinally in the apoplast until they enter cortical cells where they differentiate into arbuscules (Demchenko et al., 2004; Harrison, 2012).

During all stages of the symbiotic interaction, the fungus remains outside the plant cell, surrounded by a plant-derived periarbuscular membrane (PAM) that is continuous with the plasma membrane but distinct in its protein composition (Harrison, 2005). The phosphate transporter 4 (PT4) localizes specifically to the arbuscule branches, whereas the blue copper-binding protein 1 (BCP1) is found in arbuscule trunks and the peripheral plasma membrane (Pumplin and Harrison, 2009). In exchange for nutrients, the fungi are believed to receive carbohydrates from the host plant. However, lack of fatty acid synthase (FAS) in AM fungal genomes and the identification of AM-specific lipid biosynthetic enzymes and the ABC-transporter STR implicated in lipid transport also indicated fatty acid derivatives as transfer compounds (Bravo et al., 2017; Delaux et al., 2014; Keymer et al., 2017; Wewer et al., 2014). The fungus continues colonizing cortical cells while older arbuscules, having expired their regular lifespan of four to ten days, collapse and get completely degraded (Floss et al., 2017; Genre et al., 2008; Gutjahr and Parniske; Javot et al., 2007a; Javot et al., 2007b).

1.3. Root Nodule Symbiosis

Approximately 60 million years ago (Doyle, 2011; Sprent, 2007a; Sprent, 2007b; Sprent and James, 2007), and therefore much younger than AM, evolved the root nodule symbiosis (RNS). RNS occurs between plants of the eurosid I subclade of angiosperms (*Fabales*, *Fagales*, *Cucurbitales*, *Rosales*) and nitrogen-fixing bacteria that reside endosymbiotically inside plant root cells (Kistner and Parniske, 2002; Soltis et al., 2000). RNS is characterized by the establishment of a novel plant organ, the nodule, where the bacteria provide the fixed N to the plant in exchange for carbon and N compounds, including dicarboxylates (primarily malate) and amino acids (White et al., 2007). Legumes form RNS with Gram-negative bacteria collectively referred to as rhizobia (Sprent, 2007a; Sprent, 2007b; Sprent and James, 2007), whereas actinorhiza is established between plants of the orders *Fagales*, *Cucurbitales* and *Rosales* and Gram-positive actinobacteria of the genus *Frankia* (Pawlowski and Demchenko, 2012). The relatively close phylogenetic clustering of the nodulator clades led to the hypothesis of a common ancestor with a genetic predisposition for nodulation (Soltis et al., 1995). Since the non-legume *Parasponia* (family Cannabaceae) can be nodulated by certain rhizobia species, whereas the very closely related sister species *Trema tomentosa* does not nodulate, suggests that RNS has evolved or has been lost independently several times during evolution (Granqvist et al., 2015).

Rhizobia infect legumes in different ways using intercellular and/or intracellular entry modes (Deakin and Broughton, 2009; Madsen et al., 2010). The best studied infection mechanism takes place through the root hair and is initiated by an attachment of rhizobia to the root hair tip which curls and entraps the bacterial microcolony (Downie and Walker, 1999; Oldroyd and Downie, 2008). The enclosed bacteria are subsequently taken up by a plant-derived tubular structure, the infection thread (IT), which is formed by invagination of the plasma membrane at a site where the cell wall has been locally hydrolysed (Fournier et al., 2015; Fournier et al., 2008; Murray, 2011). The IT guides the bacteria from the rhizodermis through the outer into the inner root cortex (Oldroyd et al., 2011). The future path of the IT is determined by the plant through the formation of a preinfection thread (PIT), which consists of ER-rich cytoplasmic bridges aligned with cytoskeleton (structurally similar to the PPA in AM) (Vanbrussel et al., 1992; Yokota et al., 2009). Concomitantly, cells of the inner cortex divide and redifferentiate to form a nodule primordium. Both processes are at least partially independent as shown by mutants, which uncouple rhizobial infection and nodule organogenesis (Murray et al., 2007; Tirichine et al., 2006). Rhizobia inside ITs continue to divide until they reach the primordial cells, where they are released into the cytoplasm by an endocytotic mechanism that encapsulates the bacteria within so-called symbiosomes (Jones et al., 2008; van Rhijn et al., 1998). Controlled by plant-produced nodule cysteine-rich antimicrobial peptides (NCRs) (Van de Velde et al., 2010), the rhizobia differentiate into bacteroids, an auxotrophic form characterized by an increased size, shape, DNA content and lack of amino acid synthesis (Jones et al., 2007; Prell et al., 2009). The peribacteroid membrane surrounding the symbiosomes controls the transport of metabolites between plant and bacteria. Ammonium produced by the nitrogenase enzyme complex is transported to the plant by a yet unknown mechanism and the molecular identity of a symbiotic ammonium transporter remains to be determined. An ammonium channel, a cation channel that transports K^+ , Na^+ , and NH_4^+ and aquaporin-like channels are localized to the symbiosome membrane and were implicated in the transport (Hwang et al., 2010; Krusell et al., 2005; Niemiets and Tyerman, 2000; Tyerman et al., 1995). Inside the plant cells, the ammonium is then assimilated and incorporated into amino acids (Vance and Gantt, 1992). In return, the bacteria receive nutrients and carbon sources from the plant (Jakobsen and Rosendahl, 1990). Dicarboxylated acids like malate are assumed to be the primary carbon source (Colebatch et al., 2004; Udvardi and Day, 1997); however, a dicarboxylate transporter has not yet been identified in legumes.

2. Signaling in Root Endosymbioses

2.1. Early Symbiotic Crosstalk

Because root endosymbioses are energy-consuming processes, symbiotic establishment is tightly controlled by the plant and occurs only under nutrient-limiting conditions. Perception of symbiotic signals at the plasma membrane initiates a crosstalk between plant and microsymbiont. Under N-limiting conditions, plants secrete flavonoids into the soil (Abdel-Lateif et al., 2012), which are sensed by rhizobia and induce the synthesis and secretion of strain-specific Nod factors (NFs) (Figure 1). NFs are lipochito-oligosaccharidic (LCO) compounds of five to six β -1,4-linked N-acetyl-D-glucosamine residues, which form a chitin backbone that is acylated at the non-reducing terminal sugar residue (Oldroyd and Downie, 2008). Different rhizobia strains produce several types of NFs, which vary in their sugar chain composition, attached side groups or length and saturation degree of the fatty acid and therefore determine specificity of the interaction between plant and bacteria (Gough and Cullimore, 2011; Peck et al., 2006; Perret et al., 2000). Early responses to NFs in the epidermis include membrane depolarization caused by rapid calcium influxes, alkalization, modifications in the root hair cytoskeleton and root hair deformation (Jones et al., 2007) as well as reactivation of the mitotic cell cycle in root cortical cells to induce nodule organogenesis. In *L. japonicus*, rhizobial NFs are perceived with high affinity by lysin motif (LysM) domain receptors Nod Factor Receptor (NFR) 1 and NFR5 (Broghammer et al., 2012; Madsen et al., 2003; Radutoiu et al., 2003) (Figure 1). The extracellular LysMs are important for host specific LCO recognition as shown by domain swap and mutational analyses (Radutoiu et al., 2007). While NFRs recognize NFs, the exopolysaccharide receptor (EPR) 3, another LysM-RLK, controls entry and passage of compatible rhizobial strains through the root (Kawaharada et al., 2015; Kawaharada et al., 2017). The NFRs form heterocomplexes at the plasma membrane (Figure 1), where they interact with other signaling or regulating components including symbiotic receptor-like kinases (RLKs) (Antolin-Llovera et al., 2014), the E3 ubiquitin ligase plant U-box protein 1 (PUB1) (Mbengue et al., 2010), the Symbiosis Receptor Kinase (SYMRK)-interacting E3 ubiquitin ligase (SIE3) (Yuan et al., 2012), Seven in Absentia 4 (SINA4) (Den Herder et al., 2012), the Rho-like small Guanosine Triphosphatase (GTPase) 6 (ROP6) (Ke et al., 2012), the AT-rich interaction domain (ARID)-containing transcription factor SYMRK-interacting protein 1 (SIP1) (Zhu et al., 2008), the mitogen-activated protein kinase (MAPK) kinase SIP2 (Chen et al., 2012) or

the 3-hydroxy-3-methylglutaryl CoA reductase 1 (HMGR1) (Kevei et al., 2007). The enrichment of receptor complexes into microdomains mediated by scaffold proteins like Symbiotic Remorin 1 (SYMREM1) is assumed to increase signaling efficiency and specificity (Bapaume and Reinhardt, 2012; Jarsch and Ott, 2011).

Under P limiting conditions, plant roots produce the carotenoid-derived phytohormone strigolactone, which induces hyphal branching and alterations in fungal physiology and mitochondrial activity (Akiyama et al., 2005; Besserer et al., 2006). In turn, AM fungi secrete a mixture of signaling molecules to trigger symbiosis-related host responses including transcriptional activation, nuclear calcium oscillations, lateral root formation and starch accumulation (Gutjahr et al., 2009; Gutjahr and Paszkowski, 2013; Ortu et al., 2012; Sieberer et al., 2012). Undecorated or differently decorated mycorrhizal LCOs (Myc-LCOs), which are structurally similar to rhizobial NFs, and tetra- and pentameric chitin oligomers (CO4-CO5) were shown to be involved in the plant recognition (Genre et al., 2013; Maillet et al., 2011) (Figure 1). LysM domain receptors have been implicated in the perception of AM fungi since LCOs and COs are chitin-derived signaling molecules (Antolin-Llovera et al., 2012; Gust et al., 2012; Tirichine et al., 2006) and a single common LysM receptor, which is orthologous to *Medicago truncatula* NFP, is required for the establishment of AM and RNS in the non-legume *Parasponia andersonii* (Op den Camp et al., 2011). In *Solanum* transcript downregulation of NFR5-type receptors decreased AM colonization, while in legumes NFR1 was shown to be involved in the recognition of AM fungi and the activation of symbiotic downstream responses (Buendia et al., 2016; Zhang et al., 2007). Although a paralogue of NFR5 (LYS11) was identified in *L. japonicus* and shown to perceive LCOs (Figure 1), the mutant revealed no obvious AM symbiotic defects (Rasmussen et al., 2016). Interestingly, Chitin Elicitor Receptor Kinase 1 (CERK1), which promotes plant immunity in response to chitin oligosaccharides, is also involved in the recognition of AM fungi, suggesting that the perception of CO-based signals produced by AM fungi is conserved in LysM receptors and that diversification in the signal, the receptor domains, or the receptor/co-receptor complex compositions increased receptor functionality during evolution to activate different signaling pathways (Carotenuto et al., 2017; Zhang et al., 2015).

2.2. The Common Symbiotic Genes

After the first cross-talk between host and microsymbiont at the plasma membrane, the symbiotic signal is transmitted to the Common Symbiosis Pathway (CSP), which is shared between both types of root endosymbioses (Figure 1) and assumed to be co-opted from the ancestral AM by the evolutionary more recent RNS (Genre and Russo, 2016; Singh and Parniske, 2012). The CSP transmits the symbiotic signal from the plasma membrane to the nucleus (Figure 1), leading to nuclear calcium oscillations, which are decoded into downstream symbiosis-associated gene expression (Singh and Parniske, 2012). How the CSP transduces the symbiotic signal is still poorly understood. Recent studies suggest that the CSP may also be deployed by microbes other than AM fungi and rhizobia in non-symbiotic signaling (Genre and Russo, 2016) and that additional symbiotic signal transduction pathways exist, which bypass or run parallel to the CSP (Bonfante and Requena, 2011; Gutjahr et al., 2009).

So far at least 12 common symbiotic genes have been shown to be required for both AM and RNS (Groth et al., 2010; Imaizumi-Anraku et al., 2005; Kanamori et al., 2006; Kistner et al., 2005; Levy et al., 2004; Mitra et al., 2004; Murray, 2011; Roberts et al., 2013; Saito et al., 2007; Stracke et al., 2002; Yano et al., 2008). As a very early component immediately downstream of the initial signal perception, a Lectine Nucleotide Phosphohydrolase (LNP) was identified (Etzler et al., 1999; Roberts et al., 2013). LNP is a peripheral membrane protein, localized at the surface of root hairs and required for nodulation and AM infection. Similar to *nfr1* and *nfr5* mutant plants, an antisense line lacking LNP was impaired in calcium influx at the root hair tip, nuclear calcium spiking and *NIN* expression, but still showed root hair deformation (Roberts et al., 2013). Since LNP binds to NFs, it may act in complex or in parallel to the LysM receptor kinases. Another plasma membrane localized receptor is the RLK SYMRK (Figure 1), which consists of a signal peptide followed by an N-terminal extracellular region containing a malectin-like domain (MLD) and three leucine-rich repeats (LRR), a transmembrane segment and an intracellular kinase domain (Markmann et al., 2008; Stracke et al., 2002). Supporting the hypothesis of microdomains as symbiotic signaling platforms, SYMRK has been shown to interact with the NFRs, SYMREM1, an ARID-type DNA-binding protein, HMGR1 and SIE3 from *M. truncatula* (Kevei et al., 2007; Lefebvre et al., 2010; Toth et al., 2012; Zhu et al., 2008). Three different SYMRK versions exist in angiosperms varying in the length of their extracellular domain, which is essential for the extent of symbiotic capability (Markmann et al., 2008).

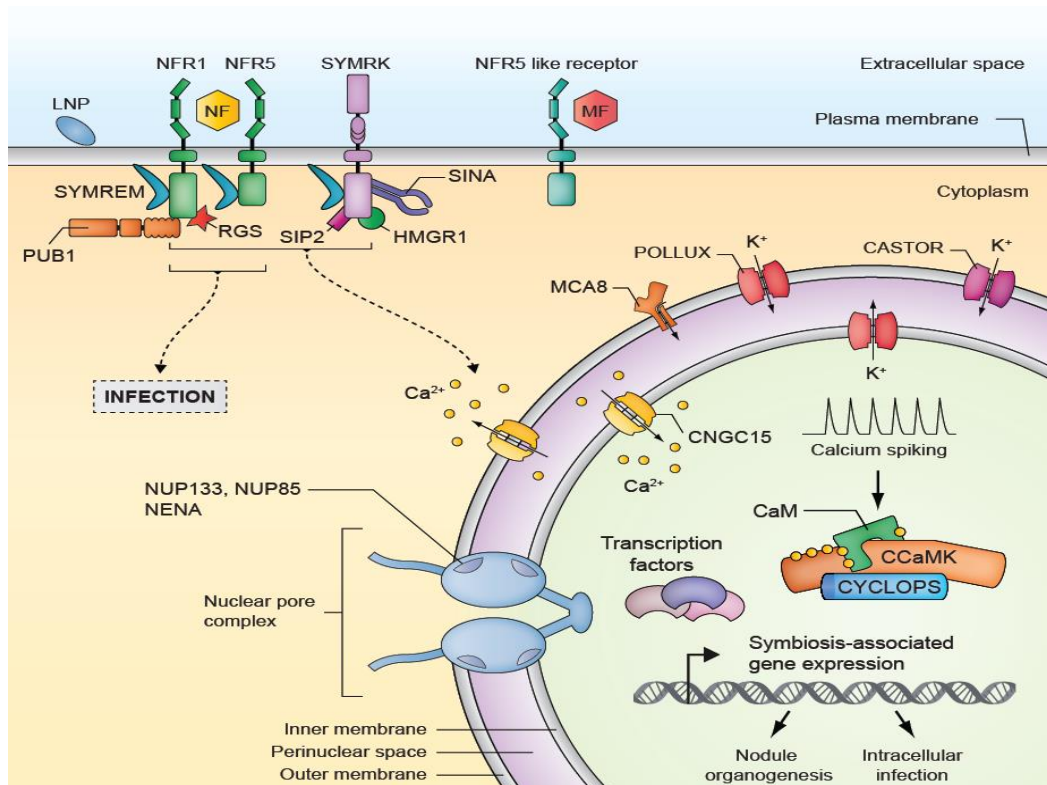


Figure 1. Symbiotic Signal Transduction in Plant Root Cells.

Perception of rhizobial Nod factors (NFs), presumably at the plasma membrane (PM) (Haney et al., 2011), is mediated by LysM-receptor-like kinases (LYKs) including *L. japonicus* Nod factor receptor 1 (NFR1) and NFR5 and in *M. truncatula* LYK3 and NFP (Amor et al., 2003; Arrighi et al., 2006; Limpens et al., 2003; Madsen et al., 2003; Radutoiu et al., 2003). An NFR5-like receptor may mediate perception of an AM fungus-derived “Myc factor” (MF) (Maillet et al., 2011; Op den Camp et al., 2011). LNP: lectine nucleotide phosphohydrolase, which binds to NFs and is involved in early symbiotic signaling (Roberts et al., 2013). RGS: regulator of G-protein signaling with GTPase activity, which is activated by NFR1 phosphorylation (Choudhury and Pandey, 2015). PUB1: plant U-box protein 1 of *M. truncatula*, is an E3 ubiquitin ligase interacting with the kinase domain of LYK3, and exerts a negative regulatory role on nodulation signaling (Mbengue et al., 2010). SINA: the SEVEN IN ABSENTIA homolog SINA4 interacts with the kinase domain of SYMRK and mediates its relocalization and degradation (Den Herder et al., 2012). The MAP kinase kinase SIP2 and HMGR1, the rate-controlling enzyme of the mevalonate pathway, were identified as interactors of SYMRK (Chen et al., 2012; Kevei et al., 2007; Liu et al., 2003). The symbiotic receptors at the PM interact with SYMREM1, a remorin protein specifically upregulated during nodulation and required for infection thread (IT) formation (Lefebvre et al., 2010; Toth et al., 2012). Within minutes, LCO perception at the PM leads to a sustained nuclear calcium-spiking response, the generation, decoding and transduction of which is mediated by components common to both types of symbioses (Ehrhardt et al., 1996; Kistner and Parniske, 2002). These are genetically positioned upstream (SYMRK/DMI2, CASTOR/POLLUX/DMI1, NUP85, NUP133, NENA, MCA8) or downstream (CCaMK/DMI3, CYCLOPS/IPD3) of the calcium-spiking response (Antolin-Llovera et al., 2014; Binder and Parniske, 2013; Capoen et al., 2011; Gleason et al., 2006; Groth et al., 2010; Markmann et al., 2008; Tirichine et al., 2006; Venkateshwaran et al., 2012; Yano et al., 2008). The cyclic nucleotide-gated channels 15 (CNGC15) mediate symbiotic calcium oscillations in the nucleus (Charpentier et al., 2016). Several transcription factors including NSP1/2, NIN, ERN1, NF-YA1 and NF-YB1 have been implicated in symbiosis-related gene expression leading to nodule organogenesis and intracellular infection (Cerri et al., 2016; Kaló et al., 2005; Laloum et al., 2014; Schausser et al., 1999; Smit et al., 2005). The observation that autoactive CCaMK does not restore epidermal IT formation in *nfr* mutants suggests the existence of a common SYM gene-independent pathway (Hayashi et al., 2010; Madsen et al., 2010). Figure and legend modified from Singh and Parniske, 2012*.

Autophosphorylation, particularly tyrosine phosphorylation in a gatekeeper position, and proteolytic cleavage of the ectodomain, potentially mediated by the interacting E3 ligase SINA4, was shown to be important for SYMRK-mediated signaling and NFR5 interaction, respectively (Antolin-Llovera et al., 2014; Saha et al., 2016). However, both the ligand and the precise function of SYMRK remain unknown yet.

Downstream of LNP and SYMRK, the nuclear-localized ion channels CASTOR, POLLUX, the *M. truncatula* calcium-dependent adenosine triphosphatase (MCA) 8 and cyclic nucleotide-gated channels (CNGCs) 15 are required for the targeted release of calcium (Binder and Parniske, 2013; Capoen et al., 2011; Charpentier et al., 2016; Venkateshwaran et al., 2012) (Figure 1). Also the nuclear pore components nucleoporin (NUP) 85, NUP133 and NENA act upstream of calcium spiking and may be involved in transport between nucleus and cytoplasm or the relocation of channels between inner and outer nuclear membrane (Binder and Parniske, 2013; Capoen et al., 2011; Groth et al., 2010), whereas CCaMK, CYCLOPS, several transcriptional regulators and VAPYRIN, a putative protein involved in membrane trafficking during symbiotic accommodation, are positioned downstream of the calcium response (Gleason et al., 2006; Murray, 2011; Pumplin et al., 2010; Singh et al., 2014; Tirichine et al., 2006; Yano et al., 2008). The components involved in signal transduction from the plasma membrane receptors to the nuclear calcium spiking machinery have not been determined yet. The MAPK cascade and the mevalonate pathway that produces sterols, isoprenoids and particularly cytokinins are likely to be downstream targets of the NF signaling pathway, since the MAPK Kinase (MAPKK) SIP2 and HMGR1, the rate controlling enzyme of the mevalonate pathway, were identified as interactors of SYMRK (Chen et al., 2012; Kevei et al., 2007; Liu et al., 2003). Silencing of either of the genes caused nodulation defects, but showed no effect on AM colonization, suggesting that additional pathways downstream of SYMRK might be involved in AM signal transduction. Another signaling pathway may involve heterotrimeric G-protein complexes and the Regulator of G-protein Signaling (RGS), a GTPase which is activated by NFR1 phosphorylation and shown to be involved in the regulation of nodulation in soybean (Choudhury and Pandey, 2015).

*Reprinted from “Singh, S., and Parniske, M. (2012). Activation of calcium- and calmodulin-dependent protein kinase (CCaMK), the central regulator of plant root endosymbiosis. *Current Opinion in Plant Biology* 15, 444-453.” with permission from Elsevier.

2.3. Symbiotic Calcium Responses

One of the earliest signals and a common feature of symbiotically stimulated plant root cells are nuclear calcium spikings (Chabaud et al., 2011; Sieberer et al., 2012). Within ten minutes after perception of symbiotic signals at the plasma membrane, sustained calcium oscillations (calcium spiking) in the nucleus can be observed (Chabaud et al., 2011; Shaw and Long, 2003). Microinjection of calcium sensitive dyes into root hair cells and the use of cytoplasmic and nucleus-targeted cameleon sensors revealed that pico- to nanomolar concentrations are sufficient to induce calcium oscillations (Ehrhardt et al., 1996; Shaw and Long, 2003) and that a minimum number of 36 spikes is required for the induction of the early nodulation marker *ENOD11:GUS* in *M. truncatula* roots upon NF application (Miwa et al., 2006a). During infection progression, a switch occurs from low frequency calcium spiking in preinfected cells to high frequency spiking in cells directly contacting ITs or PPAs, showing that throughout root infection calcium spiking is continuously activated and silenced to regulate the reprogramming of root cell development (Sieberer et al., 2012). In terms of periodicity, the calcium signatures during rhizobial and AM fungal infection were very similar, indicating that the activation of specific gene expression may not be encoded by different calcium profiles (Sieberer et al., 2012). However, the number of high frequency spikes during AM infection could not be determined. CNGC15 proteins were shown to be responsible for the calcium release from the nuclear envelope (Charpentier et al., 2016). The loss of positive charge is then compensated by the potassium-counter channels CASTOR/POLLUX (Parniske, 2008; Venkateshwaran et al., 2012), while MCA8 has been identified in *M. truncatula* to recapture the released calcium and thereby permitting generation of the next calcium spike (Capoen et al., 2011).

In addition to calcium spiking, NF induce calcium influxes in the root hair tips, which are associated with the production of reactive oxygen species (ROS) and membrane depolarization (Cardenas et al., 2008), but in contrast to calcium spiking require much higher concentrations of NF (Miwa et al., 2006b; Shaw and Long, 2003). Because many genes uncouple calcium influx and calcium spiking and structural modifications in *S. meliloti* NFs could differentially activate either of the two calcium responses, calcium influx and spiking were implicated in two different downstream pathways (Moriere et al., 2013). While calcium spiking activated nodule organogenesis, calcium influx is proposed to be associated with IT development (Miwa et al., 2006b; Moriere et al., 2013).

3. The CCaMK/CYCLOPS Complex

3.1 CCaMK

Nuclear-localized CCaMK is assumed to decode and transduce the calcium signals into downstream symbiotic gene activation (Singh et al., 2014; Singh and Parniske, 2012). The protein containing an N-terminal serine/threonine kinase domain, followed by a calmodulin (CaM) binding domain overlapping with an autoinhibition region and four C-terminal EF-hands, is unique to plants because of its dual ability to bind calcium: free calcium to the EF-hands or calcium complexed with CaM to the CaM-binding domain (CaMBD) (Hrabak et al., 2003; Patil et al., 1995). Biochemical studies on *Lilium longiflorum* CCaMK, where it was initially cloned from, showed that the kinase activity is regulated by both calcium and Ca²⁺/CaM (Patil et al., 1995; Takezawa et al., 1996). Expression of autoactive CCaMK versions in calcium spiking-deficient mutants complemented RNS and AM, proofing the main purpose for generation of calcium spikings is CCaMK activation (Hayashi et al., 2010; Madsen et al., 2010). The special domain structure of CCaMK as well as the intron/exon arrangement are evolutionary highly conserved and most likely diverged from a calcium-dependent protein kinase (CDPK) of a common ancestor of charophytes and land plants (Delaux et al., 2015). The finding of symbiotically preadapted algal ancestors indicated that the emergence of CCaMK has been one of the major events for the colonization of land plants. CCaMK is only present in symbiotic plants, but absent in asymbiotic plants like *Arabidopsis thaliana* (Hrabak et al., 2003), showing that its function in plant-microbe symbioses was conserved. Mutant *ccamk* plants are symbiosis-defective and do neither initiate neither nodule organogenesis nor infection of rhizobia and AM fungi, but still revealed root hair deformation and calcium spiking upon NF treatment (Levy et al., 2004; Mitra et al., 2004; Miwa et al., 2006b). In non-legumes, CCaMK was shown to further function in disease resistance, reactive oxygen species (ROS) accumulation and abiotic stress responses and to be transcriptionally regulated by brassinosteroid and abscisic acid (ABA) signaling (Ma et al., 2012; Shi et al., 2012; Wang et al., 2012; Yan et al., 2015; Yang et al., 2011). A NAC transcription factor, NAC84, was identified as interactor and phosphorylation substrate of CCaMK in *Zea mays*, which mediated ABA-induced antioxidant defense in a CCaMK-dependent manner (Zhu et al., 2016).

CCaMK is subject to positive and negative regulation via autophosphorylation (Figure 2). Upon low-level calcium binding to the EF-hand motifs, T265 in the kinase domain gets phosphorylated, which stabilizes an autoinhibitory conformation (Miller et al., 2013). Substitution at S337, an *in vitro* phosphorylation site in the CaMBD leading to the *ccamk-14* mutation (S337N), has been shown to negatively regulate CCaMK function (Liao et al., 2012; Routray et al., 2013). The mutant revealed increased epidermal root hair infection, but compromised cortical infection and is deficient in AM development. Using a phosphomimetic version (S337D), Ca²⁺/CaM-binding of CCaMK was impaired and kinase activity and interaction with CYCLOPS decreased, suggesting that CCaMK is locked in an inhibited state (Liao et al., 2012; Routray et al., 2013). Another CCaMK variant impaired in CaM-binding (CCaMK^{FN-ED}) could restore nodule formation but not rhizobial infection in *ccamk-3* mutant plants upon *M. loti* inoculation, confirming that cortical infection requires negative feedback regulation by autophosphorylation within the CaMBD of CCaMK (Shimoda et al., 2012).

3.2 CYCLOPS

CCaMK forms a preassembled complex with the dimeric transcription factor CYCLOPS in the nucleus (Singh et al., 2014; Yano et al., 2008). CYCLOPS is a phosphorylation substrate of CCaMK and was postulated to transduce the calcium signal into downstream symbiotic gene expression, because expression of several nodulation- and AM-specific TFs was found to be dependent on CYCLOPS (Cerri et al., 2017; Pimprikar et al., 2016; Singh et al., 2014; Yano et al., 2008). Like CCaMK, CYCLOPS is already present in algal ancestors of land plants and assumed to be an important preadaptation for symbiosis (Delaux et al., 2015). *Cyclops* mutants initiate but prematurely arrest nodule organogenesis (Horvath et al., 2011; Ovchinnikova et al., 2011; Yano et al., 2008) and respond towards rhizobia with root hair curling around entrapped bacteria. However, IT formation is impaired and the nodule primordia remain uninfected (Yano et al., 2008). Similarly, arbuscule formation is absent during AM and fungal hyphae display abnormal swellings and significantly reduced cortical colonization (Yano et al., 2008). Although *cyclops* mutants show a less severe phenotype than *ccamk* mutants, overexpression of an autoactive CCaMK version in a *cyclops* background significantly reduced nodule frequency and the nodules remained uninfected upon inoculation with rhizobia, therefore indicating a role of CYCLOPS in rhizobial infection and nodule organogenesis (Madsen et al., 2010; Yano et al., 2008).

In *M. truncatula* the ortholog of *CYCLOPS* (*IPD3*) revealed a less severe mutant phenotype depending on the genetic background, implying genetic redundant components. While *M. truncatula* R108 *ipd3* mutants displayed the same severe phenotype as *cyclops* mutants, *M. truncatula* Jemalong *ipd3* mutants formed more developed nodules and misshaped ITs (Ovchinnikova et al., 2011). Moreover, Jemalong *ipd3* mutants were impaired in bacterial release into nodule cells and revealed a significantly reduced expression of the nodule-specific remorin *SYMREMI*, which controls proper IT growth and is essential for symbiosome formation, indicating an additional later role of *CYCLOPS/IPD3* in rhizobial cell entry (Ovchinnikova et al., 2011). However, the precise role of *CYCLOPS* in symbiotic signal transduction remained unknown so far.

3.3 Structure, Mechanism and Conformational Dynamics

Since no high-resolution information about the CCaMK/*CYCLOPS* complex were available so far, most of the functional and mechanistical understanding came from computational modeling using structurally similar proteins. The N-terminal domain of CCaMK (amino acids 1-340) shares sequence homology with Calmodulin-dependent Kinase II (CaMKII), a metazoan kinase that decodes calcium signals into phosphorylation of target proteins during neuronal signaling (De Koninck and Schulman, 1998; Hudmon and Schulman, 2002; Rellos et al., 2010). Similar to CCaMK, CAMKII contains a kinase and a CaMBD that overlaps with an autoinhibitory region and is regulated by autophosphorylation in the kinase domain and CaMBD. The CCaMK autoinhibition/CaMBD shows 79 % homology to that of CaMKII (Patil et al., 1995). By x-ray crystallography and comparison with different CAMKII isoforms, it was shown that the enzyme forms a large dodecameric complex, which can interconvert from an autoinhibited into a calcium-activated state (Chao et al., 2011). A similar structural arrangement and mechanism is assumed for CCaMK, supported by the finding of autoactive versions containing the kinase domain only (CCaMK¹⁻³¹⁴) or a substitution at T265 (CCaMK^{T265D}), which conferred a gain-of-function phenotype *in planta* leading to spontaneous nodule formation in the absence of rhizobia (Gleason et al., 2006; Hayashi et al., 2010; Shimoda et al., 2012; Takeda et al., 2012; Tirichine et al., 2006).

However, while the N-terminal region of CCaMK and CAMKII are very similar, the C-terminal region of CCaMK is different since it possesses a second calcium sensor: EF-hands. EF-hands are helix-loop-helix motifs, which usually appear as pairs and contain positively charged amino acids that contact calcium ions (Denessiouk et al., 2014). Structural comparison and modeling identified two visinin-like and one non-canonical EF-hand in CCaMK, which are assumed to form two functional EF-hand pairs (Shimoda et al., 2012). Deletion of the EF-hands impaired RNS and point mutational analyses revealed the critical importance of the third EF-hand for CCaMK activity and calcium-binding ability. The integration of two independent calcium sensors and the precise role of the autophosphorylation site was a long-time conundrum, in particular because phosphomimetic and –ablative substitutions at T265 (CCaMK^{T265D/I/A}) caused a gain-of-function phenotype (Shimoda et al., 2012). A combination of biochemistry, genetics and structural modeling could prove that the CCaMK autophosphorylation site in the kinase domain is in contrast to CAMKII negatively regulating kinase activity (Miller et al., 2013). According to the mechanism (Figure 2), a hydrogen bond network is strengthened by T265 phosphorylation (or T271 in *M. truncatula* DMI3) at basal calcium concentrations, which stabilizes a closed conformation and renders the kinase inactive (Miller et al., 2013; Takezawa et al., 1996). At elevated calcium concentrations during calcium spiking, binding of Ca²⁺/CaM induces a conformational change in the CaMBD, whereby the inhibitory segment adopts an extended conformation and the unstructured CaMBD becomes helical. This structural arrangement increases CaM-binding affinity (“CaM trapping”) and activates the kinase for target phosphorylation (Sathyanarayanan et al., 2000). Subsequent autophosphorylation at S337 in the CaMBD prevents Ca²⁺/CaM from rebinding (“CaM capping”) (Liao et al., 2012).

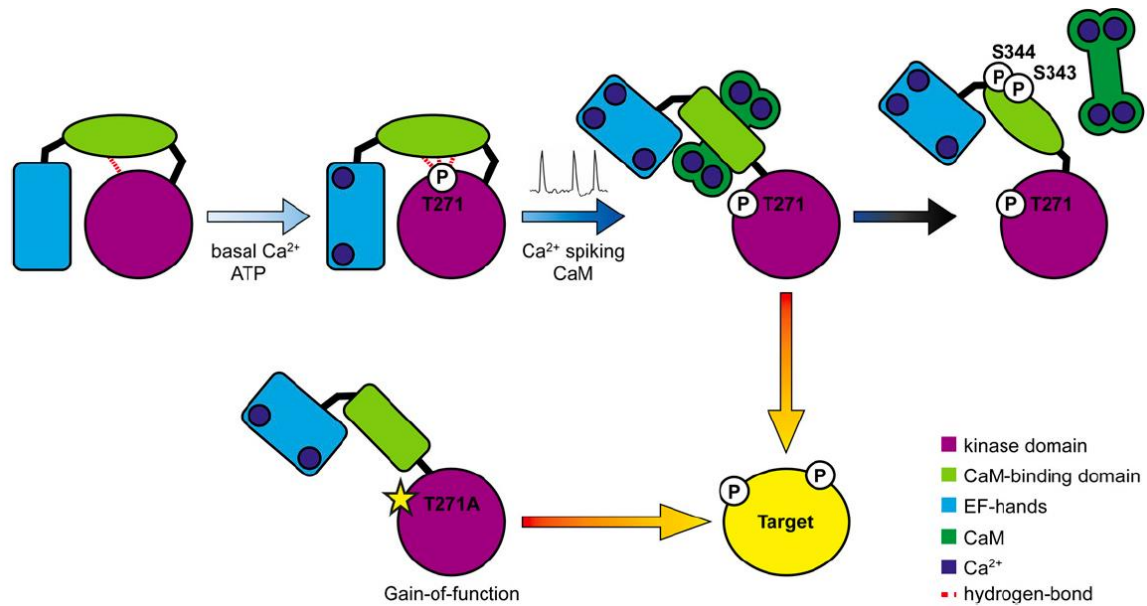


Figure 2. Schematic Overview of CCaMK Activation.

A hydrogen bond network between the kinase domain and the CaM-binding domain is strengthened by Ca^{2+} -induced T271 phosphorylation at basal calcium concentrations; in this state, CCaMK is inactive for target phosphorylation. With relatively low dephosphorylation rates, phosphorylated CCaMK is likely to be the dominant species at basal calcium concentrations. At elevated calcium concentrations during calcium spiking, CaM binds to CCaMK, and this overrides the negative regulation caused by T271 phosphorylation, making the kinase active for target phosphorylation. Phosphorylation of S343/S344 inhibits CaM-binding, and this negatively regulates CCaMK activity (Liao et al., 2012; Routray et al., 2013). The hydrogen bond network in the gain-of-function T271A mutant (yellow star) is disrupted, rendering the protein active for target phosphorylation. Figure and legend modified from Miller *et al.*, 2013*.

In contrast to CCaMK, no structural information about CYCLOPS was available and sequence analysis could not identify homologous regions with proteins of known function (Yano et al., 2008). Two nuclear localization signals (NLSs) in the C-terminal region and several CC domains were predicted, the very C-terminal one with a probability of 100 % (Singh et al., 2014). The CC is highly conserved and deletion impairs CYCLOPS' functioning in RNS and AM (Perry et al., 2009). Modeling of the C-terminal end of CYCLOPS using the EMBnet coil server suggested a canonical CC structure of four α -helices containing two serine- and threonine-rich regions and eight putative N-glycosylation sites (Messinese et al., 2007). However, computational methods are a just first approach. In order to obtain precise structural information, methods like x-ray crystallography are needed.

*Reprinted from “Miller, J.B., Pratap, A., Miyahara, A., Zhou, L., Bornemann, S., Morris, R.J., and Oldroyd, G.E. (2013). Calcium/Calmodulin-dependent protein kinase is negatively and positively regulated by calcium, providing a mechanism for decoding calcium responses during symbiosis signaling. *Plant Cell* 25, 5053-5066.” with permission from American Society of Plant Physiologists.

4. Transcriptional Regulation during Root Symbioses

Downstream of calcium signaling, complex transcriptional networks are activated to coordinate different root symbiotic developments. The expression of several symbiosis-related transcriptional regulators belonging to the RWP-RK domain, GRAS domain, CAAT-box and ethylene response factor (ERF) family were found to be dependent on CCaMK and CYCLOPS (Andriankaja et al., 2007; Cerri et al., 2016; Cerri et al., 2017; Combier et al., 2006; Gobbato et al., 2012; Kaló et al., 2005; Marsh et al., 2007; Middleton et al., 2007; Pimprikar et al., 2016; Schaarschmidt et al., 2013; Schauser et al., 1999; Smit et al., 2005; Soyano et al., 2013).

NIN, encoding an RWP-RK domain containing transcription factor, is rapidly induced in response to NF and its expression is significantly reduced in *cyclops* mutants (Horvath et al., 2011; Yano et al., 2008). *NIN* plays an important role for both nodule organogenesis and rhizobial infection (Fournier et al., 2015; Schauser et al., 1999). Ectopic expression of *NIN* induces the formation of abnormal lateral root organs partly resembling nodule primordia (Soyano et al., 2013) and it has been shown that *NIN* binds and transactivates the promoters of two subunits of the heteromeric CAAT-box-binding protein complex Nuclear Factor Y (NF-Y), *NF-YA1* and *NF-YB1*, which is believed to trigger entry into the cell division cycle and to regulate meristem persistence in root nodules (Combier et al., 2006; Laloum et al., 2013; Laporte et al., 2014; Mantovani, 1999; Soyano et al., 2013). Likewise, ectopic cell divisions and *NIN* expression are induced in the cortex by exogenous cytokinin application in the absence of rhizobia (Heckmann et al., 2011), confirming a function of *NIN* in the regulation of cortical cell divisions. *NIN* also acts antagonistically to the homologous *NIN*-like proteins (NLP) by binding to *nitrate-responsive elements* (*NREs*) and repressing nitrate-inducible genes, thereby allowing the establishment of RNS under nitrate-limiting conditions (Soyano et al., 2014). Beside its role as positive regulator of RNS, *NIN* creates a negative long-distance feedback loop through direct targeting of *CLAVATA3/ENDOSPERM SURROUNDING REGION* (*CLE*) *ROOT SIGNAL 1* (*CLE-RS1*) and *CLE-RS2*, which induces expression of small root-derived peptides that are perceived in the shoot to activate the autoregulation of nodulation (AON) pathway and restrict the number of nodules in the root (Soyano et al., 2014).

In addition to nodule organogenesis, NIN functions in signaling pathways required for rhizobial infection. Plants mutated in *NIN* show excessive root hair deformations upon inoculation with rhizobia and are impaired in the establishment of a functional infection chamber inside curled root hairs and IT formation (Fournier et al., 2015; Schauser et al., 1999). Expression of many infection-related genes are dependent on NIN including the flotillin encoding genes *FLOT2* and *FLOT4* in *M. truncatula* (Haney and Long, 2010), *SCARN* belonging to the SCAR/WAVE actin regulatory complex (Qiu et al., 2015), *NODULATION PECTATE LYASE (NPL) 1* (Xie et al., 2012) and *EPR3* in the root cortex (Kawaharada et al., 2017), the last two being directly targeted by NIN. The *daphne* mutant containing a chromosomal translocation upstream of the *NIN* gene resulting in enhanced *NIN* expression in the epidermis, revealed an hyperinfection phenotype, thus suggesting a role of NIN in the autoregulation of infection (Yoro et al., 2014). The importance of NIN as both an activator and repressor of rhizobial infection and nodule organogenesis suggests a precisely fine-tuned spatiotemporal expression, which is in agreement with the inability to fully complement *nin* mutant plants so far (Schauser et al., 1999; Soyano et al., 2014; Vernié et al., 2015; Yoro et al., 2014).

The GRAS domain TFs Nodulation Signaling Pathway (NSP) 1 and NSP2 are involved in transcriptional regulation during root symbiosis. *Nsp1* and *nsp2* mutants show reduced root hair deformation and are impaired in rhizobial infection and root nodule formation downstream of CCaMK (Heckmann et al., 2006; Kaló et al., 2005; Mitra et al., 2004; Smit et al., 2005). BD-containing NSP1 forms a heterocomplex with NSP2, which associates with promoters of NF-inducible genes, such as *ENOD11*, *ERN1* and *NIN* (Hirsch et al., 2009). In *M. truncatula* a complex interplay of ERN1 and NSP1/NSP2 is required for *ENOD11* expression (Cerri et al., 2012). NSP1 and NSP2 were originally identified as nodulation-specific genes (Catoira et al., 2000; Heckmann et al., 2006; Kaló et al., 2005; Murakami et al., 2006; Oldroyd and Long, 2003; Smit et al., 2005). However, more recent analyses also indicated a function in AM signaling (Delaux et al., 2013; Laressergues et al., 2012; Maillet et al., 2011) and strigolactone biosynthesis (Liu et al., 2011).

The GRAS domain protein DELLA was identified as positive regulator of root nodule and AM symbiosis (Floss et al., 2013; Fonouni-Farde et al., 2016; Jin et al., 2016; Pimprikar et al., 2016; Yu et al., 2014). DELLA proteins inhibit gibberellic acid (GA) signaling, an important phytohormone, which upon treatment of plant roots represses AM development, nodulation and rhizobial infection (Floss et al., 2013; Jin et al., 2016; Pimprikar et al., 2016; Takeda et al., 2015b).

Interactions with NSP2, NF-YA1 and CYCLOPS classified DELLA as important scaffold protein to bridge transcriptional regulatory complexes during root symbiotic development and thereby integrates hormonal and symbiotic responses (Fonouni-Farde et al., 2016; Jin et al., 2016; Pimprikar et al., 2016). Accordingly, *della* mutants were reduced in rhizobial colonization and *ERN1* and *ENOD11* expression (Jin et al., 2016) and severely impaired in arbuscule formation (Floss et al., 2013), while ectopic expression of a dominant GA-insensitive version of DELLA enabled arbuscule development in the presence of GA and spontaneously induced *ENOD11* expression (Floss et al., 2013; Fonouni-Farde et al., 2016). Additionally the GRAS domain proteins RAM1 and DELLA Interacting Protein (DIP) 1 are involved in AM development, since mutations in either of the genes blocked arbuscule formation or branching (Floss et al., 2013; Fonouni-Farde et al., 2016; Pimprikar et al., 2016; Yu et al., 2014). The finding that overexpression of *RAM1* or a dominant active version of *DELLA* was sufficient to activate genes critical for arbuscule development in the absence of a fungal symbiont and to complement arbuscule formation in a *cyclops* mutant background, clearly indicates a role in AM signaling (Floss et al., 2013; Pimprikar et al., 2016).

NSP1, NSP2 and NF-YA2 function in the direct transactivation of the *ERN1* promoter (Hirsch et al., 2009; Laloum et al., 2014) and rhizobia-induced expression of *ERN1* in the epidermis is dependent on CYCLOPS (Cerri et al., 2017). ERN1 is a nodulation-specific transcriptional regulator which activates the *ENOD11* promoter via the NF-box in a separate region than NSP1/NSP2 (Cerri et al., 2016; Cerri et al., 2012) and directly binds to and transactivates the *EPR3* promoter during epidermal infection (Kawaharada et al., 2017). In *M. truncatula*, *ern1* mutants form ITs but are impaired in nodule organogenesis, while *ern2* mutants develop infected, but less colonized and prematurely senescent nodules (Cerri et al., 2016). In contrast, the double mutant of *ern1* and its closest homolog *ern2* is completely blocked in rhizobial infection and nodule organogenesis, demonstrating functional redundancy between both transcriptional regulators (Cerri et al., 2016). Complementation of the respective single or double mutants by expressing *ERN1* or *ERN2* under control of their native promoters, revealed a concerted action of ERN1/ERN2 in root epidermal infection, while ERN2 was dispensable for nodule formation (Cerri et al., 2016).

5. Aim of the Thesis

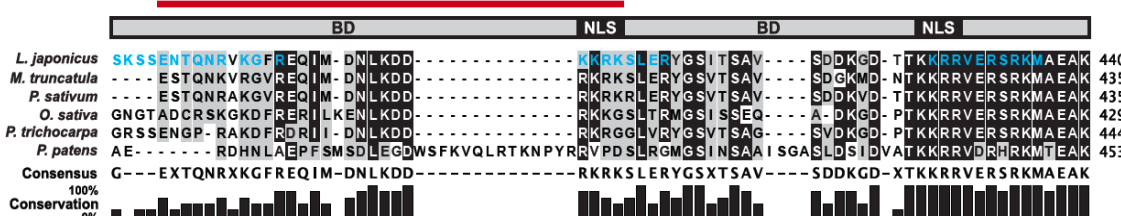
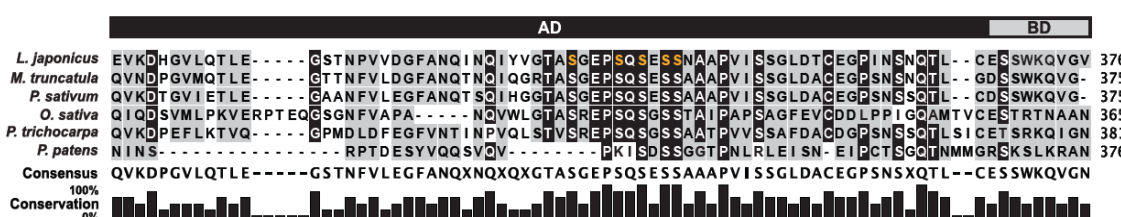
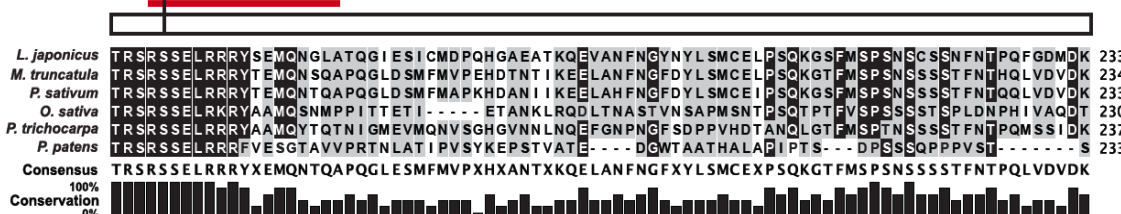
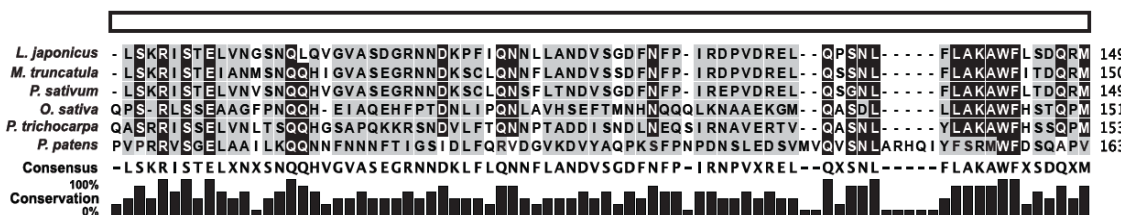
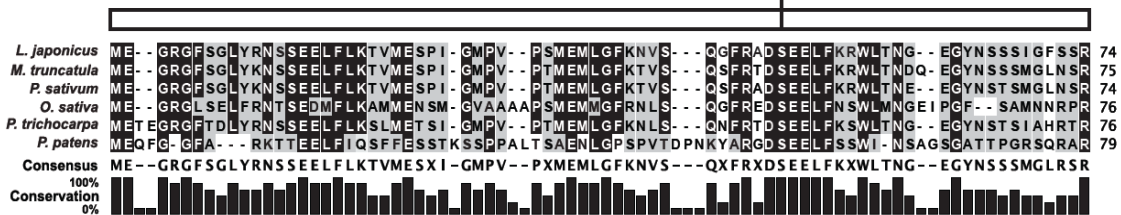
Despite the importance of CCaMK as prime decoder of symbiotic calcium oscillations, the connection between CCaMK activation and transcriptional reprogramming remained unknown. CYCLOPS was identified as interactor and phosphorylation target of CCaMK (Yano et al., 2008). RNS and AM are impaired in *cyclops* mutant plants and expression of the marker genes *NIN*, *ERN1*, *ENOD40* and *RAM1* are significantly reduced (Jin et al., 2016; Yano et al., 2008), assuming a direct or indirect involvement of CYCLOPS in downstream signal transduction. However, the molecular function of CYCLOPS was enigmatic since domain analysis could not identify homologous regions with proteins of known function. The general aim of this study was to better understand the mechanism of signal transduction from the CCaMK/CYCLOPS complex towards activation of gene expression and to characterize function, structure and regulation of CYCLOPS during root symbioses. Since both symbionts, rhizobia and AM fungi, elicit sustained calcium spikings leading to CCaMK activation (Ehrhardt et al., 1996; Gleason et al., 2006; Sieberer et al., 2012; Tirichine et al., 2006), differential phosphorylation of CYCLOPS was assumed to mediate symbiotic signaling. Two critical sites in the N-terminal region were found to be critical for CYCLOPS' activity and led to the identification of CYCLOPS as transcriptional regulator (Singh et al., 2014). One major goal of the thesis was to reveal the domains of CYCLOPS required for DNA-binding, transcriptional activation and dimerization. To approach this question, deletion versions were generated and the activity was tested *in vitro* and *in planta* (Singh et al., 2014). The C-terminal region of CYCLOPS, which is highly conserved and indispensable for CYCLOPS' function (Perry et al., 2009), was of special interest since it contains a novel type of BD and thus is an important specificity determinant by defining the binding to distinct regulatory DNA elements. Using x-ray crystallography, it was aimed to determine the structure of this domain and get insights into the molecular decision process at the level of transcriptional regulation. Structural analysis would further help to identify new complex components involved in the transcriptional coordination, since the non-congruent phenotypes of *cyclops* and *ccamk* indicated additional factors that act redundantly with CYCLOPS during root symbiotic development (Levy et al., 2004; Yano et al., 2008)

V. Results

1. CYCLOPS is a Modular Transcriptional Regulator

CCaMK-mediated phosphorylation of CYCLOPS at S50 and S154 is essential for symbiotic development, since phosphoablative replacement to alanine impaired CYCLOPS to complement *cyclops-3* roots for RNS and AM (Singh et al., 2014). Strikingly, phosphomimetic replacement of both sites to aspartate (*CYCLOPS-S50D-S154D = CYCLOPS^{DD}*) resulted in a gain-of function phenotype causing transactivation of the *NIN* promoter in *N. benthamiana* leaves and *L. japonicus* roots and formation of spontaneous nodules in the absence of CCaMK and rhizobia (Singh et al., 2014). Deletion and substitution analysis of the *NIN* promoter delimited a 30 bp *cis*-regulatory CYCLOPS response element (*CYC-RE_{NIN}*) containing a palindromic region (Singh et al., 2014). Together, these results implicated CYCLOPS directly in the transcriptional regulation of target genes.

To map the CYCLOPS-AD and -BD, truncated versions of CYCLOPS were generated and fused to either the GAL4-BD or the VP16-AD. GAL4-BD-3xHA-CYCLOPS^{DD} revealed strong transactivation of the *p5xUAS_{GAL4}:eGFP-GUS_{Intron}* reporter in *N. benthamiana* leaves, confirming the presence of an AD in CYCLOPS (Figure 3A). The CYCLOPS-AD was narrowed down to amino acid 267-380, as a GAL4-BD fusion of this truncation was sufficient to transactivate the reporter in *N. benthamiana* leaves (Figure 3A). In yeasts, a tandem repeat fusion of the CYCLOPS-AD was able to trigger autoactivation of a *p3xUAS_{GAL4}:lacZ* reporter, indicating that CYCLOPS interacts with components of the basal transcriptional machinery (Figure 3B). The CYCLOPS-AD is predicted by DIPHOS (Iakoucheva et al., 2004) to be intrinsically disordered and to contain serine-rich regions as potential phosphorylation sites (Figure 4), suggesting folding of this region upon phosphorylation-induced recruitment of transcriptional mediators. To delimit the CYCLOPS-BD, fusions to the VP16-AD were tested in *N. benthamiana* leaves to transactivate the *2xCYC-RE_{NIN}:GUS* reporter. Deletion of the C-terminal part of CYCLOPS impaired transactivation, while CYCLOPS-364-518 revealed strong transactivation, indicating the presence of a BD in this region (Figure 3C). Consistent with this, two NLS, a CC region with a probability of 100 % (Lupas et al., 1991) and DNA-binding motif residues (Wang et al., 2010) were predicted in the CYCLOPS-BD (Figure 4).



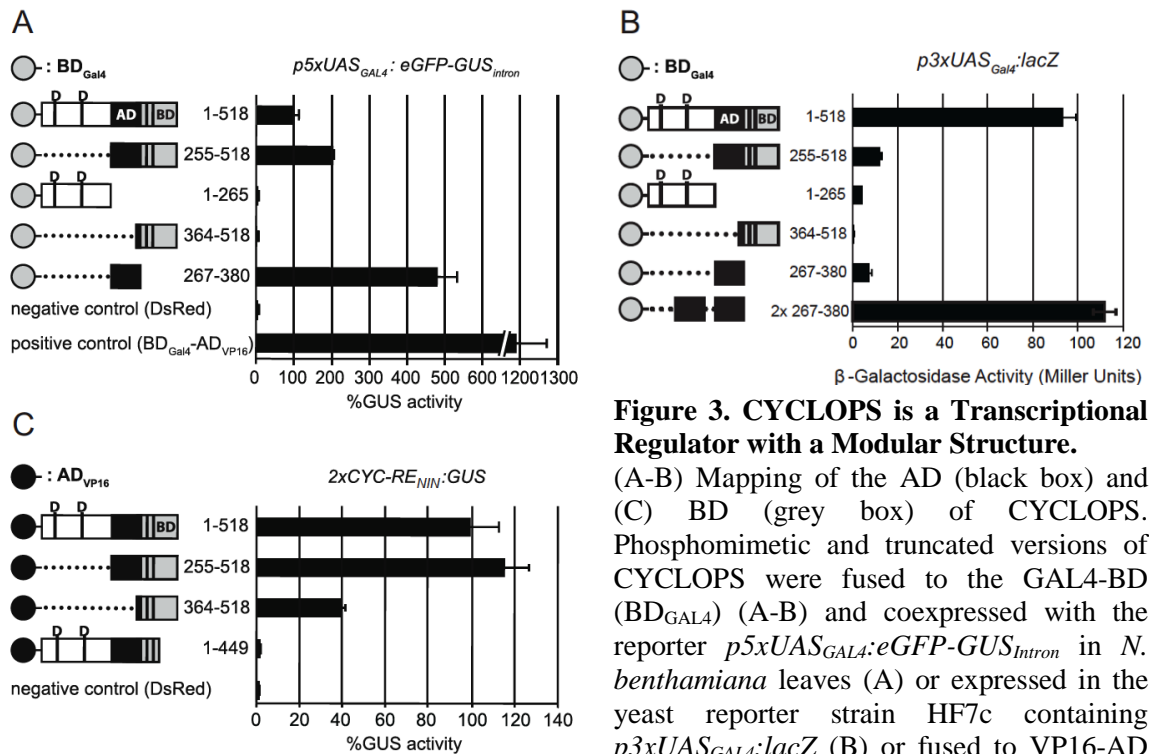


Figure 3. CYCLOPS is a Transcriptional Regulator with a Modular Structure.

(A-B) Mapping of the AD (black box) and (C) BD (grey box) of CYCLOPS. Phosphomimetic and truncated versions of CYCLOPS were fused to the GAL4-BD (BD_{GAL4}) (A-B) and coexpressed with the reporter $p5xUAS_{GAL4}:eGFP-GUS_{intron}$ in *N. benthamiana* leaves (A) or expressed in the yeast reporter strain HF7c containing $p3xUAS_{GAL4}:lacZ$ (B) or fused to VP16-AD

(AD_{VP16}) and coexpressed with the reporter $2xCYC-RE_{NIN}:GUS$ in *N. benthamiana* leaves (C). All versions were constitutively expressed under control of the 35S (A and C) or *ADH* promoter (B). The graphs show mean values and standard deviations calculated from three biological replicates. (A and C) An AD (amino acid 267-380) was delimited to the central part and a BD (amino acid 364-518) to the C-terminal region of CYCLOPS. T-DNAs encoding a GAL4-BD-VP16-AD fusion (BD_{GAL4}-AD_{VP16}) (A) or *DsRed* (C) were used as positive and negative controls, respectively. Data are represented as percentage of GUS activity relative to GAL4-BD- (A) or VP16-AD-3xHA-CYCLOPS^{DD} (B), set to 100 %.

(B) A tandem repeat fusion of the deduced AD revealed strong activation of the yeast reporter. β -Galactosidase activity is represented in Miller units.

Figures and legends modified from Singh et al., 2014*. Figures and data related to the figures were generated by K. Katzer.

Figure 4. Alignment of CYCLOPS Amino Acid Sequences. Sequence alignment of CYCLOPS species from *Lotus japonicus*, *Medicago truncatula*, *Pisum sativa*, *Oryza sativa*, *Populus trichocarpa* and *Physcomitrella patens*. The delimited regulatory N-terminal region, the AD and the BD containing two predicted NLS of CYCLOPS are indicated above the alignment as white, black and grey boxes, respectively. CC predictions (Lupas et al., 1991) are shown as red lines with the corresponding probability. Positions of S50 and S154 phosphorylation sites, BindN+ predicted DNA-binding motif residues (blue) (Wang et al., 2010) and a serine-rich region (orange) predicted by DIPHOS (Iakoucheva et al., 2004) are highlighted. Identical amino acids (>83.3 % of aligned species) are shown in white on black background, identical amino acids between some plant species (50-83.3% of aligned species) are shaded in grey and non-conserved residues are shown in black on white background. Figure and legend modified from Singh et al., 2014*. Figure was generated by K. Katzer.

*Reprinted from "CYCLOPS, a DNA-binding transcriptional activator, orchestrates symbiotic root nodule development. *Cell Host & Microbe* 15, 139-152." with permission from Elsevier.

2. The N-terminal Half of CYCLOPS has a Negatively Regulatory Function

Because both the CYCLOPS-AD and -BD were localized to the C-terminal part, a minimal CYCLOPS version (CYCLOPS-255-518 =CYCLOPS_{min}) lacking the N-terminal region was generated (Figure 5A). CYCLOPS_{min} fully transactivated the 2xCYC-RE_{NIN}:GUS reporter in *N. benthamiana* leaves and *L. japonicus* roots (Figure 5 A and B). Furthermore, transactivation was dependent on a palindromic sequence within the 2xCYC-RE_{NIN}, since mutagenized 2xCYC-RE_{NIN}:GUS versions (2xM2, 2xM3 and 2xmCYC-RE_{NIN}) led to a significantly reduced transactivation (Figure 5A). Both CYCLOPS_{min}-mediated fold activation and sequence-specificity in 2xCYC-RE_{NIN}:GUS transactivation in *N. benthamiana* leaves matched that of CYCLOPS^{DD} (Figure 5A). These results indicate the N-terminal part of CYCLOPS negatively regulates CYCLOPS' activity by inducing an inhibitory conformation, which is released upon phosphorylation at S50 and S154 or cleavage of the N-terminal part.

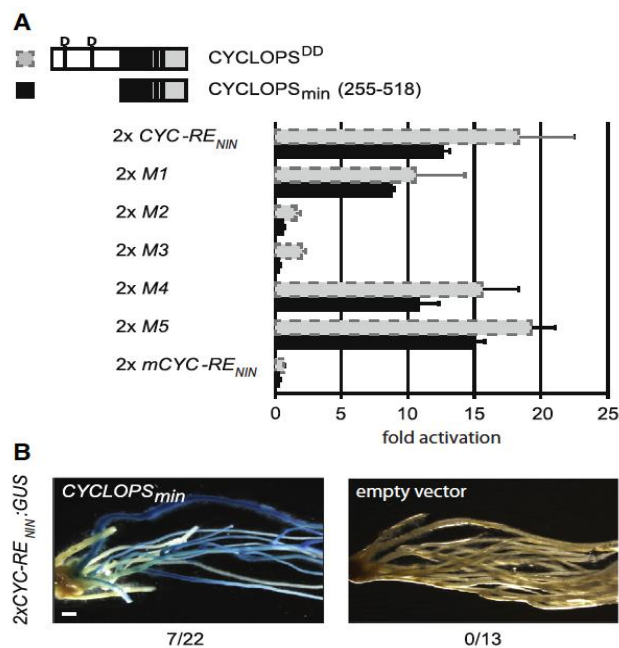


Figure 5. A Minimal CYCLOPS Version is Sufficient to Transactivate via 2xCYC-RE_{NIN} in planta.

(A) Transactivation assay in *N. benthamiana* leaves cotransformed with the 2xCYC-RE_{NIN}:GUS reporter, or the indicated mutated reporter versions, and CYCLOPS^{DD} (grey bars) or a minimal CYCLOPS (CYCLOPS-255-518 = CYCLOPS_{min}) version comprising the CYCLOPS-AD and -BD (black bars). GUS activity is shown relative to the values obtained with a pNINmin:GUS reporter (minimal NIN promoter fused to uidA), set to 1. All versions were constitutively expressed under control of the 35S promoter. The graph shows mean values and standard deviations calculated from three biological replicates. (B) The 2xCYC-RE_{NIN}:GUS reporter is

induced in *L. japonicus cyclops-3* mutant roots cotransformed with *ProUbi:3xHA-cCYCLOPS_{min}*, but not in roots cotransformed with the empty vector. Blue staining shows GUS reporter activity. Numbers indicate GUS positive root systems per total number of stained root systems. Figures and legends modified from Singh et al., 2014*. Figure and data related to CYCLOPS_{min} expression in *N. benthamiana* and *L. japonicus* roots (A-B) were generated by K. Katzer. Data related to CYCLOPS^{DD} expression in *N. benthamiana* (A) were generated by S. Singh.

*Reprinted from "CYCLOPS, a DNA-binding transcriptional activator, orchestrates symbiotic root nodule development. Cell Host & Microbe 15, 139-152." with permission from Elsevier.

3. CYCLOPS Binds to Target Genes in a Sequence-Specific and Phosphorylation-Dependent Manner

To test direct binding of CYCLOPS to DNA, EMSAs were performed (Figure 6). Both CYCLOPS^{DD} and the CYCLOPS-BD bound to labeled *CYC-RE_{NIN}*, while deletion of the CYCLOPS-BD (CYCLOPS^{DD}-1-449 =DD-ΔBD) impaired DNA-binding (Figure 6A and D), confirming the C-terminal CYCLOPS-BD. Furthermore, DNA-binding was specific, since addition of unlabeled wildtype (WT) *CYC-RE_{NIN}* or a truncated version containing the palindrome only (*IPalI*) outcompeted binding of CYCLOPS-BD and CYCLOPS^{DD} to the *CYC-RE_{NIN}*, respectively, while a mutated competitor (*mIPalI* or *mCYC-RE_{NIN}*) did not (Figure 6A and D). Sequence-specific binding was confirmed by microscale thermophoresis (MST) measurements, showing that binding of CYCLOPS-BD to labeled *CYC-RE_{NIN}* can be outcompeted by increasing amounts of *CYC-RE_{NIN}*, but not *mCYC-RE_{NIN}* (Figure 6B), while CYCLOPS^{DD}-ΔBD revealed no changes in thermophoresis values when increasing concentrations of unlabeled *CYC-RE_{NIN}* were added (Figure 6C), indicating an impairment in *CYC-RE_{NIN}* binding. Taken together these results demonstrate CYCLOPS as transcriptional regulator containing a C-terminal BD with a sequence-specificity matching the one of CYCLOPS^{DD}, and narrowed down the DNA sequence sufficient for CYCLOPS' activity to a palindrome within the *CYC-RE_{NIN}*.

CYCLOPS is a phosphorylation target of CCaMK (Singh et al., 2014). To analyze whether DNA-binding of CYCLOPS is phosphorylation-dependent, phosphomimetic (CYCLOPS^{DD}) and phosphoablative (CYCLOPS^{AA}) CYCLOPS versions were tested in EMSA. GST-CYCLOPS^{DD}, but not CYCLOPS^{AA} or CYCLOPS^{WT} could induce a mobility shift with labeled *CYC-RE_{NIN}* (Figure 6E). Binding of CYCLOPS^{WT} was only observed after coexpression with CCaMK (Figure 6E) and was lost after phosphatase treatment (Singh et al., 2014). These findings indicate that phosphorylation of CYCLOPS by CCaMK promotes CYCLOPS' DNA binding activity.

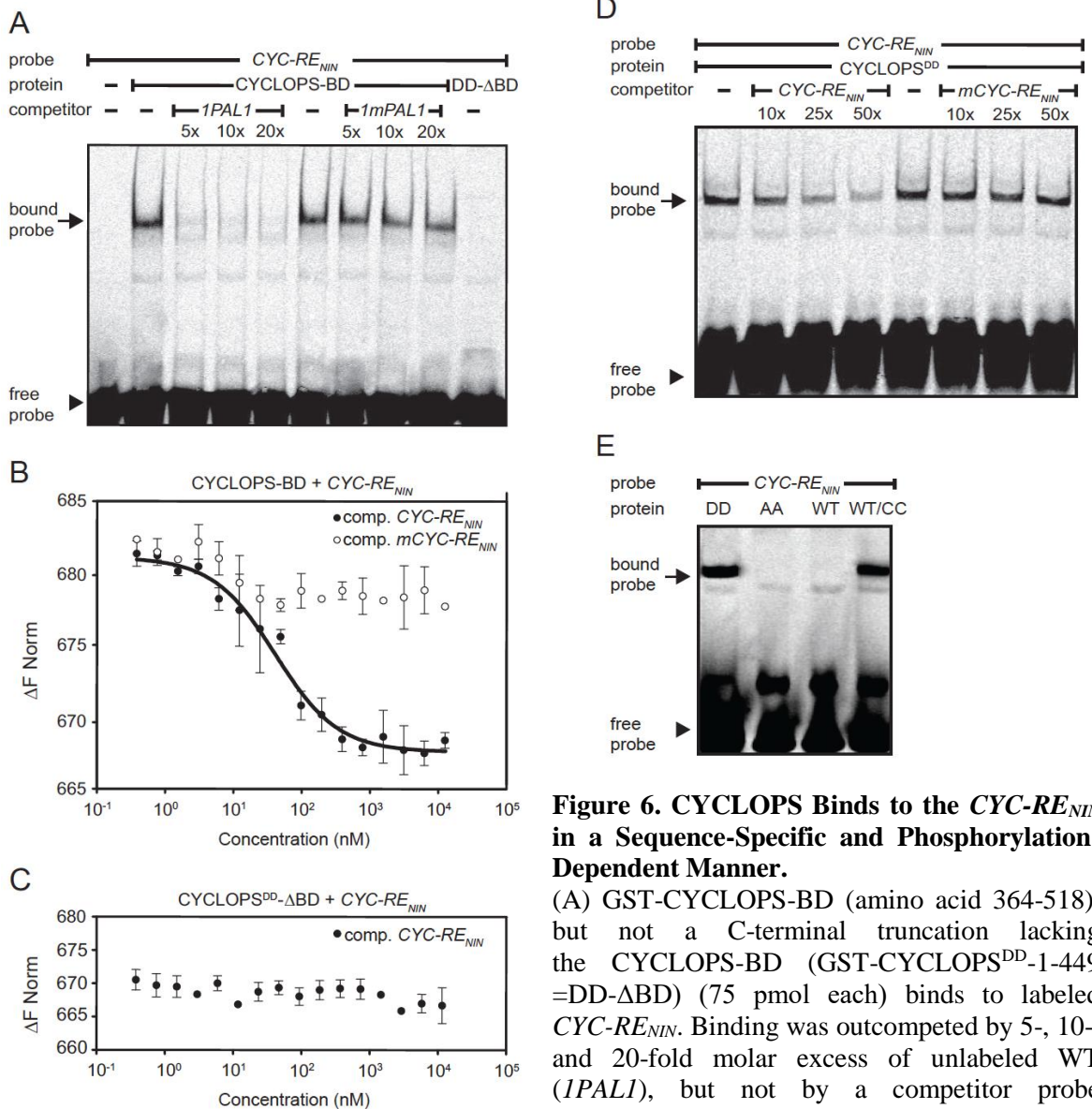


Figure 6. CYCLOPS Binds to the *CYC-RE_{NIN}* in a Sequence-Specific and Phosphorylation-Dependent Manner.

(A) GST-CYCLOPS-BD (amino acid 364-518), but not a C-terminal truncation lacking the CYCLOPS-BD (GST-CYCLOPS^{DD}-1-449 =DD-ΔBD) (75 pmol each) binds to labeled *CYC-RE_{NIN}*. Binding was outcompeted by 5-, 10-, and 20-fold molar excess of unlabeled WT (*IPALI*), but not by a competitor probe containing a mutated palindrome (*ImPALI*).

(B-C) Binding of GST-CYCLOPS-BD to CY5-labeled *CYC-RE_{NIN}* (B) was outcompeted by increasing concentrations of unlabeled *CYC-RE_{NIN}* (black circles), but not mutated *CYC-RE_{NIN}* (*mCYC-RE_{NIN}*) (white circles) in MST experiments. In contrast, GST-CYCLOPS^{DD}-ΔBD (C) showed no change in thermophoresis values when increasing concentrations of unlabeled *CYC-RE_{NIN}* were added, indicating an impairment in *CYC-RE_{NIN}* binding. Average thermophoresis values and standard deviations of three experimental replicates are shown. MST was performed with 25 nM labeled *CYC-RE_{NIN}* and 1.3 mM GST-CYCLOPS-BD or GST-CYCLOPS^{DD}-ΔBD.

(D) GST-CYCLOPS^{DD} (35 pmol) sequence-specifically binds to *CYC-RE_{NIN}*. 10-, 25-, and 50-fold molar excess of unlabeled WT or mutated *CYC-RE_{NIN}* were used as competitors.

(E) CYCLOPS binds to the *CYC-RE_{NIN}* in a phosphorylation-dependent manner, since only GST-CYCLOPS^{DD} (DD) and Strep-CYCLOPS co-expressed with 6xHis-CCaMK (WT/CC) (40 pmol), but not GST-CYCLOPS^{AA} (AA) or GST-CYCLOPS (WT) (each 35 pmol) led to a mobility shift.

(A, D, E) EMSAs were performed using IR-labeled *CYC-RE_{NIN}* (0.1 pmol) as probe. Arrows and arrowheads indicate position of specifically bound and free probe, respectively. Samples were resolved on 6% (A, D) or 4% (E) polyacrylamide gels.

Figures and legends modified from Singh et al., 2014*. Figures and data related to the figures were generated by K.Katzer.

*Reprinted from “CYCLOPS, a DNA-binding transcriptional activator, orchestrates symbiotic root nodule development. *Cell Host & Microbe* 15, 139-152.” with permission from Elsevier.

By induction of *NIN*, *CYCLOPS* initiates cortical cell divisions for root nodule development (Singh et al., 2014). Two additional *CYC-REs* were identified in the nodulation-specific *ERNI* and the AM-specific *RAMI* promoter required for bacterial infection and arbuscule development during AM, respectively (Cerri et al., 2017; Pimprikar et al., 2016). Sequence-specific binding to both elements (*CYC-RE_{ERNI}* and *CYC-RE_{RAMI}*) was demonstrated by EMSAs (Figure 7). Addition of increasing amounts of WT *CYC-RE_{ERNI}* and *CYC-RE_{RAMI}* could outcompete binding of GST-*CYCLOPS_{min}* or 6x-His-*CYCLOPS_{min}* to the labeled probes, respectively, while mutagenized versions did not (Figure 7A and B). These results positioned the CCaMK/*CYCLOPS* complex as central integrator of symbiotic development by initiating transcriptional cascades leading to nodule organogenesis, bacterial and AM fungal infection (Cerri et al., 2017; Pimprikar et al., 2016).

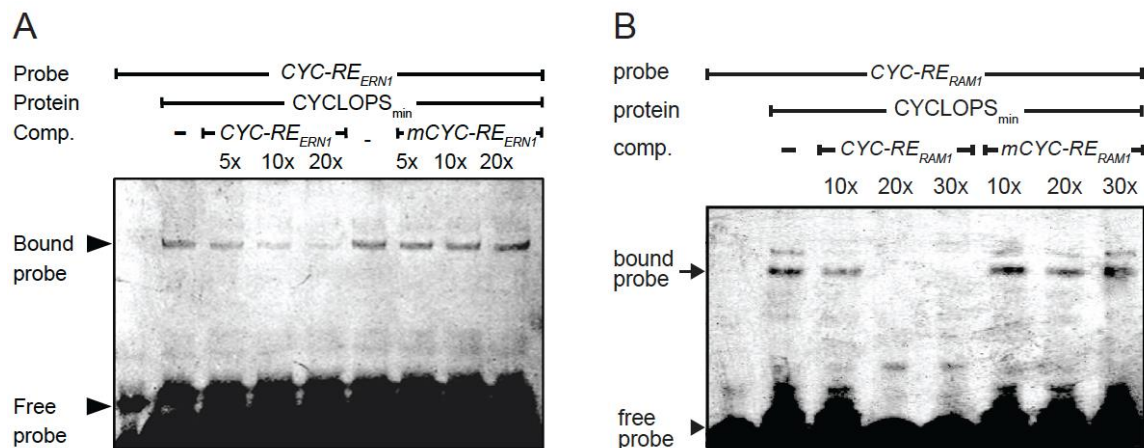


Figure 7. *CYCLOPS* Sequence-Specifically Binds to the *ERNI* and *RAMI* Promoter. *CYC-REs* were identified within the nodulation-specific *ERNI* and the AM-specific *RAMI* promoter (Cerri et al., 2017; Pimprikar et al., 2016). EMSAs were performed using GST-*CYCLOPS_{min}* (A) or 6xHis-*CYCLOPS_{min}* (each 100 pmol) and CY5-labeled *CYC-RE_{ERNI}* (A) or *CYC-RE_{ERNI}* (each 0.1 pmol) as probes. Binding was outcompeted by addition of unlabeled WT, but not mutated *CYC-RE_{ERNI}* (A) or *CYC-RE_{ERNI}* (B) (as indicated), confirming sequence-specific binding to the target elements. Arrows and arrowheads indicate position of specifically bound and free probe, respectively. Samples were resolved on 6 % polyacrylamide gels. Figures and legends modified from Cerri et al., 2017* (A) and Pimprikar et al., 2016** (B). Figures and data related to the figures were generated by K.Katzer.

*Reprinted from “Cerri, M.R., Wang, Q., Stolz, P., Folgmann, J., Frances, L., Katzer, K., Li, X., Heckmann, A.B., Wang, T.L., Downie, J.A., et al. (2017). The *ERNI* transcription factor gene is a target of the CCaMK/*CYCLOPS* complex and controls rhizobial infection in *Lotus japonicus*. *New Phytologist* 215, 323-337.” with permission from John Wiley and Sons.

**Reprinted from “Pimprikar, P., Carbonnel, S., Paries, M., Katzer, K., Klingl, V., Bohmer, M.J., Karl, L., Floss, D.S., Harrison, M.J., Parniske, M., et al. (2016). A CCaMK-*CYCLOPS*-*DELLA* complex activates transcription of *RAMI* to regulate arbuscule branching. *Current Biology* 26, 1126. *Current Biology* 26, 1126.” with permission from Elsevier.

4. The C-terminal DNA-binding Domain of CYCLOPS Contains a Coiled-Coil Region

The ability of legumes to engage in two root symbioses one with nitrogen-fixing rhizobia and another with AM fungi poses a specific cell developmental problem: Distinct developmental programs must be activated depending on the symbiotic partner on one hand and on whether microbial infection is supported or a new organ is initiated (Gutjahr and Parniske, 2013; Oldroyd, 2013). Since both symbioses employ the same regulatory hub, comprising the CCaMK/CYCLOPS complex, it is especially important to ensure activation of appropriate and distinct developmental programs. CYCLOPS has been shown to regulate three key transcription factors, two of which are specific for nodulation and one specific for AM (Cerri et al., 2017; Pimprikar et al., 2016; Singh et al., 2014). However, since the recognition sequences of the *CYC-REs* are very similar, it remained unknown how specific DNA-binding to the different promoters is achieved.

Fundamental to specific protein-DNA interactions are BDs, which adopt unique structural folds and at the same time maintain conformational flexibility to dynamically respond to a variety of external signals. The C-terminal sequence of CYCLOPS harboring the BD is highly conserved (Figure 4) and indeed, deletion or frameshift mutation within that region results in a premature arrest of both types of symbioses (Perry et al., 2009; Yano et al., 2008). To gain structural information of this important domain, the CYCLOPS-BD (amino acid 421-518) was expressed in *E. coli* and purified for crystallization (Figure 8). The crystal structure was determined at 2.4 Å by single-wavelength anomalous diffraction with seleno-methionine-substituted crystals (Se-SAD) (J. Basquin; Table 1) and revealed a homodimeric CC domain (also referred to as zipper) formed by winding of two CYCLOPS helices of amino acid 450-515 around each other (Figure 8A). The remaining amino acids were not structurally resolvable, suggesting a disordered condition.

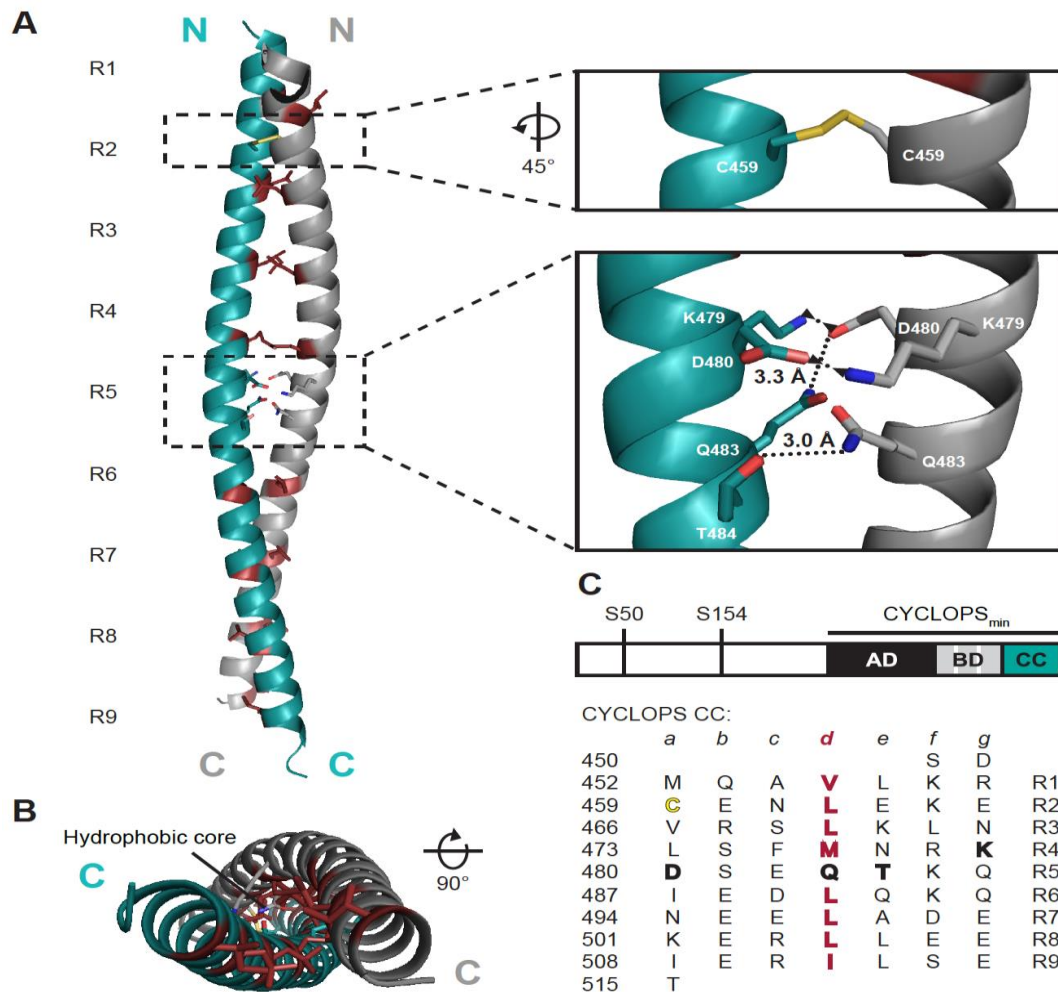


Figure 8. Crystal Structure of the CYCLOPS Zipper. Overall structure of the CYCLOPS zipper from N- to C-terminus (labeled with capital N and C) and viewed parallel (A) or perpendicular (B) to the zipper axis.

(A) The CYCLOPS zipper is formed between two interacting CYCLOPS helices (colored cyan and grey, amino acid 450-515) each containing nine heptad repeats (R1-9). Hydrophobic amino acids in position *d* (shown as sticks, colored ruby) are buried inbetween the two helices, thereby forming a hydrophobic core. Close-ups: the zipper is additionally stabilized by an interhelical disulfide bond (shown as sticks, colored yellow, turned 45°) between two cysteines (C459) in position *a* of R2 and a network of hydrogen (shown as dots) and electrostatic interactions (shown as dots with facing arrow heads) surrounding R5 formed by K479, D480, Q483 and T484 (shown as sticks, colored by element: C in cyan or grey, N in blue, O in red). Distances of hydrogen bondings are indicated in angstrom.

(B) View of the CYCLOPS zipper perpendicular to the zipper axis (turned by 90°) from C- to N-terminus showing the hydrophobic amino acids in position *d* packed into the hydrophobic core of the zipper.

(C) Position and sequence of the CYCLOPS CC domain. Upper panel: Protein domain structure of CYCLOPS. The AD, BD and the CC region are highlighted in black, grey and cyan, respectively. Two phosphorylated serines important for CYCLOPS' activity and two predicted NLS in the BD are marked as black and white lines, respectively. Position of CYCLOPS_{min} is indicated as line above the model. Lower panel: Sequence of the CYCLOPS CC region (R1-9) aligned by heptad repeat position (*a-g*). Hydrophobic amino acids in position *d*, the cysteine residue of the disulfide bridge and the amino acids of the polar network surrounding R5 are indicated in ruby, yellow or bold, respectively. Numbering refers to the CYCLOPS amino acid sequence.

Crystallization and x-ray structure determination were performed by J. Basquin.

Typical for canonical CCs (Vinson et al., 2002), the CYCLOPS zipper contains two parallel left-handed, amphiphatic α -helices and is based on tandem heptad sequence repeats (R, designated $a-g$) (Figure 8C). The a and d residues are hydrophobic and pack into a 'knobs and holes' pattern along the helical interface to form a stabilizing hydrophobic core (Figure 8B). Additionally, CYCLOPS CC formation is supported by hydrophobic $e-g'$ interactions at the extreme ends of the zipper (R1, 8 and 9), eight salt bridges and three hydrogen bonds (Figure 9A). A covalent disulfide bridge between two C459 residues of position a in R2 was revealed in the crystal structure (Figure 8A), which was shown to enhance helicity and stability of CC proteins (Ciaccio and Laurence, 2009). Two exceptional features characterize the CYCLOPS zipper: it is unusually long, comprising nine repeats (R1-9), and contains a polar repeat in the central region (R5). Instead of the canonical hydrophobic interactions, the zipper is stabilized in R5 by a network of salt bridges between K479 and D480 ($g-a'$) and hydrogen bondings between D480-Q483 ($a-d'$) and Q483-T484 ($d-e'$) (Figure 8A and 9A). Taken together, the crystal structure revealed a conformation different to the previously modeled structure that did not predict a homodimeric zipper (Messinese et al., 2007).

Figure 9. Comparison of Zipper Interaction Surfaces.

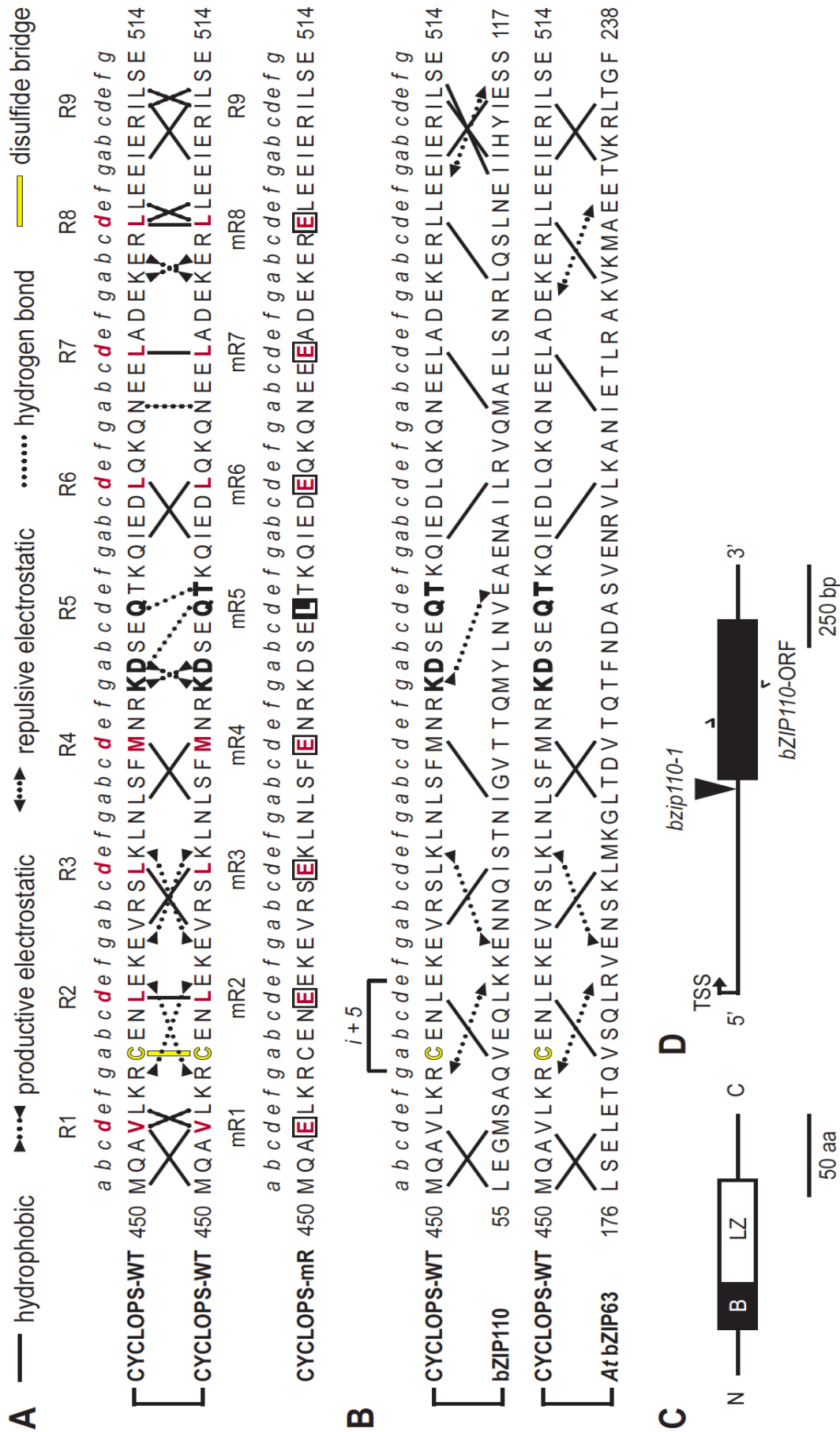
(A-B) Schematic alignment of the homodimeric CYCLOPS zipper sequence (A) and prediction of heterodimeric CC formations with bZIP transcriptional regulators (B). Hydrophobic (black solid line), productive and repulsive electrostatic interactions (black dotted line with facing or opposing arrow heads) and hydrogen bonds (black dotted line) between two helices are indicated. Hydrophobic amino acids in position d , the disulfide bridge in R2 and the amino acids forming a polar network in R5 of the CYCLOPS zipper are highlighted in ruby, yellow or bold, respectively. Heptad repeats letters ($a-g$) are indicated above the sequences.

(A) The CYCLOPS zipper (homodimeric CC formation between two helices of amino acid 450-515) contains 9 heptad repeats (R1-9). Upper panel: CC formation is supported by hydrophobic interactions between amino acids in positions $a+d$ and $d+e$. Charged amino acids in position $e+g$ and $a+g$ interact electrostatically to form interhelical salt bridges. R5 does not contain a hydrophobic core, but is instead stabilized by a network of salt bridges and hydrogen bondings. Lower panel: Mutagenesis of the CYCLOPS zipper. Amino acids in the d position of R1-8 (mR1-8) were substituted by glutamate to destabilize (white boxes) or leucine to stabilize (black box) the zipper interface, respectively.

(B) CC formations between CYCLOPS and bZIP110 (amino acid 55-121) or *At* bZIP63 (amino acid 176-238) were predicted *in silico*. Heptad repeats were aligned by the maximal number of productive hydrophobic interactions between amino acids in position $a+d$ and salt bridges between $e+g$ ($i+5$). Although both heterodimers contain two repulsive interactions, zipper formation with *At* bZIP63 is less stable compared to bZIP110 because of a destabilized central region.

(C) Schematic illustration of the bZIP110 protein domain structure. The basic region (B) and the leucine zipper domain (LZ) are shown as black and white boxes, respectively. N- and C-terminus are indicated. Bar size indicates 50 amino acids.

(D) Genomic structure of the *bZIP110* gene containing the coding sequence (black box) and 5'- and 3'-untranslated regions (UTRs) (black line). Insertion site of the LORE1 mutant line is marked by a triangle. Positions of primers used for qPCR analysis are indicated. Bar length represents 250 base pairs. TSS: translational start site.



	#1
Wavelength (Å...)	0.9794
Resolution range (Å...)	39.8 - 2.498 (2.587 - 2.498) ^a
Space group	C 1 2 1
Unit cell	161.727 29.856 32.321 90 100.15 90
Total reflections	35168 (3285) ^a
Unique reflections	5445 (508) ^a
Multiplicity	6.5 (6.5) ^a
Completeness (%)	99.60 (97.32) ^a
Mean I/sigma(I)	17.65 (4.52) ^a
Wilson B-factor	36.09
R-merge	0.08871 (0.4132) ^a
R-meas	0.09648
CC1/2	0.999 (0.961) ^a
CC*	1 (0.99) ^a
Reflections used for R-free	
R-work	0.2234 (0.3080) ^a
R-free	0.2752 (0.4289) ^a
CC(work)	
CC(free)	
Number of non-hydrogen atoms	1068
macromolecules	1056
ligands	
water	12
Protein residues	132
RMS(bonds)	0.010
RMS(angles)	1.08
Ramachandran favored (%)	1e+02
Ramachandran allowed (%)	
Ramachandran outliers (%)	0
Clashscore	1.42
Average B-factor	41.10
macromolecules	41.10
ligands	
solvent	37.80

Table 1. Data Collection and Refinement Statistics.

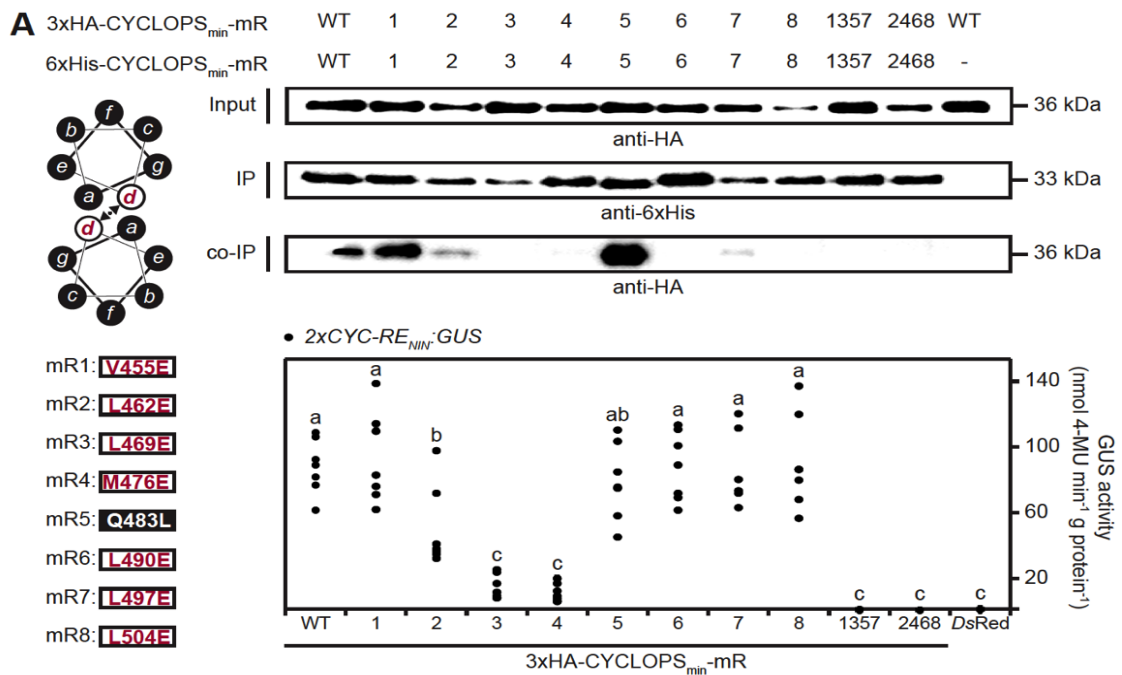
Data collection and refinement statistics were performed by J. Basquin.

^aStatistics for the highest-resolution shell are shown in parentheses.

5. The Coiled-Coil Domain of CYCLOPS Homodimerizes *in planta*

Because *in vitro* crystallization can lead to artificial protein-protein interactions, homodimerization of the CYCLOPS CC needs to be verified *in planta*. To test the validity of the interaction sites observed in the crystal, point mutations were specifically introduced into the CYCLOPS zipper to produce productive or repulsive interactions, which support or impair homodimer formation, respectively. The corresponding CC versions were called mR1-8 referring to the position of the mutation in the heptad repeat succession (Figure 9A). Position *d* of the hydrophobic core contributes the most to the thermodynamic stability of zipper domains (Moitra et al., 1997), thus, introduction of a polar glutamic acid residue (mR1-4, 6-8) should lead to repulsive interactions, while replacement to a hydrophobic leucine (mR5) should stabilize the homodimer. To completely disrupt the CYCLOPS zipper interaction, two additional versions were generated in which all even or uneven numbers of repeats (mR1357 and mR2468) were mutated in position *d*.

CYCLOPS homodimerization was analyzed by co-immunopurification (co-IP) using extracts of *N. benthamiana* leaves co-expressing WT or mutant 3xHA- together with 6xHis-CYCLOPS_{min} versions (Figure 10A). A minimal CYCLOPS version comprising the AD and BD (CYCLOPS_{min}) was used to remove potential effects of predicted CCs in the regulatory N-terminal domain (Figure 8C). While 3xHA-CYCLOPS_{min} was co-immunopurified with 6xHis-CYCLOPS_{min}, all zipper mutants except mR1, mR2 and the stabilizing amino acid exchange in mR5 significantly reduced the ability of CYCLOPS_{min} to dimerize *in planta*. Thus, the results of the *in vivo* binding assays verified that the homodimeric CC structure formed in the crystal also occurs in the context of the larger CYCLOPS_{min} version *in planta*. Homodimerization was further confirmed by chemical cross-linking *in vitro* (Figure 11A), showing that 6xHis-CYCLOPS_{min} formed dimeric and higher oligomeric complexes in solution when treated with BS³ (bis[sulfosuccinimidyl] suberate) cross-linker.



B *cyclops-3*, *M. loti* DsRed 4 wpi

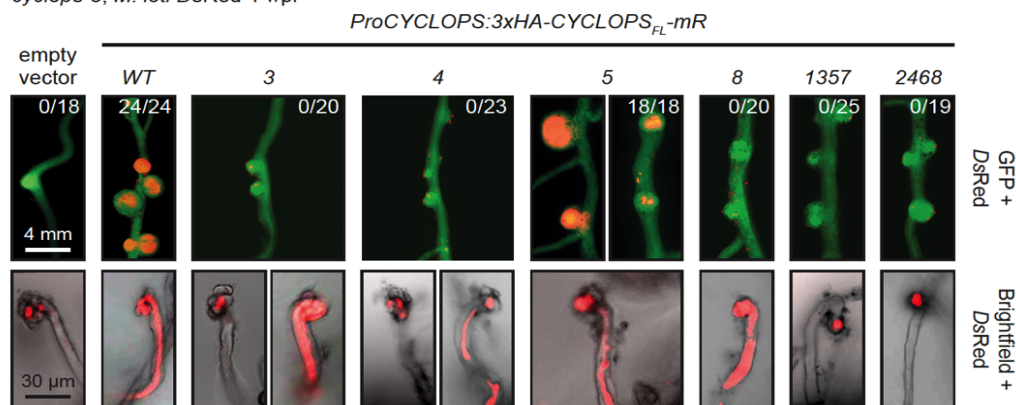


Figure 10. Homo- and Heterodimerization of the CYCLOPS Zipper.

(A-B) Site-directed mutagenesis of the CYCLOPS zipper. To confirm the crystal structure of the CYCLOPS zipper, hydrophobic amino acids in position *d* of the heptad repeats (illustrated by a helical wheel diagram) were mutagenized to polar glutamate residues in mR1-4 and mR6-8 (indicated by ruby letters in white boxes), which was predicted to induce repulsive electrostatic interactions to destabilize the zipper (shown as dotted line with opposing arrow heads). As a control, the *d* position in mR5 was mutagenized to leucine (indicated by white letters in black box), which was predicted to stabilize the hydrophobic core of the zipper.

(A) Analyses of the CYCLOPS zipper mutants in *N. benthamiana*. Leaves were transformed with the indicated versions expressed under the 35S promoter 60 hpi. Upper panel: Protein-protein interaction analysis by co-IP from leaf extracts using an anti-6xHis antibody. Dimerization was tested between two differentially tagged CYCLOPS_{min} versions indicated above each lane of the protein blot. Except for CYCLOPS_{min}-mR1, 2 and 5, site-directed mutagenesis of the zipper abolished CYCLOPS_{min} dimerization *in planta*. Protein blots of Input (10 % of the amount used for co-immunopurification), IP and co-IP samples were detected with anti-HA and anti-6xHis antibodies as indicated. Protein sizes are shown. Lower panel: Transactivation of a 2xCYC-RE_{NIN}:GUS reporter. All CYCLOPS_{min} versions impaired in homodimerization were transcriptionally inactive, except CYCLOPS_{min}-mR6-8, which indicates that dimer formation may be restored by interaction with other plant CC proteins. T-DNA encoding *DsRed* was used as negative control. GUS activities (nmol 4-MU min⁻¹ g protein⁻¹) were quantified by MUG fluorimetric assay. Letters indicate different statistical groups (ANOVA, post hoc Tukey; $p \leq 0.05$; $n = 87$).

Previous yeast-two hybrid interaction studies of CYCLOPS deletion series have delimited a central region (amino acid 81-366) necessary for dimerization (Yano et al., 2008). To test if the CYCLOPS CC is required for homodimerization of the full-length protein, a version deleted in this region (CYCLOPS_{ΔCC}) was generated. Homodimerization of CYCLOPS_{ΔCC} was confirmed by co-IP assays from *N. benthamiana* leaf extracts and bimolecular fluorescence complementation (BiFC) (Figure 11B and 12A). However, although CYCLOPS homodimerization still occurred in the absence of the C-terminal zipper, the amount of co-immunopurified protein was significantly reduced compared to interaction between full-length 6xHis-CYCLOPS and 3xHA-CYCLOPS (Figure 11B), showing that this region contributes to but is not the only dimerization domain of CYCLOPS.

6. CYCLOPS Dimerization is Required for DNA-Binding

The palindromic *CYC-RE_{NIN}* sequence suggested that CYCLOPS binds this target as a dimer of which each CYCLOPS-BD contacts one half of the palindromic sequence repeat (Singh et al., 2014) and indeed DNA-binding of many zipper-containing transcriptional regulators is dependent on a functional dimerization interface (Pogenberg et al., 2014). To analyze whether DNA-binding of CYCLOPS requires homodimerization, CYCLOPS_{min} mutants, which were incapable to dimerize (Figure 10A), were tested in electrophoretic mobility shift assays (EMSAs). 6xHis-CYCLOPS_{min} caused a shift of CY5-labeled *4Pal8* probe, a deletion version of the *CYC-RE_{NIN}* comprising the palindromic sequence surrounded by 4 and 8 bp to the 5' and 3' end, respectively (Figure 11C). In contrast, binding of 6xHis-CYCLOPS_{min}-mR4 and mR1357 to *4Pal8* was not detected.

(B) Complementation of *L. japonicus cyclops-3* mutant roots with the coding sequence of WT or CC mutated 3xHA-CYCLOPS_{FL} (all expressed under control of the 2.4 kb *CYCLOPS* promoter) and the empty vector control. Transformed roots were inoculated with *DsRed*-tagged *M. loti* and the nodulation phenotype was analyzed 4 wpi for infected root nodules and IT formation. RNS was restored by 3xHA-CYCLOPS_{FL}-WT and -mR5 (around 65 % of the nodules were smaller and partially infected, 35 % were mature and fully infected). ITs were initiated in 3xHA-CYCLOPS_{FL}-mR8 and occasionally in mR3 and mR4 transformed roots but got prematurely arrested, inferring the existence of heterodimeric interaction partner. The nodulation phenotype is presented as overlay images recorded with GFP (indicates transformed plant roots) and *DsRed* filter. IT formation is shown as overlay of brightfield images and micrographs recorded with *DsRed* filter. Numbers indicate root systems with infected root nodules per number of total root systems analyzed. Bar sizes with identical magnification for all images are presented inside the figure.

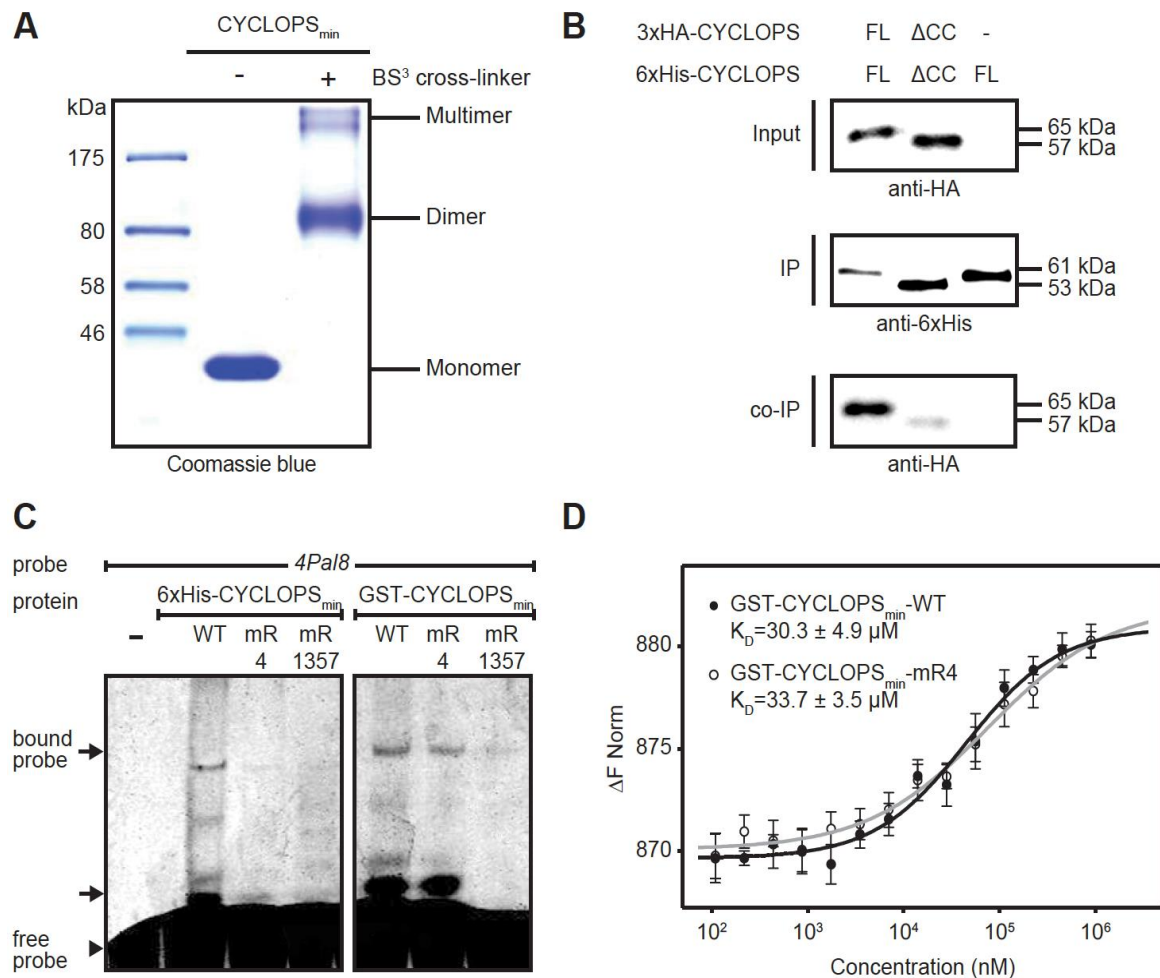


Figure 11. Homodimerization Analyses of the CYCLOPS Zipper Domain.

(A) Chemical cross-linking of 6xHis-CYCLOPS_{min} showed dimer and higher oligomeric complex formations *in vitro*. Cross-linking was performed with BS³ (bis[sulfosuccinimidyl] suberate) crosslinker for 5 min at room temperature with 2.9 nmol protein. Samples were separated by SDS-PAGE and Coomassie stained. Molecular weight marker is indicated.

(B) Protein-protein interaction analyses by co-IP from extracts of *N. benthamiana* leaves co-transformed with the indicated versions expressed under the 35S promoter 60 hpi using anti-His antibody (as described in Figure 10). Homodimerization of CYCLOPS_{ΔCC} lacking the C-terminal zipper domain is significantly reduced compared to CYCLOPS_{FL}.

(C-D) DNA-binding ability of CYCLOPS depends on a functional zipper domain.

(C) EMSAs were performed using 100 pmol protein and CY5-labeled 4Pal8 (0.1 pmol) as probe. Compared to 6xHis-CYCLOPS_{min}-WT, 6xHis-CYCLOPS_{min}-mR4 and -mR1357 were impaired in DNA-binding. GST-tag-mediated dimerization could restore DNA-binding of CYCLOPS_{min}-mR4 but not of CYCLOPS_{min}-mR1357. An arrow and an arrowhead indicate positions of bound and free probe, respectively. Samples were resolved on 6 % polyacrylamid gels.

(D) MST demonstrating similar DNA binding affinities of GST-CYCLOPS_{min}-WT (black dots and line) and GST-CYCLOPS_{min}-mR4 (white dots and gray line). MST was performed with 25 nM 5'-CY5 labeled 4Pal8 and increasing amounts of protein (from 109 nM to 896 μM). Average thermophoresis values and standard deviations of three experimental replicates are shown. A K_D-value of 30.3 ± 4.9 μM and 33.7 ± 3.5 μM was calculated for GST-CYCLOPS_{min}-WT and GST-CYCLOPS_{min}-mR4, respectively.

Importantly, an N-terminal fusion to glutathione S-transferase (GST), carrying an intrinsic dimerization domain (Riley et al., 1996), rescued binding of 6xHis-CYCLOPS_{min}-mR4 to the labeled probe, confirming that DNA affinity of CYCLOPS is based on its ability to dimerize. Binding of CYCLOPS_{min}-mR1357 instead was only insufficiently restored by GST-mediated dimerization, possibly due to conformational changes that prevented DNA-binding. Using MST, DNA-binding affinities were measured (Figure 11D). K_D -values of $30.3 \pm 4.9 \mu\text{M}$ and $33.7 \pm 3.5 \mu\text{M}$ were calculated for GST-CYCLOPS_{min}-WT and GST-CYCLOPS_{min}-mR4, respectively, showing low DNA-binding affinity, which either suggests non-optimal *in vitro* conditions or cooperative binding with other TFs *in vivo*. The K_D -values of 6xHis-CYCLOPS_{min}-WT and -mR4 could not be obtained due to limitations in protein concentrations.

7. Homo- and Heterodimerization of the CYCLOPS Zipper Determine Root Symbiotic Development

Singh *et al.*, 2014 have shown that CYCLOPS_{min} is sufficient to transactivate via the *CYC-RE_{NIN}*. To test if transactivation requires CYCLOPS_{min} dimerization, assays were performed using *N. benthamiana* leaves co-transformed with WT or zipper-mutated *CYCLOPS_{min}* versions and a *2xCYC-RE_{NIN}:GUS* reporter (Figure 10A). CYCLOPS_{min}-mR2, 3, 4, 1357 and 2468, which were decreased or impaired in homodimerization, also caused a significantly reduced reporter transactivation, while CYCLOPS_{min}-mR1 and 5, which were not affected in homodimerization, showed GUS expression similar to WT levels. Surprisingly, CYCLOPS_{min}-mR6, 7, and 8, which did not homodimerize, still fully transactivated the reporter. Since the DNA affinity of CYCLOPS was very low and zipper-dependent (Figure 11C), these results suggest that introduction of a polar glutamate residue in mR6-8 may have impaired homodimerization, while heterodimerization with other plant transcriptional activators was still feasible and sufficient to mediate binding and transactivation of the *2xCYC-RE_{NIN}:GUS* reporter in *N. benthamiana* leaves.

To examine the role of CYCLOPS homo- and heterodimerization during RNS, zipper amino acids replacements analyzed in Figure 10A (homodimerization/transactivation: +/+, -/-, -/+) were introduced into full-length *CYCLOPS* (*CYCLOPS_{FL}*) and tested for complementation of the *L. japonicus cyclops-3* mutant phenotype.

Hairy roots expressing the different versions were inoculated with *M. loti* containing *DsRed* (Figure 10B). Amino acid replacement in mR3, 4, 8, 1357 and 2468 of the zipper prevented *3xHA-cCYCLOPS_{FL}* to restore RNS, and a *cyclops-3*-like mutant phenotype was retained characterized by uninfected nodule primordia with surface attached rhizobia and aborted ITs or unsuccessful IT initiation attempts (Figure 10B). By contrast, *3xHA-cCYCLOPS-mR5* containing a zipper-stabilizing amino acid replacement, maintained CYCLOPS' function. Strikingly, roots transformed with *3xHA-cCYCLOPS-mR3, 4* and *8* occasionally initiated IT growth but aborted early in its development, indicating that these zipper mutants can form heterodimers with other plant CC proteins during early stages of the symbiosis sufficient to initiate IT growth, while heterodimerization with zipper-proteins at later stages was impaired, leading to a premature arrest of infection and nodule organogenesis. Taken together, these findings led to the hypothesis that cell-type-specific gene expression during root symbiotic development may be governed by zipper-dependent heterodimerization of CYCLOPS.

8. CYCLOPS Interacts with Plant bZIP Transcriptional Regulators

To identify interaction partners of CYCLOPS, we investigated the structural properties of the CYCLOPS zipper. Important criteria used to define CC heterodimerization are the number of heptad repeats and the amino acid composition at the specificity determining *e* and *g* positions (Vinson et al., 2002). We screened the *L. japonicus* genome for CC proteins with nine heptad repeats and among the 16 candidates, one was independently identified in a yeast-two-hybrid screen (B. Fussbroich, unpublished data) to interact with a truncated version of CCaMK (CCaMK¹⁻³⁵¹). The protein belongs to the bZIP family and was named bZIP110 after the closest homolog and thus potential ortholog from *G. max* (R.E. Andrade, unpublished data). bZIP110 is classified as S-group member according to the nomenclature established by Jakoby *et al.*, 2002 for *A. thaliana* bZIPs because of its small size (17.7 kDa, amino acid 1-157) and single exon number encoding a central bZIP domain of nine heptad repeats with small N- and C-terminal extensions (Figure 9C-D).

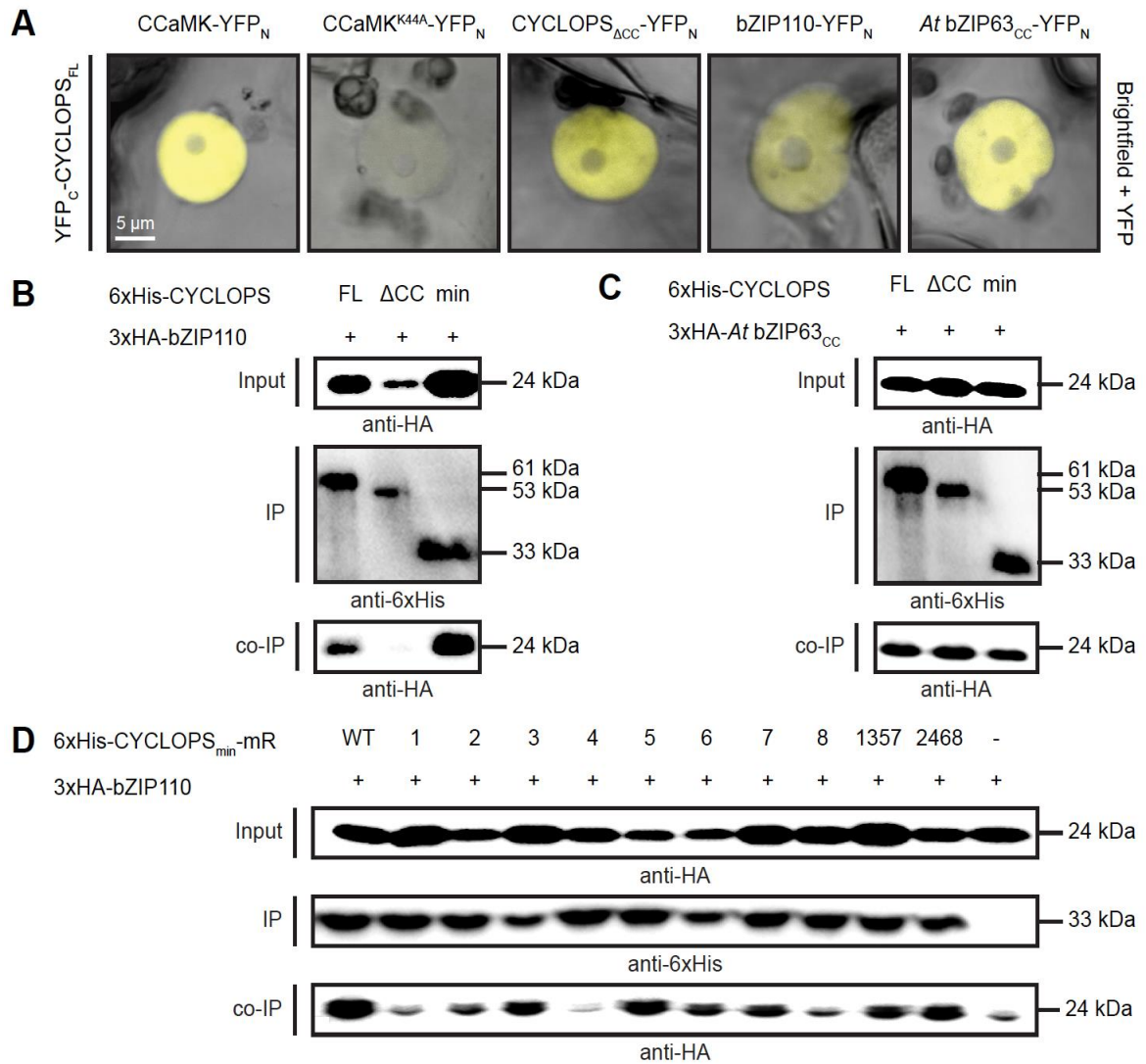


Figure 12. Interaction between CYCLOPS and Plant bZIP Transcriptional Regulators.

(A) Heterodimerization of CYCLOPS and bZIP transcriptional regulators was confirmed by BiFC in *N. benthamiana*. Leaves were co-transformed with YFP_C-CYCLOPS_{FL} and CCaMK-YFP_N (positive control), CCaMK^{K44A}-YFP_N (negative control), CYCLOPS-1-449 (CYCLOPS_{ΔCC})-YFP_N, bZIP110-YFP_N or At bZIP63_{CC}-YFP_N expressed under the 35S promoter 60 hpi. YFP fluorescence (shown in yellow) indicates interaction. YFP_N: N-terminal half of YFP, YFP_C: C-terminal half of YFP. Images represent merged overlays of brightfield pictures and micrographs recorded with a YFP filter. Bar size with identical magnification for all images is presented inside the figure.

(B-D) Protein-protein interaction analyses by co-IP from extracts of *N. benthamiana* leaves co-transformed with the indicated versions expressed under the 35S promoter 60 hpi using an anti-6xHis antibody (as described in Figure 10). Protein sizes are shown.

(B-C) Rough mapping of CYCLOPS interaction domains with plant bZIP transcriptional regulators. 6xHis-CYCLOPS_{FL}, 6xHis-CYCLOPS_{ΔCC} or 6xHis-CYCLOPS_{min} were co-transformed with 3xHA-bZIP110 (B) or 3xHA-At bZIP63_{CC} (C). bZIP110 specifically interacted with the C-terminal CC domain of CYCLOPS, while heterodimerization with At bZIP63_{CC} was narrowed down to the N-terminal part.

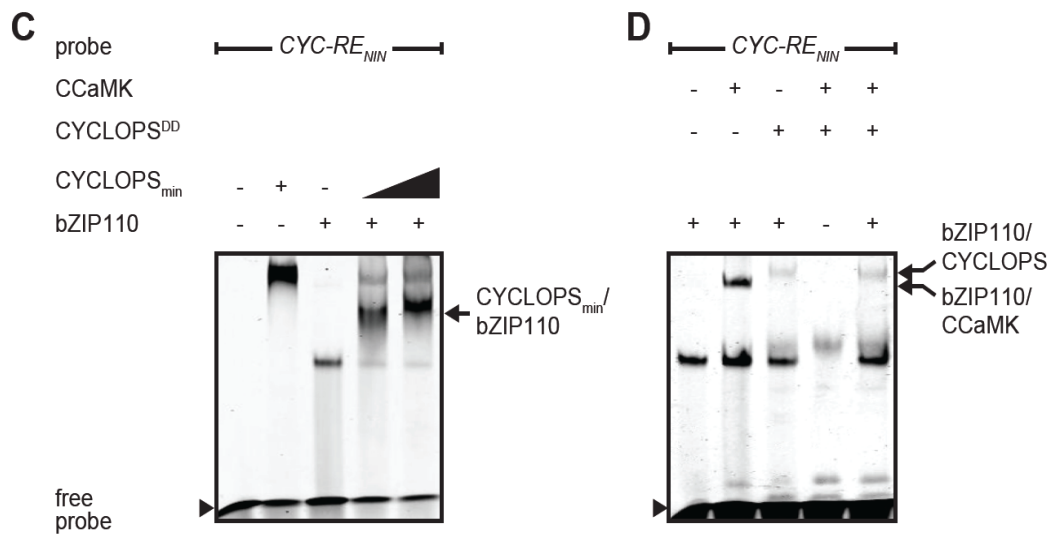
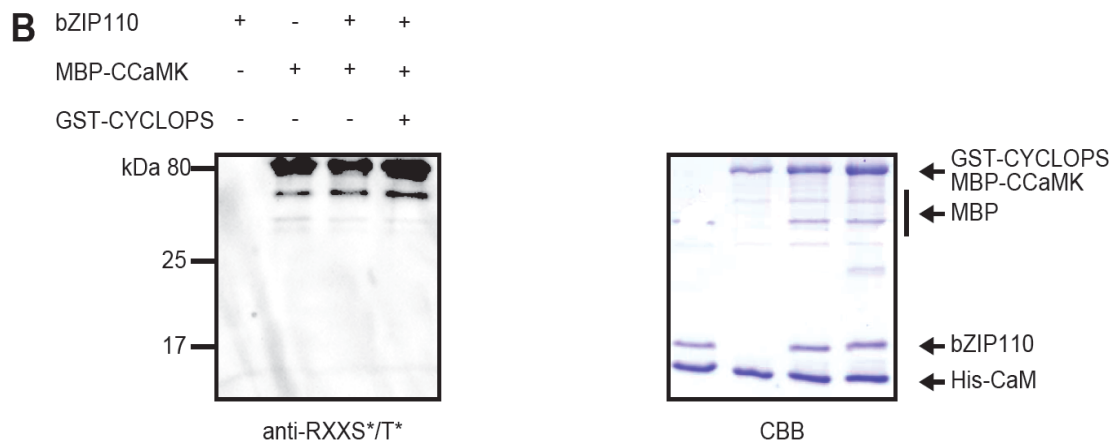
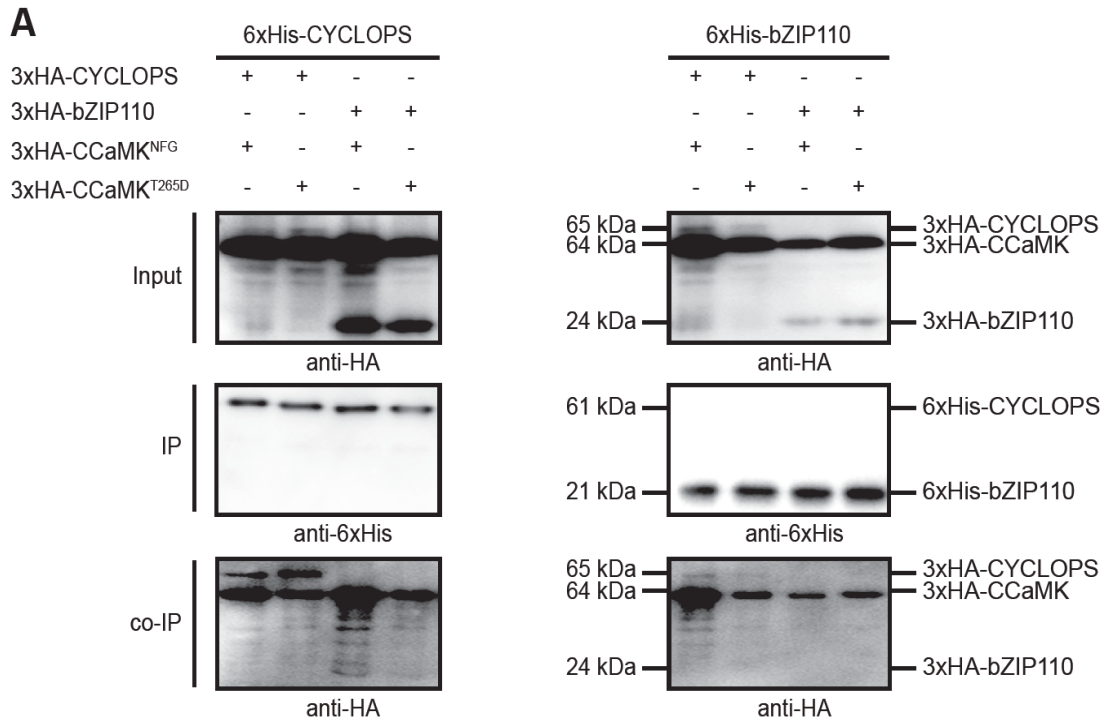
(D) Sequence-specific interaction between bZIP110 and the C-terminal helix of CYCLOPS. Site directed mutagenesis in 6xHis-CYCLOPS_{min}-mR1, 2, 4 and 8 significantly reduced heterodimerization with 3xHA-bZIP110 compared to 6xHis-CYCLOPS_{min}-WT.

A phylogenetic analysis of S-group bZIP amino acid sequences from different legume and non-legume species revealed that bZIP110 is legume-specific (R.E. Andrade, unpublished data). Interaction of bZIP110 and CYCLOPS was predicted *in silico* based on intermolecular hydrophobic interactions between amino acids in position $a+d$ and productive or repulsive salt bridges between position $e+g$ ($i+5$) of the CC regions (Figure 9B) and was confirmed by fluorescence lifetime imaging microscopy (FLIM)-FRET measurements (C. Cathebras, unpublished data), co-IP analyses and BiFC in *N. benthamiana* leaves (Figure 12). Moreover, bZIP110 specifically heterodimerized with the C-terminal CC of CYCLOPS, since 6xHis-CYCLOPS $_{\Delta CC}$ and 6xHis-CYCLOPS $_{min-mR1, 2, 4 \text{ and } 8}$ were significantly reduced in heterodimerization with 3xHA-bZIP110 by co-IP assays from *N. benthamiana* leaf extracts (Figure 12B and D). As a control, the CC region of bZIP63 from *A. thaliana* (*At* bZIP63 $_{CC}$) was tested, which also contains nine heptad repeats, but was *in silico* predicted to not associate with the C-terminal CC of CYCLOPS due to the absence of productive bondings in the central zipper region (Figure 9B). Interaction between CYCLOPS and *At* bZIP63 $_{CC}$ was detected by BiFC and co-IP experiments in *N. benthamiana* leaves, but was narrowed down to the N-terminal part of CYCLOPS (Figure 12A and C).

9. CCaMK/CYCLOPS Form a Preassembled Complex with bZIP110 on the *CYC-RE_{MIN}*

Because bZIP110 was identified as an interactor of both CCaMK and CYCLOPS, we analyzed if (i) a trimeric complex is formed, (ii) bZIP110 prevents CCaMK/CYCLOPS interaction or (iii) bZIP110 is released from the complex upon binding of CYCLOPS to CCaMK or activation of CCaMK. Co-expressed and co-purified Strep-CYCLOPS, 6xHis-CCaMK and MBP-bZIP110 from *E. coli* coeluted as a high molecular weight oligomeric complex of a size of around 700-800 kDa (V. Gimenez Oya, unpublished data). Heterodimerization of 6xHis-bZIP110 with 3xHA-CCaMK and 3xHA-CYCLOPS was further confirmed by co-IP assays from *N. benthamiana* leaf extracts (Figure 13A). Moreover, 3xHA-bZIP110 appeared to have a higher stability when being co-expressed with 6xHis-CYCLOPS compared to 6xHis-bZIP110 and preferred heterodimerization with CYCLOPS and CCaMK over homodimerization (Figure 13A). Together these results show that CCaMK/CYCLOPS and bZIP110 form a trimeric complex.

To monitor if critical conformational changes undergo upon CCaMK activation, FLIM measurements were performed in nuclei of *N. benthamiana* leaf cells (C. Cathebras, unpublished data). Two gain-of-function versions of CCaMK were used: the kinase-only CCaMK (3xHA-CCaMK³¹⁴) and a deregulated construct substituted at an inhibitory autophosphorylation site (3xHA-CCaMK^{T265D}). As kinase inactive version of CCaMK, a construct mutated in the conserved DFG motif within the activation-loop of protein kinases was generated (3xHA-CCaMK^{NFG}), which is still capable to interact with CYCLOPS (Figure 13A; C. Cathebras, unpublished data). Strong reduction of fluorescence lifetime resulted from FRET between bZIP110 and CCaMK or CYCLOPS, confirming previous *in vitro* protein-protein interaction analyses (C. Cathebras, unpublished data). Furthermore, phosphomimetic substitution at two critical serines in CYCLOPS^{DD} did not disrupt heterodimer formation with bZIP110 (C. Cathebras, unpublished data). Strikingly, in the presence of untagged CCaMK^{T265D} and CCaMK³¹⁴, FRET was slightly decreased between CYCLOPS and bZIP110, revealing conformational alterations within the complex, while there were no changes in fluorescence lifetime in the presence of kinase-inactive CCaMK^{NFG} (C. Cathebras, unpublished data). As negative and positive controls, FLIM-FRET was measured in the presence of free mCherry or between CCaMK/CYCLOPS or CCaMK/CYCLOPS^{DD}, respectively. These results indicate that upon activation of CCaMK by Ca²⁺/CaM-binding, bZIP110 is not released from the complex but rather structural rearrangements are induced. In agreement with this, size-exclusion chromatography revealed no stoichiometrical changes of the trimeric complex in the presence of deregulated 6xHis-CCaMK^{T265D} (V. Gimenez Oya, unpublished data) and co-IP analyses from *N. benthamiana* leaf extracts showed that heterodimerization of 6xHis-bZIP110 with 3xHA-CCaMK and 3xHA-CYCLOPS was independent of the kinase activity of CCaMK (Figure 13A). Potential phosphorylation of bZIP110 by CCaMK was examined by *in vitro* kinase assays but no phosphorylation was identified by mass spectrometry and by western blotting using a phospho-specific antibody, while the MBP-tag as control was phosphorylated by CCaMK (Figure 13B).



MST analyses revealed a low DNA-binding affinity of CYCLOPS (Figure 11D). Since interaction between TFs can improve DNA-binding affinity (Flammer et al., 2006), we analyzed by EMSA if a heterodimeric CYCLOPS/bZIP110 complex is formed on the *CYC-RE_{NIN}*. Homodimeric GST-CYCLOPS_{min} and MBP-bZIP110 alone caused a band-shift of labeled probe, while combination of both proteins resulted in an intermediate band and reduction of the homodimeric bands, indicating heterodimerization of CYCLOPS/bZIP110 on the *CYC-RE_{NIN}* (Figure 13C). To see if CCaMK is stably associated with CYCLOPS/bZIP110 bound to target DNA elements, EMSA was carried out in the presence of CCaMK. MBP-bZIP110 caused a mobility shift with MBP-CCaMK or GST-CYCLOPS, showing higher-order DNA-complexes (Figure 13D). However, combination of all three proteins abolished heterodimeric interaction between bZIP110 and CCaMK, but did not reveal an additional shift, which may be accounted for by the resolution limit of the gel. Together these results indicate that CCaMK/CYCLOPS form a preassembled, transcriptional complex on the *CYC-RE_{NIN}*.

Figure 13. bZIP110 Forms a Trimeric Complex with CCaMK/CYCLOPS Bound to DNA.

(A) Protein-protein interaction analyses by co-IP from extracts of *N. benthamiana* leaves co-transformed with the indicated versions expressed under the 35S promoter 60 hpi using an anti-6xHis antibody (as described in Figure 10). Homo- and heterodimerization between bZIP110 and CYCLOPS was compared in the presence of 3xHA-CCaMK^{T265D} or 3xHA-CCaMK^{NFG}. Heterodimerization of bZIP110 with CCaMK or CYCLOPS was favoured over homodimerization and increased stability of bZIP110 *in planta*. However, co-IP of CCaMK, CYCLOPS and bZIP110 was independent of the kinase activity of CCaMK. Proteins and corresponding sizes are indicated. (B) *In vitro* kinase assay of bZIP110. *In vitro* phosphorylation of bZIP110 (18 kDa) by MBP-CCaMK (96 kDa) was tested in the absence or presence of GST-CYCLOPS (86 kDa) (as indicated). The MBP-tag (40 kDa) of MBP-bZIP110 was cleaved by a HRV 3C protease prior to the kinase assay. Left panel: Protein blot probed with anti-RXXS/T antibody. Right panel: Coomassie blue (CBB) staining. Proteins are indicated by an arrow and molecular weight marker is shown. His-CaM: 6xHis-tagged Calmodulin.

(C-D) bZIP110 forms higher-order DNA-complexes with CYCLOPS and CCaMK bound to *CYC-RE_{NIN}*. EMSAs were performed using MBP-bZIP110 (10 pmol), GST-CYCLOPS_{min} (50 and 100 pmol), GST-CYCLOPS^{DD} (100 pmol), MBP-CCaMK (100 pmol) and CY5-labeled *CYC-RE_{NIN}* (0.1 pmol) as probe. Free probe and positions of heterodimeric complexes are indicated by an arrowhead or arrow, respectively. Samples were resolved on 6 % (B) or 4 % (C) polyacrylamid gels.

(C) Homodimeric bZIP110 or CYCLOPS_{min} bound to *CYC-RE_{NIN}*. An intermediate mobility shift of heterodimeric CYCLOPS_{min}/bZIP110 was revealed upon mixing of both proteins.

(D) bZIP110/CYCLOPS or bZIP110/CCaMK form trimeric complexes with the *CYC-RE_{NIN}*. Although heterodimeric interaction between bZIP110 and CCaMK was lost upon combination of all three proteins, no additional shift indicating complex formation of CCaMK/CYCLOPS/bZIP110 was observed, which is probably caused by the resolution limit of the gel.

10. Heterodimerization with bZIP110 Specifically Anchors CYCLOPS to *CYC-REs* of Nodulation Promoters.

Homodimeric and heterodimeric CYCLOPS and bZIP110 complexes were indicated by EMSA (Figure 13C). The affinity of both TFs to target *cis*-elements was determined by surface plasmon resonance (SPR) analysis (R. Heermann, unpublished data). Because CYCLOPS is involved in the transcriptional regulation of both RNS and AM, binding to the nodulation-specific elements *CYC-RE_{NIN}* and *CYC-RE_{ERNI}* and the AM-specific target *CYC-RE_{RAMI}* was analyzed (Cerri et al., 2017; Pimprikar et al., 2016; Singh et al., 2014). Although weak attachment of co-expressed 6x-His-CCaMK/Strep-CYCLOPS complex to the tested *CYC-REs* was observed, no affinity constant could be calculated, supporting the low affinity K_D value (μM -range) determined by MST for GST-CYCLOPS_{min} (Figure 11D). In contrast, MBP-tagged bZIP110 bound to the *CYC-REs* with a much higher affinity ($K_D = 169\text{-}256\text{ nM}$) (R. Heermann, unpublished data). However, when both proteins were mixed in equal stoichiometry it was not possible to measure the affinity of the heterodimeric complex, possibly due to the low heterodimer to homodimer ratio formed under the applied *in vitro* conditions, which was also observed in EMSAs (Figure 13D). Interestingly, EMSA revealed a preference of MBP-bZIP110 for the nodulation-specific *CYC-RE_{NIN}* over the AM-specific *CYC-RE_{RAMI}* element (Figure 14). Binding of MBP-bZIP110 to labeled *CYC-RE_{RAMI}* probe could be out-competed by 40-fold excess of unlabeled *CYC-RE_{NIN}* in EMSA, while 40-fold excess of unlabeled *CYC-RE_{RAMI}* was not sufficient to out-compete the binding to labeled *CYC-RE_{NIN}* probe. Furthermore, 20x more MBP-bZIP110 protein was required to induce a mobility shift with the *CYC-RE_{RAMI}* compared to the *CYC-RE_{NIN}* probe in EMSA, which is in agreement with the low response units (RUs) observed by SPR for this element (R. Heermann, unpublished data). These results suggest that CYCLOPS is specifically anchored to nodulation-specific target promoters by heterodimerization with bZIP110.

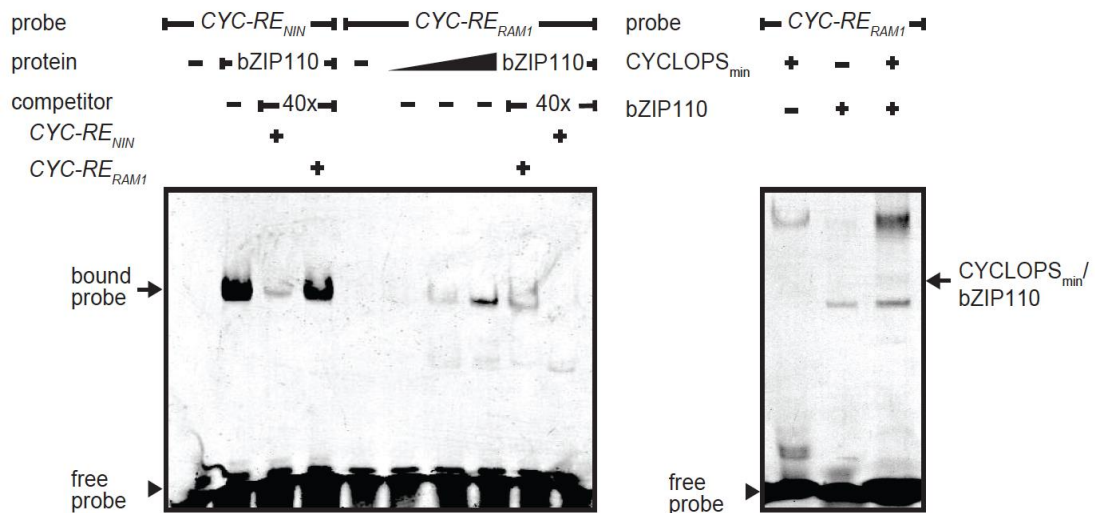


Figure 14. bZIP110 Preferentially Binds to Nodulation- over AM-Specific Promoter Elements. Preferential binding of bZIP110 to $CYC-RE_{NIN}$ was shown by EMSA. Left panel: Binding of MBP-bZIP110 (10 pmol) to CY5-labeled $CYC-RE_{NIN}$ (0.1 pmol) can be outcompeted by 40-fold excess of unlabeled $CYC-RE_{NIN}$ but not $CYC-RE_{RAM1}$. Increasing amounts of MBP-bZIP110 (10, 200 and 400 pmol) were applied to induce a mobility shift with CY5-labeled $CYC-RE_{RAM1}$ (0.1 pmol). Binding of MBP-bZIP110 (400 pmol) to CY5-labeled $CYC-RE_{NIN}$ (0.1 pmol) can be outcompeted by 40-fold excess of unlabeled $CYC-RE_{NIN}$ and $CYC-RE_{RAM1}$. Right panel: Only a slight mobility shift of heterodimeric GST-CYCLOPS_{min} (100 pmol) and MBP-bZIP110 on $CYC-RE_{RAM1}$ was revealed by EMSA (indicated by an arrow). An arrow and an arrowhead show positions of bound and free probe, respectively. Samples were resolved on 6 % polyacrylamid gels.

11. CYCLOPS-Mediated Transactivation is Inhibited by Heterodimerization with bZIP110.

To test the influence of bZIP110 on CCaMK/CYCLOPS complex activity, transactivation assays were performed in *N. benthamiana* leaves co-transformed with deregulated CYCLOPS versions and a $2xCYC-RE_{NIN}:GUS$ reporter. In the presence of 3xHA-bZIP110, 3xHA-CYCLOPS^{DD}- or 3xHA-CYCLOPS_{min}-mediated $2xCYC-RE_{NIN}:GUS$ transactivation was significantly decreased (Figure 16). In contrast, no reporter inhibition was observed using a mutated version of bZIP110 (mbZIP110), in which I114 in position *d* was exchanged to a destabilizing glutamate. Neither 3xHA-bZIP110 nor 3xHA-mbZIP110 alone elicited *GUS* expression. bZIP110-mediated inhibition via $CYC-RE_{NIN}$ was also observed in *L. japonicus* roots (Figure 15). Gifu WT plants were co-transformed with a T-DNA containing the $2xCYC-RE_{NIN}:GUS$ reporter alone or $ProUbi:CYCLOPS^{DD}+2xCYC-RE_{NIN}:GUS$ (visualized by a *GFP* transformation marker) and a T-DNA expressing $ProUbi:bZIP110$ or the empty vector (visualized by a *mCherry* transformation marker).

Co-transformation of two independent T-DNAs frequently resulted in root systems with differentially transformed roots with either one or both T-DNAs. These mosaic roots provided ideal internal controls for the study of the local effect of bZIP110 on *CYCLOPS*^{DD}-mediated *2xCYC-RE_{NIN}:GUS* activation. Expression of *ProUbi:bZIP110* did not induce the *2xCYC-RE_{NIN}:GUS* reporter. Only in part of the roots co-transformed with *ProUbi:CYCLOPS*^{DD}+*2xCYC-RE_{NIN}:GUS* and the empty vector, but not with *ProUbi:bZIP110*, *CYCLOPS*^{DD}-mediated activation of the *2xCYC-RE_{NIN}:GUS* and spontaneous nodule formation were observed.

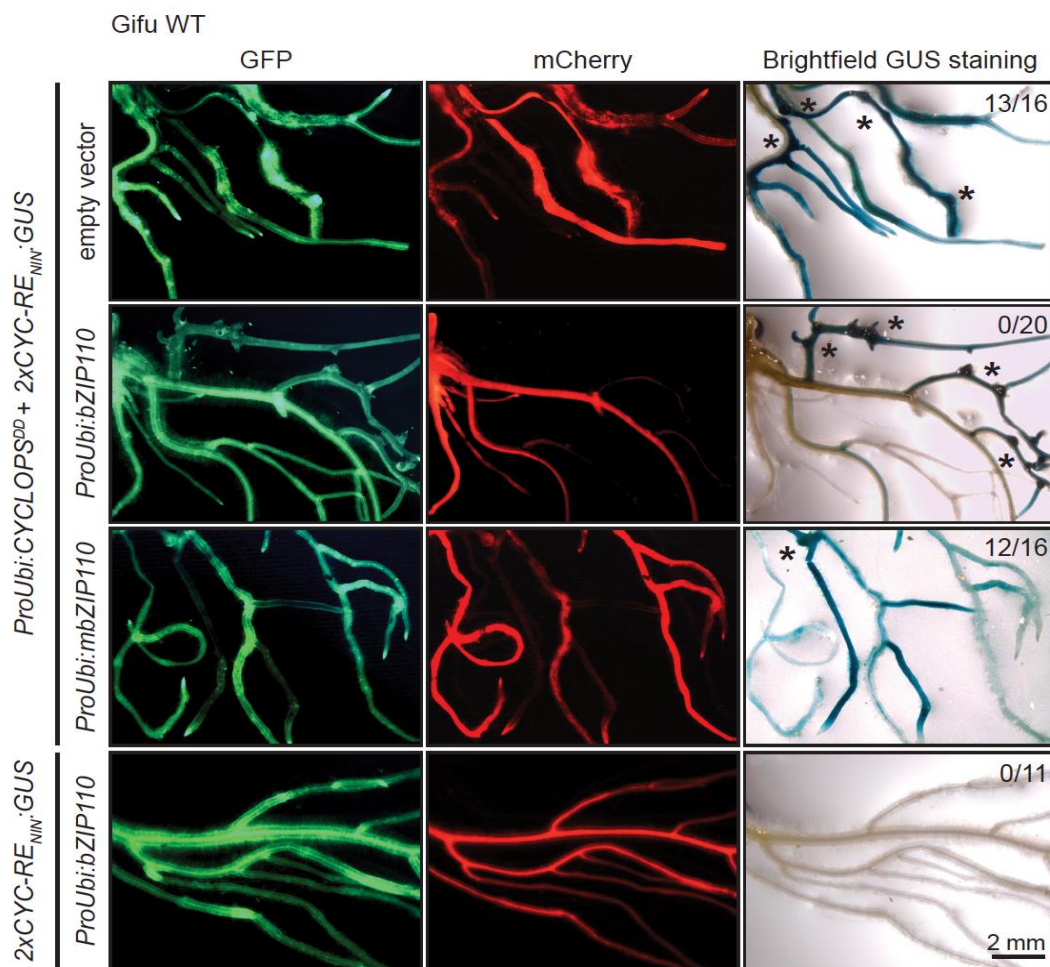


Figure 15. bZIP110 Inhibits *CYCLOPS*^{DD}-mediated Transactivation in *L. japonicus* Roots. Transactivation assay in *L. japonicus* Gifu WT roots co-transformed with a T-DNA containing the *2xCYC-RE_{NIN}:GUS* reporter alone or *ProUbi:CYCLOPS*^{DD}+*2xCYC-RE_{NIN}:GUS* (visualized by a *GFP* transformation marker) and a T-DNA expressing *ProUbi:bZIP110* or the empty vector (visualized by a *mCherry* transformation marker). Roots expressing *ProUbi:gCYCLOPS*^{DD} activated *2xCYC-RE_{NIN}:GUS* (shown by blue staining) and formed spontaneous nodules (marked by asterisks). Co-transformation of *ProUbi:CYCLOPS*^{DD}+*2xCYC-RE_{NIN}:GUS* with *ProUbi:bZIP110* but not with *ProUbi:mbZIP110* or the empty vector inhibited *CYCLOPS*^{DD}-mediated *2xCYC-RE_{NIN}:GUS* activation and spontaneous nodule formation. Expression of *ProUbi:bZIP110* did not induce the *2xCYC-RE_{NIN}:GUS* reporter. Numbers indicate GUS positive co-transformed root systems per total number of root systems analyzed. Bar size with identical magnification for all images is presented inside the figure.

Co-expression of *ProUbi:CYCLOPS^{DD}+2xCYC-RENIN:GUS* with *ProUbi:mbZIP110* caused a faint reporter activation. Taken together, these findings reveal a role of bZIP110 as transcriptional repressor by forming an inhibitory heterodimeric complex with CYCLOPS on the *CYC-RENIN*.

Since CCaMK activation resulted in conformational changes of the complex (C. Cathebras, unpublished data), the effect on functionality of the inhibited, trimeric complex was analyzed (Figure 16). Transactivation assays were performed in *N. benthamiana* leaves co-transformed with *3xHA-CYCLOPS* or *3xHA-CYCLOPS^{DD}*, deregulated (*3xHA-CCaMK^{T265D}* and *3xHA-CCaMK³¹⁴*) or kinase-inactive CCaMK (*3xHA-CCaMK^{NFG}*) versions and the *2xCYC-RENIN:GUS* reporter and were compared in the absence or presence of *3xHA-bZIP110*. While 3xHA-CYCLOPS- or 3xHA-CYCLOPS^{DD}-mediated reporter activation was 9-10-times repressed by 3xHA-bZIP110 in the presence of 3xHA-CCaMK^{NFG}, a significantly reduced repression was observed using the deregulated CCaMK versions (Figure 16), indicating that upon activation of CCaMK structural changes of the complex are induced which release bZIP110-mediated transcriptional repression of CYCLOPS. None of the tested *CCaMK* versions alone caused reporter activation.

12. Fine-tuned Expression Pattern of CYCLOPS and bZIP110 Contribute to Cell-Type-Specific Development during RNS.

Defined negative and positive regulatory mechanisms are important for legumes in order to control cell-type-specific nodule development. To obtain spatiotemporal information about the trimeric complex during RNS, the expression pattern of *bZIP110* and *CYCLOPS* using fluorescent reporter genes in *L. japonicus* hairy roots driven by the endogenous promoter sequences were analyzed (C. Cathebras, unpublished data). In non-inoculated roots, *bZIP110* and *CYCLOPS* were co-expressed in root hairs, the primary sites for rhizobial infection. Additionally, *bZIP110* promoter activity was found in the root cortex and around the vascular bundle. Upon inoculation with BFP-labeled *M. loti* R7A, *CYCLOPS* and *bZIP110* were co-expressed in inner cortical cells of primordia and emerging nodules. Interestingly, at later stages of nodule development, expression of both genes was mutually exclusive. While *CYCLOPS* expression became restricted to infected cells, *bZIP110* was expressed in the outer nodule tissue surrounding this region and, in contrast to *CYCLOPS*, was still highly expressed in the root cortex and vascular tissue.

Strikingly, using a transgenic *L. japonicus ProNIN:GUS* line, expression of *NIN* was induced by *M. loti* in inner cortical cells of primordia and nodules, but was absent in outer nodule tissue layers and the root cortex where solely *bZIP110* expression was found (C. Cathebras, unpublished data). These findings indicate dual-negative regulatory roles of bZIP110 for cell-type-specific nodule development, as a heterodimeric complex partner of CCaMK/CYCLOPS in nuclei of root hairs and inner cortical cells of primordia and as a homodimeric inhibitor in outer cells of mature nodules to confine *NIN* expression to the nodule interior.

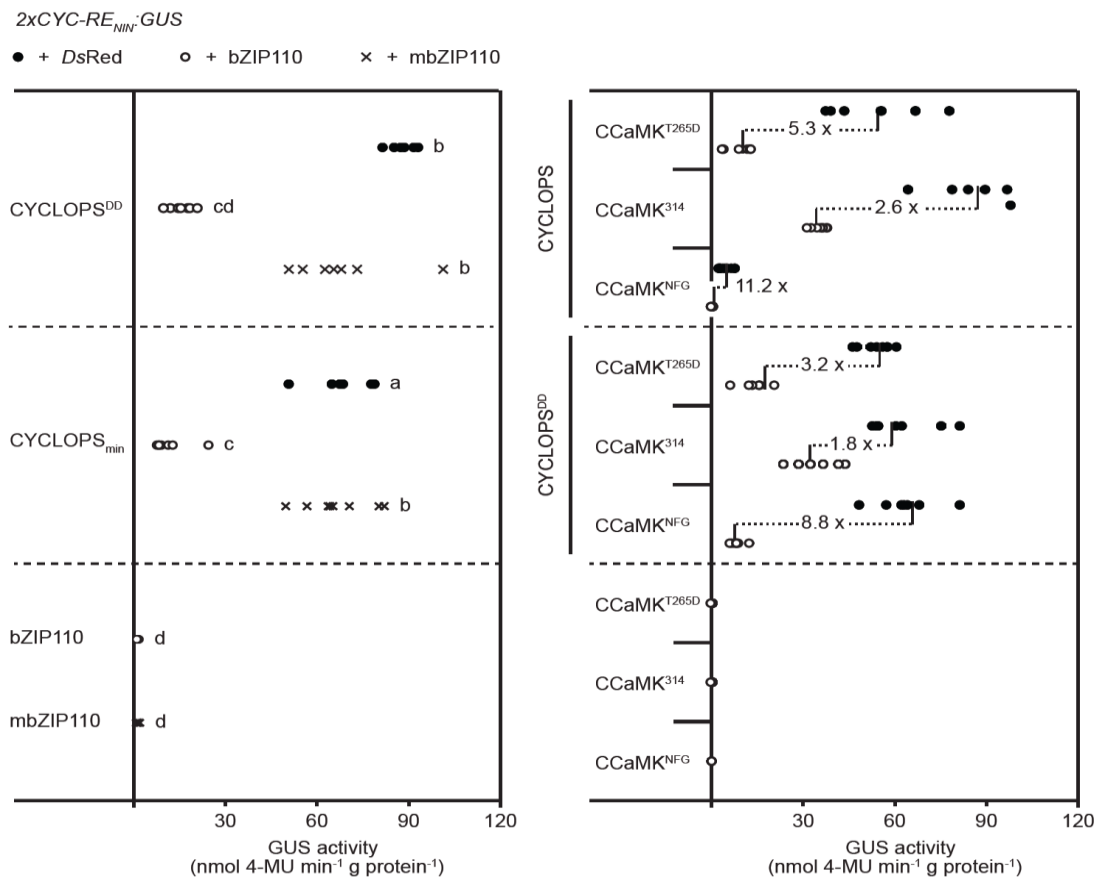


Figure 16. bZIP110-Mediated Repression is Released upon CCaMK Activation. Transactivation assays from extracts of *N. benthamiana* leaves co-transformed with the indicated versions expressed under the 35S promoter 60 hpi. Left panel: Transactivation of 2xCYC-RE_{NIN}:GUS by 3xHA-CYCLOPS^{DD} and 3xHA-CYCLOPS_{min} is significantly reduced in the presence of 3xHA-bZIP110 (white circles), while no reporter inhibition was observed in the presence of DsRed (black circles) or a mutated version of bZIP110 (mbZIP110), in which I114 in position *d* was exchanged to a destabilizing glutamate (black crosses). Right panel: 3xHA-CYCLOPS- or 3xHA-CYCLOPS^{DD}-mediated transactivation of 2xCYC-RE_{NIN}:GUS is inhibited in the presence of a kinase-inactivate CCaMK version (3xHA-CCaMK^{NFG}), while co-transformation with gain-of-function CCaMK versions (3xHA-CCaMK^{T265D} and 3xHA-CCaMK³¹⁴) resulted in a de-repression. Neither 3xHA-bZIP110 and 3xHA-mbZIP110 alone nor in the presence of kinase-active and -inactive 3xHA-CCaMK versions elicited *GUS* expression. bZIP110-mediated inhibition is indicated as fold change of the median *GUS* activity. *GUS* activities (nmol 4-MU min⁻¹ g protein⁻¹) were quantified by MUG fluorimetric assay. Letters indicate different statistical groups (ANOVA, post hoc Tukey; p≤0.05; n= 60-113).

13. bZIP110 is a Negative Regulator and Specifically Inhibits Root Nodule Development, but not Arbuscular Mycorrhiza.

Because bZIP110 was identified as interactor of CCaMK/CYCLOPS, the key regulatory complex in the developmental decision between RNS and AM (Figure 12 and 13), a role of bZIP110 in the two types of symbiosis was examined. A homozygous *bzip110-1* line was derived from a heterozygous mother plant carrying a *Lotus* retrotransposon 1 insertion (LORE1) (Fukai et al., 2012) in the 5'-UTR of *bZIP110* (plant ID 30010948, Figure 9D), which showed significantly reduced *bZIP110* expression level compared to Gifu WT plants (M.R., Cerri, unpublished data). Phenotypic analysis revealed an increased number of nodules 4 wpi with *M. loti* DsRed (M.R., Cerri, unpublished data). Indicative for a recessive mutation, heterozygous plants developed an intermediate nodule number. Consistent with the hypernodulation phenotype, empty vector transformed *bzip110-1* mutant roots showed significantly increased expression of the nodulation-specific marker genes *NIN* and *ERN1* 8 dpi with *M. loti*, whereas *CYCLOPS* induction was similar to Gifu WT plants transformed with the empty vector (M.R., Cerri, unpublished data).

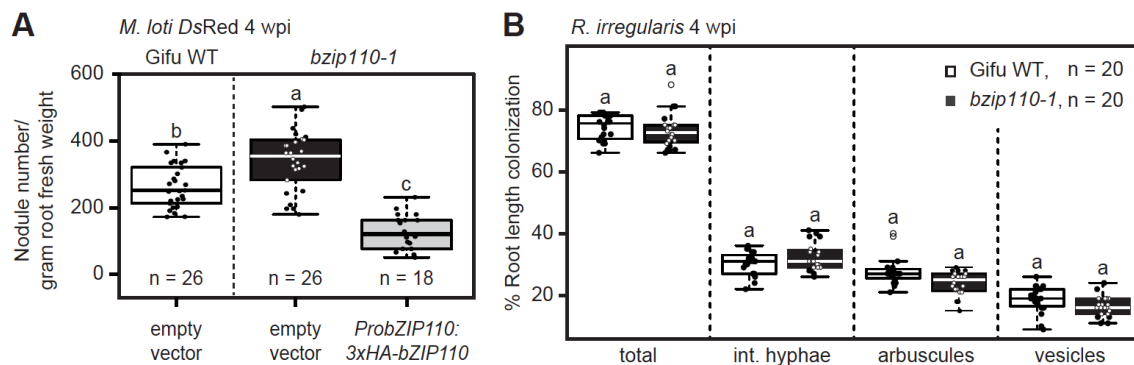


Figure 17. bZIP110 is a Negative Regulator of Root Nodule Symbiosis but not Arbuscular Mycorrhiza.

(A) Complementation analysis. The number of infected root nodules/gram fresh weight was measured of hairy roots from *bzip110-1* plants transformed with the empty vector (black box) or the genomic *bZIP110* sequence including its endogenous promoter (grey box) and Gifu WT plants transformed with the empty vector (white box) 4 wpi with DsRed-tagged *M. loti*. Expression of *ProbZIP110:3xHA-bZIP110* in *bzip110-1* plants significantly reduced the number of nodules compared to the empty vector.

(B) AM phenotype of *bzip110-1* mutant plants. No significant differences in percent root length colonization were observed between *bzip110-1* mutant (black box) and Gifu WT plants (white box) 4 wpi with *R. irregularis*. Percent root length colonization was determined by the gridline intersect method.

(A-B) Data are presented as box plots. Bold black line: median; box: interquartile range; whiskers: highest and lowest data point within 1.5 interquartile range; dots: data points. Different letters indicate different statistical groups (ANOVA, post hoc Tukey; $p \leq 0.05$), n= number of plants (A) and (t-test; $p \leq 0.05$; n= 20-30) (B).

Line	Ecotype	Genotype	Number of plants	Average root length (cm)	Average lateral root number	Average lateral root number/cm root length	Average arbuscule length (μm) ^a
	Gifu	wildtype	31	2.6 \pm 0.6	2 \pm 1	1.0 \pm 0.3	47.2 \pm 11.3
<i>bzip110-1</i>	Gifu	homozygous	33	1.2 \pm 0.3	2 \pm 1	2.0 \pm 0.8	36.7 \pm 8.9

Table 2. Growth Phenotype of *bzip110-1* Mutant Plants.

Mutant *bzip110-1* seedlings show a stunted growth phenotype compared to Gifu WT plants. Root length and lateral root number of 12-days-old seedlings were measured.

^aLength of 100 arbuscules was measured 4 wpi with *R. irregularis* from 5 root systems in total.

Line	Ecotype	Genotype	Average root length (cm)	Number of plants
<i>bZIP110</i>	Gifu	wildtype	1.5 \pm 0.5	12
<i>bzip110-1</i>	Gifu	heterozygous	1.4 \pm 0.6	12
<i>bzip110-1</i>	Gifu	homozygous	1.6 \pm 0.6	23

Table 3. Segregation of a Stunted Root Phenotype in the Progeny of a Heterozygous *bzip110-1* Mother Plant.

Progeny of a heterozygous *bzip110-1* mother revealed that the *bzip110-1* allele did not co-segregate with stunted roots. Root length of 12-days-old seedlings was measured.

Furthermore, a stunted root phenotype segregated in the 30010948 LORE1 line for *bzip110-1* plants (Table 2). However, progeny of a heterozygous *bzip110-1* mother revealed that the *bzip110-1* allele did not co-segregate with stunted roots, suggesting that other mutations in the LORE1 line are responsible for the phenotype (Table 3). Hairy root transformation of *bzip110-1* plants with the genomic *bZIP110* sequence including its endogenous promoter, significantly decreased nodule number (Figure 17A and Table 4) and *NIN* and *ERN1* expression (M.R., Cerri, unpublished data) compared to plants transformed with the empty vector control, confirming that the *bZIP110* mutation was causative for the nodulation phenotype. As expected from the independent segregation (Table 3), the stunted root phenotype was not restored by the *bZIP110* transgene.

To examine the AM phenotype, *bzip110-1* roots were inoculated with *R. irregularis* and 4 wpi AM infection was quantified. Although arbuscule length was significantly smaller in the mutant due to reduced root cell sizes, the amount of intraradical hyphae, arbuscules and vesicles were not significant different compared to Gifu WT plants (Figure 17B and Table 2). Successful AM colonization was further confirmed by qRT-PCR analysis, showing that the AM marker genes *RAM1* and *PT4* were equally induced in the mutant (M.R., Cerri, unpublished data).

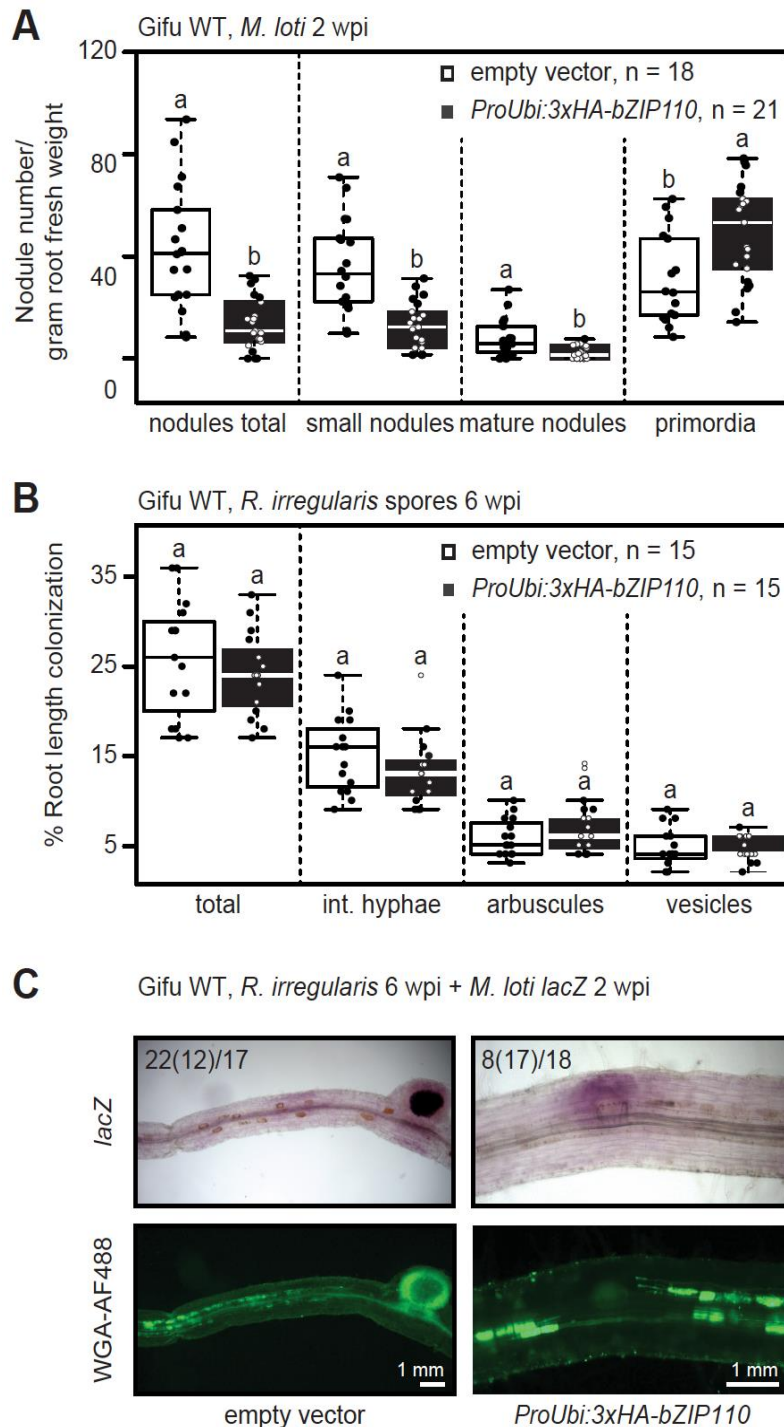


Figure 18. Overexpression of *bZIP110* Negatively Affects Nodule Development but not AM Colonization.

Two-weeks old Gifu WT plants transformed with *ProUbi:bZIP110* (black boxes) or the empty vector (white boxes) were grown sterile for 4 weeks before inoculation with *M. loti lacZ* for 2 weeks (A), spore-inoculated with *R. irregularis* and grown for 6 weeks (B) or grown for 4 weeks and co-inoculated with *M. loti* carrying *lacZ* for 2 more weeks (C).

(A) Plants ectopically expressing *bZIP110* showed a reduced and delayed nodule development since the total number of nodules and the number of small and mature nodules per gram root fresh weight were significantly decreased, whereas the number of primordia was significantly increased compared to the empty vector control.

(B) Total root length AM colonization, the number of internal hyphae, arbuscules and vesicles were not significantly different between plants transformed with *ProUbi:bZIP110* or the empty vector. Percent root length colonization was determined by the gridline intersect method.

(A-B) Data are presented as box plot. Bold black line: median; box: interquartile range; whiskers: highest and lowest data point within 1.5 interquartile range; dots: data points. Letters indicate different statistical groups (t-test; $p \leq 0.05$), n= number of plants.

(C) Coinoculation experiment. Plants ectopically expressing *bZIP110* developed a significantly decreased number of nodules, while arbuscule development was not affected. Pictures are presented as brightfield and images recorded with GFP (indicates fungi stained with WGA-AlexaFluor488). Numbers indicate average number of nodules (primordia) per total number of root systems analyzed. Bar sizes with identical magnification for all images are presented inside the figure.

Line	Ecotype	Genotype	Transgene	Number of plants	Nodule number	Root fresh weight (mg)	Nodule number/mg root fresh weight
	Gifu	wildtype	empty vector	26	47 ± 15	218 ± 93	230 ± 60
<i>bzip110-1</i>	Gifu	homozygous	empty vector	26	25 ± 10	83 ± 31	306 ± 84
<i>bzip110-1</i>	Gifu	homozygous	<i>ProbZIP110:3xHA-bZIP110</i>	18	4 ± 2	46 ± 30	100 ± 50

Table 4. Complementation Analysis of *bzip110-1* Mutant Plants.

Mutant *bzip110-1* plants were transformed by *A. rhizogenes* mediated hairy root transformation with the empty vector control or a T-DNA encoding the genomic *bZIP110* sequence with an N-terminal 3xHA-tag driven by the native *bZIP110* promoter sequence. As a control, Gifu WT plants transformed with the empty vector were used. Transgenic plants were visualized by a GFP transformation marker. Plants were inoculated with *DsRed*-tagged *M. loti* and the number of infected root nodules/gram fresh weight was measured 4 wpi.

Consistent with a specific negative regulatory role as homodimer at later stages of nodule formation, ectopic expression of *bZIP110* driven by the *L. japonicus ubiquitin* promoter in Gifu WT plants caused a delay in nodule development showing significantly higher amounts of primordia, but reduced nodule numbers (Figure 18A). Overexpression of *bZIP110* was confirmed by qPCR analysis and revealed a significantly reduced expression level of *NIN* and *ERN1*, but not *CYCLOPS* compared to Gifu WT plants transformed with the empty vector (M.R., Cerri, unpublished data). In contrast, AM colonization of *bzip110-1* mutants was similar to Gifu WT plants (Figure 18B). This was confirmed by co-inoculation experiments with *M. loti* and *R. irregularis* showing that Gifu WT plants ectopically expressing *bZIP110* develop significantly more nodule primordia, but a decreased nodule number, while arbuscule formation is not affected (Figure 18C).

VI. Material and Methods

1. Experimental Model and Subject Details

1.1. Plant Lines

Experiments were performed using *L. japonicus* ecotype Gifu B-129 WT (Handberg and Stougaard, 1992) and *cyclops-3* mutant plants (Szczyglowski et al., 1998; Yano et al., 2008). Homozygous *bzip110-1* mutants were derived from the LORE1 insertion line 30010948 obtained from the *Lotus* Base at Aarhus University, Denmark (Fukai et al., 2012). Plant lines and seed bag numbers are listed in VI. 4. Plant Sed Bag Numbers. Transactivation assays, co-IP analyses and BiFC were performed in *N. benthamiana*. AM experiments were set up in a chive (*Allium schoenoprasum*) nurse pot system (Demchenko et al., 2004).

1.2. Microbial and Yeast Strains

For root symbiotic phenotyping, *M. loti* MAFF303099 carrying *DsRed* as marker (Maekawa et al., 2008), *M. loti* R7A carrying *lacZ* (Leong et al., 1985) or *R. irregularis* DAOM197198 were used (Agronutrition, Toulouse, France). Transgenic hairy roots were induced by *A. rhizogenes* strain AR1193 (Offringa et al., 1986) as described (Díaz et al., 2005). Transformation of *N. benthamiana* leaves was performed with *A. tumefaciens* strains GV3101 pMP90 (Koncz and Schell, 1986) or AGL1 (Lazo et al., 1991) as described (Yano et al., 2008). Proteins used for *in vitro* assays and crystallography were expressed in *E. coli* Rosetta™(DE3) pLacI Competent Cells - Novagen (Merck, Darmstadt, Germany). Yeast experiments were performed in the yeast reporter strain HF7c (Feilotter et al., 1994). All strains were stored in 20 % glycerol at -80 °C.

2. Method Details

2.1. Cross-linking

WT or CC-mutated proteins (2.9 nmol) were prepared in buffer (20 mM HEPES pH 7.5, 150 mM NaCl) and incubated for 5 min at RT with 30-fold molar excess of BS3 (bis(sulfosuccinimidyl)suberate) crosslinker (ThermoFisher Scientific, Darmstadt, Germany). The reaction was quenched with 50 mM Tris pH 7.5 for 30 min and the products separated on a 10 % SDS-PAGE.

2.2. Crystallization and Structural Determination

Crystallization of the CYCLOPS zipper was carried out at 4 °C using the vapor diffusion method by mixing equal volumes of protein complex at 8 mg/ml and crystallization buffer. The best diffracting crystals of the CYCLOPS zipper were obtained in 50 mM Tris pH 8.0, 15 % PEG 6K and 0.2 M CaCl₂, after 10 days. Crystals were flash-frozen in liquid nitrogen directly from the crystallization drop and diffracted to 2.4 Å resolution. X-ray data collection at the macromolecular crystallography super-bending magnet beamline X06DA (PXIII) of the Swiss Light Source, Villigen, Switzerland and structural determination were performed by J. Basquin. Data collection and refinement statistics are summarized in Table 1. Figures were created using PyMOL 1.3 Edu (<https://pymol.org/edu/>).

2.3. Domain Analyses

CYCLOPS domain analyses in *N. benthamiana* leaves and in yeast were performed as described in Singh et al., 2014.

2.4. Electrophoretic Mobility Shift Assay

EMSA of GST-CYCLOPS-BD, GST-CYCLOPS^{DD}-ΔBD, GST-CYCLOPS^{WT/DD/AA}, co-expressed 6x-His-CCaMK/Strep-CYCLOPS and IR-labeled *CYC-RE_{NIN}* (Figure 6) were performed as described in Singh et al., 2014. EMSAs of GST-CYCLOPS_{min} and 5' CY5-labeled *CYC-RE_{ERNI}* and of 6xHis-CYCLOPS_{min} and 5' CY5-labeled *CYC-RE_{RAMI}* (Figure 7) were performed as described in Cerri et al., 2017 or Pimprikar et al., 2016, respectively. For EMSAs of 6xHis- and GST-CYCLOPS_{min}-WT, -mR4 and -mR1357, GST-CYCLOPS^{DD}, MBP-bZIP110, MBP-CCaMK and 5' CY5-labeled *CYC-RE_{NIN}* or *4PAL8* (Figure 11, 13 and 14), proteins were incubated in binding buffer (10 mM Tris-HCl pH 6.8, 200 mM KCl, 2.5 mM DTT, 2.5 % (vol/vol) glycerol, 5 mM MgCl₂, 25 ng/μl Poly (dI-dC) (ThermoFisher Scientific, Darmstadt, Germany), 0.2 mM EDTA, 100 fmol 5' CY5-labeled DNA) for 15 min at room temperature. Reactions were resolved on 6 % native, pre-run polyacrylamide gels and CY5-labeled DNA was visualized with the Typhoon TriO phosphoimager (Amersham Biosciences, Freiburg im Breisgau, Germany). Complementary pairs of labeled probes and competitors are listed in VI. 7. Oligonucleotides.

2.5. Fluorimetric Assays and Histochemical Staining

Fluorimetric and histochemical GUS assays in *N. benthamiana* leaves or *L. japonicus* roots were performed as described previously (Singh et al., 2014) using 4-MUG (Biosynth, Staad, Switzerland) and 4-MU (Sigma-Aldrich, Taufkirchen, Germany) or X-Gluc (X-Gluc DIRECT, <http://x-gluc.com>), respectively. Fungal structures were stained with 1 µg Alexa Fluor 488 conjugated WGA (ThermoFisher Scientific, Darmstadt, Germany). *LacZ* staining of *M. loti* R7A was performed using Magenta-Gal (Biosynth, Staad, Switzerland).

2.6. Interaction Studies *in planta*

Protein-protein-interactions were analyzed by co-IP from *N. benthamiana* leaf extracts with µMACS His isolation kit according to the manufacture's protocol (Miltenyi Biotec, Bergisch Gladbach, Germany). Two leaf discs per assay were pooled and homogenized by a tissue lyser (Retsch, Haan, Germany). Protein extraction was performed with lysis buffer (Miltenyi Biotec, Bergisch Gladbach, Germany) supplemented with cOmplete, Mini, EDTA-free Protease Inhibitor Cocktail (Roche, Penzberg, Germany) and 5 mM DTT and plant lysate was incubated for 2 hours at 4 °C with anti-His microbeads. Samples of input, IP and co-IP from two biological replicates were analyzed by Western blotting. BiFC was performed as described previously (Singh et al., 2014).

2.7. *In vitro* Kinase Assay

In vitro kinase assay was performed as described (Liao et al., 2012) using 0.2 nmol MBP-bZIP110, MBP-CCaMK and GST-CYCLOPS. Proteins were incubated for 2 h at RT with 1 µM His-tagged human Calmodulin1 (Sigma-Aldrich, Taufkirchen, Germany) in the presence of 0.1 mM CaCl₂ and 200 µM ATP (New England Biolabs, Frankfurt am Main, Germany) using the same buffer conditions as described by Liao et al. (2012). Kinase reaction was stopped by addition of SDS-PAGE sample buffer and boiled for 5 min.

2.8. Microscale Thermophoresis

DNA-binding affinity and specificity was measured by MST as described (Jerabek-Willemsen et al., 2011). Specific binding between GST-CYCLOPS-BD or GST-CYCLOPS^{DD}-ΔBD and 5'-CY5-labeled *CYC-RE_{NIN}* was performed as described in Singh et al., 2014.

Affinity experiments were performed with 25 nM 5'-CY5-labeled *4Pal8* and increasing amounts of GST-CYCLOPS_{min}-WT or GST-CYCLOPS_{min}-mR4 (from 109 nM to 896 µM) in buffer containing 50 mM Tris-HCl pH 6.8, 200 mM NaCl, 10 mM MgCl₂, 0.05 % Tween-20 and 0.1 mg/ml BSA. Samples were loaded into Monolith NT.115TM hydrophilic capillaries (Nanotemper Technologies, Munich, Germany) and thermophoresis was carried out at 25 °C, 40 % LED and 20 % IR-laser power using the Monolith NT.115 (Nanotemper Technologies, Munich, Germany). Data analysis was performed with Nanotemper Analysis software v.1.2.101. Average thermophoresis values, standard deviations and affinity constants were calculated from three independent measurements. Curve fitting was done by SigmaPlot 11.0 software (Systat Software GmbH, Erkrath, Germany).

2.9. Microscopy

Root transformation and infection with *M. loti* was evaluated using a fluorescence stereomicroscope (Leica M165FC) and a CLSM (Leica TCS SP5) equipped with a HCX PL APO CS 20×/0.7 IMM CORR CS objective (Leica, Wetzlar, Germany). BiFC analyses were performed using a CLSM (Leica TCS SP5) equipped with a HCX PL APO CS 63×/1.2 W CORR CS2 objective. Root length colonization with *R. irregularis* was quantified by a modified gridline intersect method (Mcgonigle et al., 1990) using an inverted microscope (Leica DMI6000B). GUS activity in roots and nodules was examined using a stereomicroscope (Leica M165FC) and an upright microscope (Leica DM6B).

2.10. Plant Growth, Transformation and Inoculation

L. japonicus and *N. benthamiana* cultivation and transformation were as described by Singh et al., 2014. For nodulation experiments, plants were inoculated with *M. loti* MAFF303099 carrying *DsRed* as marker (Maekawa et al., 2008) set to a final OD₆₀₀ of 0.05 and incubated for four weeks. For AM colonization, plants were either inoculated with 500 spores per plant of *R. irregularis* DAOM197198 (Agronutrition, Toulouse, France) and incubated for 6 weeks or grown for 4 weeks in a *R. irregularis* inoculated chive (*Allium schoenoprasum*) nurse pot system (Demchenko et al., 2004). For co-inoculation experiments, spore-inoculated plants were fertilized once a week with quarter-strength Hoagland medium (Hoagland and Arnon, 1950) containing 10 mM nitrogen for 3 weeks and one week with quarter-strength Hoagland medium containing 1 mM nitrogen before inoculation with *M. loti* R7A carrying *lacZ* (Leong et al., 1985).

2.11. Protein Blot Analysis

Proteins expressed in *N. benthamiana* leaves were extracted as described by Singh et al., 2014. 3xHA-tagged proteins were detected using rat monoclonal anti-HA HRP-conjugated antibody (clone 3F10, Roche, Penzberg, Germany). Immunodetection of 6xHis-tagged proteins was performed using mouse monoclonal anti-His₆ (2) (Roche, Penzberg, Germany) as primary antibody and goat polyclonal anti-mouse HRP-conjugated (Biomol, Hamburg, Germany) as secondary antibody. Protein blotting was performed as described by Singh et al., 2014. Proteins were detected by chemiluminescence in a Vilber Lourmat Fusion-SL-3500 WL (PeqLab, Erlangen, Germany) using SuperSignal™ West Femto Maximum Sensitivity Substrate (ThermoFisher Scientific, Darmstadt, Germany).

2.12. Protein Expression and Purification

Expression of 6xHis-Sumo-CYCLOPS_{CC} was induced in *E. coli* Rosetta™(DE3) pLacI Competent Cells - Novagen (Merck, Darmstadt, Germany) for 12 h at 18 °C by addition of 0.3 mM IPTG (Roth, Karlsruhe, Germany) in M9 minimal medium substituted with L(+)-Selenomethionine (ThermoFisher Scientific (ACROS Organics), Darmstadt, Germany). Pelleted cells were lysed by French pressure cell press (SLM Aminco; ThermoFisher Scientific, Darmstadt, Germany) in the presence of 1 mg/ml Dnase I (AppliChem, Darmstadt, Germany) and 5 mM MgCl₂ and subsequently sonicated. Soluble proteins were purified by affinity chromatography with HisTrap™ FF crude 5ml column (GE Healthcare, Munich, Germany) as described by the protocol of the resin manufacturer. 6xHis-Sumo-tag was cleaved off by 6xHis-Sentrin-specific protease 2 (SEN2) (Biomol, Hamburg, Germany) over night at 4 °C during dialysis in buffer (20 mM Tris, 200 mM NaCl, 2 mM β-Mercapto-Ethanol, pH 7.0) using Slide-A-Lyzer™ Dialysis Cassettes (3.5K MWCO, 30 mL) (ThermoFisher Scientific, Darmstadt, Germany) and removed by a second affinity chromatography with HisTrap™ FF crude 5ml column (GE Healthcare, Munich, Germany). For crystallization, proteins were concentrated to about 8 mg/ml using Amicon Ultra-15 (3 kDa NMWL, PLBC Ultracel-PL Membran) centrifugal filter devices (Merck, Darmstadt, Germany).

Expression and purification of 6xHis- and GST-CYCLOPS_{min}-WT, -mR4 and -mR1357, GST-CYCLOPS^{WT/DD/AA}, GST-CYCLOPS-BD, GST-CYCLOPS^{DD}-ΔBD and co-expression of 6x-His-CCaMK/Strep-CYCLOPS^{DD} and 6x-His-CCaMK/Strep-CYCLOPS were performed using cOMplete His-Tag purification resin (Roche, Penzberg, Germany), Pierce™ Glutathione Agarose (ThermoFisher Scientific, Darmstadt, Germany) or Strep-

Tactin Sepharose (IBA, Goettingen, Germany) as described by Singh et al., 2014. GST-bZIP110 was expressed and purified applying the same conditions as for GST-CYCLOPS_{min}. Purification of MBP-CCaMK and MBP-bZIP110 was performed using amylose resin as described by the protocol of the manufacturer (New England Biolabs, Frankfurt am Main, Germany). Protein concentrations were determined by absorbance at 280 nm (DeNovix DS-11) using values for molar extinction coefficient (M⁻¹ cm⁻¹) and molecular weight of the respective proteins. Protein purity was analyzed by SDS-PAGE and Coomassie staining of the gel.

2.13. Root Growth Analysis

12-days old seedlings were scanned and root length and number of lateral roots were measured using Fiji ImageJ version 2.0.0-rc-44/1.50e (<http://imagej.net/>).

2.14. Sequence Alignment and Structure Prediction

CYCLOPS amino acid alignment and structure predictions were performed as described in Singh et al., 2014.

3. Quantification and Statistical Analysis

All statistical analyses were performed in R-studio (version 0.99.484) (<http://www.r-studio.com>). Statistical details including the statistical tests used, significance levels, exact value and representation of n, definition of precision measures (mean, median, confidence intervals, standard deviation) are indicated in the figure legends.

4. Plant Seed Bag Numbers

Line	Ecotype	Genotype	Progenitor	Seed Bag Number	Used for
<i>bzip110-1</i>	Gifu	homozygous	LORE1 line (plant ID 30010948)	92694, 92552	Figure 17A and Table 2 and 4
<i>bzip110-1</i>	Gifu	heterozygous	LORE1 line (plant ID 30010948)	92546, 92547, 111135	Table 3
<i>cyclops-3</i>	Gifu	homozygous	EMS126 line	67839, 78645, 78646, 78647	Figure 10C
	Gifu	wildtype		110882	Figure 17A
	Gifu	wildtype		91197, 91753	Table 2 and 4
	Gifu	wildtype		91751, 91752, 91750, 91749, 91744	Figure 15 and 18

5. Key Resources Table

Reagent or Resource	Source	Identifier
Antibodies		
Rat monoclonal anti-HA HRP-conjugated (clone 3F10)	Roche, Penzberg, Germany	Cat#12013819001; RRID:AB_390917
Mouse monoclonal anti-His ₆ (2)	Roche, Penzberg, Germany	Cat#04905318001; RRID:AB_840258
Goat polyclonal anti-mouse HRP-conjugated	Biomol, Hamburg, Germany	Cat#ARG65350.500
Biological Samples		
<i>L. japonicus</i> (Gifu) LOREI insertion line (plant ID 30010948)	Lotus Base, Aarhus University, Denmark	https://lotus.au.dk
<i>L. japonicus</i> (Gifu) <i>cyclops-3</i> EMS line	Szczyglowski et al., 1998; Yano et al., 2008	Please refer to the originator.
<i>L. japonicus</i> (Gifu) WT	Handberg and Stougaard, 1992	Please refer to the originator.
Plant lines and seed bag numbers, see VI. 4. Plant Sed Bag Numbers.	This thesis	Please refer to the originator.
Chemicals, Peptides, and Recombinant Proteins		
Adenosine 5'-Triphosphate (ATP)	New England Biolabs	Cat#P0756
BS3 (bis(sulfosuccinimidyl)suberate)	ThermoFisher Scientific, Darmstadt, Germany	Cat#21580
Calmodulin1, His tagged human	Sigma-Aldrich, Taufkirchen, Germany	Cat#SRP5169
cOmplete, Mini, EDTA-free Protease Inhibitor Cocktail	Roche, Penzberg, Germany	Cat#04693159001
DNaseI	AppliChem, Darmstadt, Germany	Cat#A3778,0050
IPTG (Isopropyl- β -D-thiogalactopyranosid)	Roth, Karlsruhe, Germany	Cat#2316
Magenta-Gal (5-Bromo-6-chloro-3-indoxyl-beta-D-galactopyranoside)	Biosynth, Staad, Switzerland	Cat#B-7200, CAS: 93863-88-8
4-MU (4-Methylumbelliferone sodium salt)	Sigma-Aldrich, Taufkirchen, Germany	Cat#M1508, CAS: 5980-33-6
4-MUG (4-Methylumbelliferyl-beta-D-glucuronic acid dihydrate)	Biosynth, Staad, Switzerland	Cat#M-5700, CAS: 881005-91-0
PMSF BioChemica	AppliChem, Darmstadt, Germany	Cat#A0999,0100
L(+)-Selenomethionine	ThermoFisher Scientific (ACROS Organics), Darmstadt, Germany	Cat#AC259960010, CAS: 3211-76-5
Wheat Germ Agglutinin, Alexa Fluor® 488 Conjugate	ThermoFisher Scientific, Darmstadt, Germany	Cat#W11261
X-Gluc	X-Gluc DIRECT	http://x-gluc.com

Critical Commercial Assays		
SuperSignal™ West Femto Maximum Sensitivity Substrate	ThermoFisher Scientific, Darmstadt, Germany	Cat#34095
µMACS His Isolation Kit	Miltenyi Biotec, Bergisch Gladbach, Germany	Cat#130-091-124
Experimental Models: Organisms/Strains		
<i>A. rhizogenes</i> strain AR1193	Offringa et al., 1986	Please refer to the originator.
<i>A. tumefaciens</i> AGL1	Lazo et al., 1991	Please refer to the originator.
<i>A. tumefaciens</i> GV3101 pMP90	Koncz and Schell, 1986	Please refer to the originator.
<i>M. loti</i> MAFF303099 carrying <i>DsRed</i> as marker	Maekawa et al., 2008	Please refer to the originator.
<i>M. loti</i> R7A carrying <i>lacZ</i>	Leong et al., 1985	Please refer to the originator.
<i>R. irregularis</i> DAOM197198	Agronutrition, Toulouse, France	http://www.agronutrition.com/
Rosetta™(DE3) pLacI Competent Cells - Novagen	Merck, Darmstadt, Germany	Cat#70956
Yeast HF7c	Feilotter et al., 1994	Please refer to the originator.
Recombinant DNA		
Poly (dI-dC)	ThermoFisher Scientific, Darmstadt, Germany	Cat#20148E
Plasmids, see VI. 6. Plasmid Construction.	This thesis	N/A
Sequence-Based Reagents		
Primers, Oligonucleotides and EMSA probes, see VI. 7. Oligonucleotides.	This thesis	N/A
Software and Algorithms		
Fiji ImageJ version 2.0.0-rc-44/1.50e	ImageJ	https://fiji.sc/
Nanotemper Analysis software v.1.2.101	Nanotemper technologies, Munich, Germany	http://www.nanotemper-technologies.com/
PyMOL 1.3 Edu	Pymol	https://pymol.org/edu/
R-studio version 0.99.484	RStudio, Inc.	http://www.r-studio.com
SigmaPlot 11.0	Systat Software GmbH, Erkrath, Germany	http://www.systat.de

Other		
6xHis-Sentrin-specific protease 2 (SENP2)	Biomol, Hamburg, Germany	Cat#BPS-81096
Amicon Ultra-15, PLBC Ultracel-PL Membran, 3 kDa	Merck, Darmstadt, Germany	Cat#UFC900308
Amylose resin	New England Biolabs, Frankfurt am Main, Germany	Cat#E8021S
cOmplete His-Tag Purification Resin	Roche, Penzberg, Germany	Cat#05893682001
HisTrap™ FF crude 5ml	GE Healthcare, Munich, Germany	Cat#17-5286-01
Monolith NT.115™ hydrophilic capillaries	Nanotemper technologies, Munich, Germany	Cat#K004
Pierce™ Glutathione Agarose	ThermoFisher Scientific, Darmstadt, Germany	Cat#16100
Slide-A-Lyzer™ Dialysis Cassettes, 3.5K MWCO, 30 mL	ThermoFisher Scientific, Darmstadt, Germany	Cat#66130
Strep-Tactin Sepharose 50 % suspension	IBA, Goettingen, Germany	Cat#2-1201-025

6. Plasmid Construction

Plasmid Name	Construction/Reference
Entry Clones	
pENTR: <i>cCYCLOPS</i>	Yano et al., 2008
pENTR: <i>cCYCLOPS-1-449</i> (=CYCLOPS _{ΔCC})	
pENTR: <i>3xHA-cCYCLOPS_{FL}-WT</i>	Phusion PCR products of <i>3xHA-cCYCLOPS-1-254</i> amplified from pAMPATPro35S: <i>3xHA-cCYCLOPS</i> with <i>3xHA-CYCLOPS-1-254_fwd/rev</i> and of <i>cCYCLOPS-255-518</i> amplified from pENTR: <i>cCYCLOPS_{min}-WT</i> , pENTR: <i>cCYCLOPS_{min}-mR3-5</i> , <i>8</i> , <i>1357</i> or <i>2468</i> with <i>CYCLOPS-255-518_fwd/rev</i> were re-assembled into <i>BsaI</i> sites of pENTR- <i>BsaI</i> (BB04) (Binder et al., 2014) via Golden Gate assembly
pENTR: <i>3xHA-cCYCLOPS_{FL}-mR3</i>	
pENTR: <i>3xHA-cCYCLOPS_{FL}-mR4</i>	
pENTR: <i>3xHA-cCYCLOPS_{FL}-mR5</i>	
pENTR: <i>3xHA-cCYCLOPS_{FL}-mR8</i>	
pENTR: <i>3xHA-cCYCLOPS_{FL}-mR1357</i>	
pENTR: <i>3xHA-cCYCLOPS_{FL}-mR2468</i>	
pENTR: <i>cCYCLOPS_{min}-mR1</i>	
pENTR: <i>cCYCLOPS_{min}-mR2</i>	
pENTR: <i>cCYCLOPS_{min}-mR3</i>	
pENTR: <i>cCYCLOPS_{min}-mR4</i>	
pENTR: <i>cCYCLOPS_{min}-mR5</i>	
pENTR: <i>cCYCLOPS_{min}-mR6</i>	
pENTR: <i>cCYCLOPS_{min}-mR7</i>	
pENTR: <i>cCYCLOPS_{min}-mR8</i>	
pENTR: <i>cCYCLOPS_{min}-mR1357</i>	

pENTR:cCYCLOPS _{min} -mR2468	
pENTR:bZIP110	Phusion PCR product of the 474 bp genomic <i>bZIP110</i> nucleotide sequence amplified from <i>L. japonicus</i> Gifu genomic DNA with <i>LI C-D bZIP110_fwd/rev</i> and cloned into <i>BsaI</i> sites of pENTR- <i>BsaI</i> (BB04) (Binder et al., 2014) via Golden Gate assembly
pENTR:bZIP110 ^{114E} (=mbZIP110)	Whole plasmid site directed mutagenesis Phusion PCR with <i>bZIP110^{114E}_fwd/rev</i> on pENTR:bZIP110
pENTR:cCYCLOPS-S50D-S154D (=CYCLOPS ^{DD})	Singh et al., 2014
pENTR:cCYCLOPS-255-518 (=CYCLOPS _{min})	
pENTR:bZIP63-166-314 (=At <i>bZIP63cc</i>)	gift from A. Binder
Level II - III Golden Gate Construction Plasmids	
LIIβ F 1-2 (<i>ProUbi10:mCherry</i>)	gift from D. Chiasson
LIIβ F 1-2 (<i>ProUbi10:sGFP</i>)	
LIIβ F 4-5 (<i>ProUbi:3xHA-bZIP110</i>)	Golden Gate <i>BsaI</i> cut-ligation using LIIβ F 4-5 (BB26), LI A-B <i>ProUbi</i> (G007), LI B-C <i>HA</i> (G067), LI D-E <i>dy</i> (BB08), LI E-F <i>nos-T</i> (G006), LI F-G <i>dy</i> (BB09) (Binder et al., 2014) and Phusion PCR product of the genomic <i>bZIP110</i> sequence amplified from pENTR: <i>bZIP110</i> with <i>LI C-D bZIP110_fwd/rev</i>
LIIβ F 4-5 (<i>Esp3I-lacZ dy-3xHA-bZIP110</i>)	Golden Gate <i>BsaI</i> cut-ligation using LIIβ F 4-5 (BB26), LI A-B <i>Esp3I-lacZ dy</i> (G82), LI B-C <i>HA</i> (G067), LI D-E <i>dy</i> (BB08), LI E-F <i>nos-T</i> (G006), LI F-G <i>dy</i> (BB09) (Binder et al., 2014) and Phusion PCR product of the genomic <i>bZIP110</i> sequence amplified from pENTR: <i>bZIP110</i> with <i>LI C-D bZIP110_fwd/rev</i>
LIIIβ F A-B (1-2 <i>ProUbi10:sGFP</i> , 4-5 <i>Esp3I-lacZ dy-3xHA-bZIP110</i>)	Golden Gate <i>BpiI</i> cut-ligation using LIIIβ F A-B (BB53), LIIβ F 1-2 (A-B <i>ProUbi10:sGFP</i>), LII <i>ins</i> 2-3 (BB43), LII <i>dy</i> 3-4 (BB64), LIIβ F 4-5 (<i>Esp3I-lacZ dy-3xHA-bZIP110</i>) and LII <i>dy</i> 5-6 (BB65) (Binder et al., 2014)
Plasmids for Expression in <i>L. japonicus</i> Hairy Roots	
p <i>ProUbi:3xHA-cCYCLOPS_{min}</i>	Singh et al., 2014
p <i>ProUbi:bZIP110</i>	LR reaction (ThermoFisher Scientific, Darmstadt, Germany) of pENTR: <i>bZIP110</i> or pENTR: <i>bZIP110^{114E}</i> (=mbZIP110) and p <i>ProUbi:GW_GFP</i> (Maekawa et al., 2008)
p <i>ProUbi:mbZIP110</i>	
LIIIβ F A-B (1-2 <i>ProAct:eGFP-NLS</i> , 3-4 <i>2xCYC-RE-Pro_{min}NIN:GUS</i> , 5-6 <i>ProUbi:gCYCLOPS^{DD}-3xHA</i>)	gift from A. Sandré
LIIIβ F A-B (1-2 <i>ProAct:eGFP-NLS</i> , 3-4 <i>2xCYC-RE-Pro_{min}NIN:GUS</i> , 5-6 <i>dy</i>)	gift from A. Sandré
LIIIβ F A-B (1-2 <i>ProUbi10:mCherry</i> , 4-5 <i>ProUbi:3xHA-bZIP110</i>)	Golden Gate <i>BpiI</i> cut-ligation using LIIIβ F A-B (BB53), LIIβ F 1-2 (<i>ProUbi10:mCherry</i>), LII <i>ins</i> 2-3 (BB43), LII <i>dy</i> 3-4 (BB64), LIIβ F 4-5 (<i>ProUbi:3xHA-bZIP110</i>) and LII <i>dy</i> 5-6 (BB65) (Binder et al., 2014)

LIIIβ F A-B (1-2 <i>ProUbi10:mCherry</i> , 4-5 <i>dy</i>)	Golden Gate <i>Bpi</i> I cut-ligation using LIIIβ F A-B (BB53), LIIβ F 1-2 (<i>ProUbi10:mCherry</i>), LII <i>ins</i> 2-3 (BB43), LII <i>dy</i> 3-4 (BB64), LII <i>dy</i> 4-5 (BB40) and LII <i>dy</i> 5-6 (BB65) (Binder et al., 2014)
LIIIβ F A-B (1-2 <i>ProUbi10:sGFP</i> , 4-5 <i>ProbZIP110:3xHA-bZIP110</i>)	Golden Gate <i>Esp</i> 3I cut-ligation using LIIIβ F A-B (1-2 <i>ProUbi10:sGFP</i> , 4-5 <i>Esp</i> 3I- <i>lacZ dy-3xHA-bZIP110</i>) and a Phusion PCR product of the genomic <i>bZIP110</i> promoter sequence 2 kb upstream of the translational start site amplified from <i>L. japonicus</i> Gifu genomic DNA with <i>LIII 4-5 ProbZIP110_fwd/rev</i>
LIIIβ F A-B (1-2 <i>ProUbi10:sGFP</i> , 4-5 <i>dy</i>)	Golden Gate <i>Bpi</i> I cut-ligation using LIIIβ F A-B (BB53), LIIβ F 1-2 (<i>ProUbi10:sGFP</i>), LII <i>ins</i> 2-3 (BB43), LII <i>dy</i> 3-4 (BB64), LII <i>dy</i> 4-5 (BB40) and LII <i>dy</i> 5-6 (BB65) (Binder et al., 2014)
pK7 <i>ProCYCLOPS:3xHA-cCYCLOPS_{FL}-WT</i>	LR reaction (ThermoFisher Scientific, Darmstadt, Germany) of pENTR: <i>cCYCLOPS</i> , pENTR: <i>cCYCLOPS-1-449</i> (=CYCLOPS _{ΔCC}), pENTR: <i>cCYCLOPS-S50D-S154D</i> (=CYC-LOPS ^{DD}), pENTR: <i>3xHA-cCYCLOPS_{FL}-WT</i> , pENTR: <i>3xHA-cCYCLOPS_{FL}-mR3-5</i> , 8, 1357, 2468 and pK7 <i>ProCYCLOPS:GW</i> (Singh et al., 2014)
pK7 <i>ProCYCLOPS:3xHA-cCYCLOPS_{FL}-mR3</i>	
pK7 <i>ProCYCLOPS:3xHA-cCYCLOPS_{FL}-mR4</i>	
pK7 <i>ProCYCLOPS:3xHA-cCYCLOPS_{FL}-mR5</i>	
pK7 <i>ProCYCLOPS:3xHA-cCYCLOPS_{FL}-mR8</i>	
pK7 <i>ProCYCLOPS:3xHA-cCYCLOPS_{FL}-mR1357</i>	
pK7 <i>ProCYCLOPS:3xHA-cCYCLOPS_{FL}-mR2468</i>	
Plasmids for Expression in <i>N. benthamiana</i> Leaf Cells	
p2x <i>CYC-RE_{NIN}:GUS</i>	Singh et al., 2014
p2xm <i>CYC-RE_{NIN}:GUS</i>	
p2x <i>CYC-RE_{NIN} M1-5:GUS</i>	
p5x <i>UAS_{GAL4}:eGFP-GUS_{intron}</i>	
pAMPAT <i>Pro35SS:3xHA-GW</i>	Singh et al., 2014
pAMPAT <i>Pro35SS:GAL4-BD-3xHA-cCYCLOPS^{DD}</i>	
pAMPAT <i>Pro35SS:GAL4-BD-3xHA-cCYCLOPS_{min}</i>	
pAMPAT <i>Pro35SS:GAL4-BD-3xHA-cCYCLOPS-BD</i>	
pAMPAT <i>Pro35SS:GAL4-BD-3xHA-cCYCLOPS-AD</i>	
pAMPAT <i>Pro35SS:GAL4-BD-3xHA-cCYCLOPS^{DD}-1-265</i>	

pAMPATPro35SS:VP16-AD-3xHA-cCYCLOPS ^{DD}	Singh et al., 2014
pAMPATPro35SS:VP16-AD-3xHA-cCYCLOPS _{min}	
pAMPATPro35SS:VP16-AD-3xHA-cCYCLOPS-BD	
pAMPATPro35SS:VP16-AD-3xHA-cCYCLOPS ^{DD} -1-449	
pAMPATPro35SS:3xHA-cCYCLOPS	Singh et al., 2014
pAMPATPro35SS:3xHA-cCYCLOPS ^{DD}	
pAMPATPro35SS:3xHA-cCYCLOPS _{min}	
pAMPATPro35SS:3xHA-cCCaMK	
pAMPATPro35SS:3xHA-cCCaMK ^{T265D}	
pAMPATPro35SS:DsRed	
pAMPATPro35SS:GAL4-BD-VP16-AD	
pAMPATPro35SS:3xHA-cCCaMK ^{NFG}	Whole plasmid site directed mutagenesis Phusion PCR with cCCaMK ^{D186N} _fwd/rev on pAMPATPro35SS:3xHA-cCCaMK
pAMPATPro35SS:3xHA-cCYCLOPS _{min} -mR1	LR reaction (ThermoFisher Scientific, Darmstadt, Germany) of pENTR:cCYCLOPS _{min} -mR1-8, 1357, 2468 or pENTR:cCYCLOPS _{ACC} with pAMPATPro35SS:3xHA-GW
pAMPATPro35SS:3xHA-cCYCLOPS _{min} -mR2	
pAMPATPro35SS:3xHA-cCYCLOPS _{min} -mR3	
pAMPATPro35SS:3xHA-cCYCLOPS _{min} -mR4	
pAMPATPro35SS:3xHA-cCYCLOPS _{min} -mR5	
pAMPATPro35SS:3xHA-cCYCLOPS _{min} -mR6	
pAMPATPro35SS:3xHA-cCYCLOPS _{min} -mR7	
pAMPATPro35SS:3xHA-cCYCLOPS _{min} -mR8	
pAMPATPro35SS:3xHA-cCYCLOPS _{min} -mR1357	
pAMPATPro35SS:3xHA-cCYCLOPS _{min} -mR2468	
pAMPATPro35SS:3xHA-cCYCLOPS _{ACC}	
pAMPATPro35SS:6xHis-GW	Removal of 3xHA-tag and replacement with 6xHis-tag by site-directed mutagenesis Phusion PCR of pAMPATPro35SS:3xHA-GW with pAMPATPro35SS:6xHis-GW_fwd/rev and sub-sequent re-ligation

pAMPATPro35SS:6xHis-cCYCLOPS	LR reaction (ThermoFisher Scientific, Darmstadt, Germany) of pENTR:cCYCLOPS, pENTR:cCYCLOPS _{ACC} , pENTR:cCYCLOPS _{min} or pENTR:cCYCLOPS _{min-mR1-8} , 1357, 2468 with pAMPATPro35SS:6xHis-GW
pAMPATPro35SS:6xHis-cCYCLOPS _{ACC}	
pAMPATPro35SS:6xHis-cCYCLOPS _{min}	
pAMPATPro35SS:6xHis-cCYCLOPS _{min-mR1}	
pAMPATPro35SS:6xHis-cCYCLOPS _{min-mR2}	
pAMPATPro35SS:6xHis-cCYCLOPS _{min-mR3}	
pAMPATPro35SS:6xHis-cCYCLOPS _{min-mR4}	
pAMPATPro35SS:6xHis-cCYCLOPS _{min-mR5}	
pAMPATPro35SS:6xHis-cCYCLOPS _{min-mR6}	
pAMPATPro35SS:6xHis-cCYCLOPS _{min-mR7}	
pAMPATPro35SS:6xHis-cCYCLOPS _{min-mR8}	
pAMPATPro35SS:6xHis-cCYCLOPS _{min-mR1357}	
pAMPATPro35SS:6xHis-cCYCLOPS _{min-mR2468}	
pAMPATPro35SS:3xHA-bZIP110	LR reaction (ThermoFisher Scientific, Darmstadt, Germany) of pENTR:bZIP110, pENTR:bZIP110 ^{114E} (=mbZIP110) or pENTR: At bZIP63 _{CC} with pAMPATPro35SS:3xHA-GW
pAMPATPro35SS:3xHA-mbZIP110	
pAMPATPro35SS:3xHA-At bZIP63 _{CC}	
pAMPATPro35SS:6xHis-bZIP110	LR reaction (ThermoFisher Scientific, Darmstadt, Germany) of pENTR:bZIP110, pENTR:bZIP110 ^{114E} (=mbZIP110) with pAMPATPro35SS:6xHis-GW
pAMPATPro35SS:6xHis-mbZIP110	
CCaMK ³¹⁴ -RFP+NLS (pK7WGR2)	Takeda et al., 2012
pSPYNEPro35S:cCCaMK	Yano et al., 2008
pSPYNEPro35S:cCCaMK ^{K44A}	
pAMPATPro35SS:YFP _C -cCYCLOPS	LR reaction (ThermoFisher Scientific, Darmstadt, Germany) of pENTR:cCYCLOPS with pAMPATPro35SS:YFP _C -GW (Lefebvre et al., 2010)
pSPYNEPro35S:cCYCLOPS _{ACC}	LR reaction (ThermoFisher Scientific, Darmstadt, Germany) of pENTR: cCYCLOPS _{ACC} , pENTR:bZIP110 or pENTR: At bZIP63 _{CC} with pSPYNEPro35S:GW (Walter et al., 2004)
pSPYNEPro35S:bZIP110	
pSPYNEPro35S:At bZIP63 _{CC}	

Plasmids for Expression in Yeast	
pBDGAL4: <i>cCYCLOPS</i> ^{DD}	Singh et al., 2014
pBDGAL4: <i>cCYCLOPS</i> _{min}	
pBDGAL4: <i>cCYCLOPS</i> ^{DD} -1-265	
pBDGAL4: <i>cCYCLOPS</i> -BD	
pBDGAL4: <i>cCYCLOPS</i> -AD	
pBDGAL4: <i>cCYCLOPS</i> -2xAD	
Plasmids for Protein Expression in <i>E. coli</i>	
pETM11-SUMO3: <i>cCYCLOPS</i> -421-518 (=CYCLOPS _{cc})	Phusion PCR product of <i>cCYCLOPS</i> -421-518 coding sequence amplified from pENTR: <i>cCYCLOPS</i> with primers <i>CYCLOPS</i> -421-518_fwd/rev inserted into the expression vector pETM11-SUMO3: <i>GFP</i> (EMBL, Heidelberg, Germany) via <i>AgeI/HindIII</i> sites
pDEST15: <i>cCYCLOPS</i> -BD	Singh et al., 2014
pDEST15: <i>cCYCLOPS</i> ^{WT/DD/AA}	
pDEST15: <i>GST-cCYCLOPS</i> ^{DD} -ΔBD	
pDEST15: <i>cCYCLOPS</i> _{min}	LR reaction (ThermoFisher Scientific, Darmstadt, Germany) of pENTR: <i>cCYC-LOPS</i> _{min} , pENTR: <i>cCYCLOPS</i> _{min} -mR4 or pENTR: <i>cCYCLOPS</i> _{min} -mR1357 and pDEST15:GW (ThermoFisher Scientific, Darmstadt, Germany)
pDEST15: <i>cCYCLOPS</i> _{min} -mR4	
pDEST15: <i>cCYCLOPS</i> _{min} -mR1357	
pDEST17: <i>cCYCLOPS</i> _{min}	LR reaction (ThermoFisher Scientific, Darmstadt, Germany) of pENTR: <i>cCYC-LOPS</i> _{min} , pENTR: <i>cCYCLOPS</i> _{min} -mR4 or pENTR: <i>cCYCLOPS</i> _{min} -mR1357 and pDEST17:GW (ThermoFisher Scientific, Darmstadt, Germany)
pDEST15: <i>cCYCLOPS</i> _{min} -mR4	
pDEST15: <i>cCYCLOPS</i> _{min} -mR1357	
pETM-44: <i>bZIP110</i>	LR reaction (ThermoFisher Scientific, Darmstadt, Germany) of pENTR: <i>bZIP110</i> and pETM-44:GW (EMBL, Heidelberg, Germany)
pKM596: <i>cCCaMK</i>	LR reaction (ThermoFisher Scientific, Darmstadt, Germany) of pENTR: <i>CCaMK</i> (Singh et al., 2014) and pKM596:GW (Addgene, Cat#8837)
pETDUET_6xHis- <i>cCCaMK</i> _Strep- <i>cCYCLOPS</i>	Singh et al., 2014

7. Oligonucleotides

Name	Sequence	Restriction Site
Primer (5'-3')		
<i>3xHA-CYCLOPS-1-254_fwd</i>	ATGGTCTCTCACCATGGCTGGATCTCG	<u>BsaI</u>
<i>3xHA-CYCLOPS-1-254_rev</i>	ATGGTCTCACTTTCTCAAGTTGACTGCTGAGTCTCC	<u>BsaI</u>
<i>CYCLOPS-255-518_fwd</i>	ATGGTCTCTAAAGAAGCTGCAGAAGATGACTTAAATG	<u>BsaI</u>
<i>CYCLOPS-255-518_rev</i>	ATGGTCTCACCTTGCGCCACCCTTTTACAT	<u>BsaI</u>
<i>CYCLOPS^{V455E}_fwd</i>	TGCAAGCTGAGTTGAAGCG	
<i>CYCLOPS^{V455E}_rev</i>	CGCTTCAACTCAGCTTGCA	
<i>CYCLOPS^{L462E}_fwd</i>	GAAGAGAAGGAAGTTCGATCGCTAA	
<i>CYCLOPS^{L462E}_rev</i>	P-GTTTTTCGCACCGCTTCAA	
<i>CYCLOPS^{L469E}_fwd</i>	AAGTTCGATCGGAAAACTCAACTT	
<i>CYCLOPS^{L469E}_rev</i>	AAGTTGAGTTTTTCCGATCGAACTT	
<i>CYCLOPS^{M476E}_fwd</i>	AACTTGTCTTCGAGAATAGAAAGG	
<i>CYCLOPS^{M476E}_rev</i>	CCTTCTATTCTCGAAGGACAAGTT	
<i>CYCLOPS^{Q483L}_fwd</i>	AAGGATTCTGAACTAACAAGCAGATA	
<i>CYCLOPS^{Q483L}_rev</i>	TATCTGCTTTGTTAGTTCAGAATCCTT	
<i>CYCLOPS^{L490E}_fwd</i>	GAACAGAAGCAGAATGAAGAGCTG	
<i>CYCLOPS^{L490E}_rev</i>	P-GTCTTCTATCTGCTTTGTTTGTCA G	
<i>CYCLOPS^{L497E}_fwd</i>	AGAATGAAGAGGAGGCAGATGAAA	
<i>CYCLOPS^{L497E}_rev</i>	TTTCATCTGCCTCCTCTTCATTCT	
<i>CYCLOPS^{L504E}_fwd</i>	GAACCTCGAAGAGATTGAAAGAATTCTATC	
<i>CYCLOPS^{L504E}_rev</i>	P-GCGCTCTTTTTCATCTGCC	
<i>bZIP110^{I114E}_fwd</i>	GAGTTTCATGAGGCTCAGGAGACTC	
<i>bZIP110^{I114E}_rev</i>	GTAGTTGTTGCTTGATTCAATGTAATG	
<i>LI C-D bZIP110_fwd</i>	ATGGTCTCACACCATGGCTTCTCCTGGTGGAG	<u>BsaI</u>
<i>LI C-D bZIP110_rev</i>	ATGGTCTCACCTTTCAATACATTAACATGTCAGCAGC	<u>BsaI</u>
<i>LIII 4-5 ProbZIP110_fwd</i>	ATCGCGTCTCAGCGGCATGATTGGTATGAGAGAAAATTGAGAC	<u>Esp3I</u>
<i>LIII 4-5 ProbZIP110_rev</i>	CGATCGTCTCTCAGAATGCGCTAATTACGAATTACCCTTAC	<u>Esp3I</u>
<i>CCaMK^{D186N}_fwd</i>	CTCAAGATCATGAACTTTGGGTTGAGCTC	
<i>CCaMK^{D186N}_rev</i>	GAGCTCAACCCAAAGTTCATGATCTTGAG	
<i>pAMPATPro35SS:6 xHis-GW_fwd</i>	TCGTA CTACCATCACCATCACCATCACGGTACC GAATCCCCATCAC	
<i>pAMPATPro35SS:6 xHis-GW_rev</i>	P-CATGGTTAATTAACAATTGCTCGA	
<i>CYCLOPS-421-518_fwd</i>	AACCGGTGGAATGAAGGGAGACACCACTAAAAAGC	<u>AgeI</u>
<i>CYCLOPS-421-518_rev</i>	CTAAGCTTTTACATTTTTTTCAGTTTCTGATAGAA TTC	<u>HindIII</u>

EMSA and MST Probes (5'-3')		
<i>CYC-RE_{NIN}</i>	Singh et al., 2016	
<i>CYC-RE_{NIN}</i> <i>palindrome +/- 1 bp</i> <i>(1PAL1)</i>	Singh et al., 2016	
<i>mCYC-RE_{NIN}</i> <i>palindrome +/- 1 bp</i> <i>(1mPAL1)</i>	Singh et al., 2016	
<i>CYC-RE_{NIN}</i> <i>palindrome +4/8 bp</i> <i>(4PAL8)_fwd</i>	CGATT <u>GGCCATGTGGC</u> ACGCAGAGA	
<i>CYC-RE_{NIN}</i> <i>palindrome +4/8 bp</i> <i>(4PAL8)_rev</i>	TCTCTGCGT <u>GGCCACATGGC</u> AATCG	
<i>CYC-RE_{ERN1}</i>	Cerri et al., 2017	
<i>mCYC-RE_{ERN1}</i>	Cerri et al., 2017	
<i>CYC-RE_{RAM1}</i>	Pimprikar et al., 2016	
<i>mCYC-RE_{RAM1}</i>	Pimprikar et al., 2016	

VI. General Discussion

This study was performed to characterize function and structure of CYCLOPS, a hitherto unknown protein of high CC content. *Cyclops* mutants are impaired in RNS and AM formation, thus demonstrating an important role of CYCLOPS for symbiotic development (Yano et al., 2008). Since CYCLOPS interacts and is directly phosphorylated by CCaMK (Yano et al., 2008), the presumed decoder of symbiotic calcium signatures, it was assumed to play an important role in signal transduction leading to symbiosis-associated gene expression. In this context, CYCLOPS function and the specificity mechanisms causing distinct symbiotic responses (e.g. nodule formation in RNS but not during AM) downstream of calcium spiking should be analyzed. A combination of domain analysis, x-ray crystallography and protein-protein/protein-DNA interaction studies has been used as a powerful tool in this study to identify CYCLOPS as a novel type of transcriptional regulator. Depending on the celltype-specific expression and the activational status of CCaMK, heterodimeric interactions with zipper-containing proteins are formed to facilitate specific and high affinity binding of CYCLOPS during root symbiotic development.

1. CYCLOPS is a Novel Type of Transcriptional Regulator

Deletion analyses in *N. benthamiana* and *S. cerevisiae* led to the identification of a CYCLOPS-AD and -BD (Figure 3). The BD was localized to the very C-terminus of CYCLOPS and contains a canonical left-handed CC arrangement with 9 heptad repeats (Figure 8). Zipper-dependent CYCLOPS dimerization, DNA-binding and transactivation via *CYC-RE_{NN}* were tightly connected (Figure 10 and 11). Consistently, mutation within the zipper impaired CYCLOPS' function in RNS. In agreement with the evolutionary conservation of the BD (Figure 4; Delaux et al., 2015), these results highlight the importance of the CYCLOPS zipper for root symbiotic development. A number of TFs including bZIP and bHLH proteins contain a CC dimerization region in the BD (Blackwood and Eisenman, 1991; Jakoby et al., 2002). However, although the zipper structure is similar, the adjacent N-terminal basic region (BR) of CYCLOPS shares no homology (Figure 9), classifying CYCLOPS as novel transcriptional regulator. While the BR of bZIP proteins is highly conserved and contains two clusters of Lys/Arg residues separated by a linker of 10–12 residues, the two predicted NLS of CYCLOPS are 20 amino acids apart and do not contain the invariant Asn and Arg residues of BRs from bZIP proteins (Miotto and Struhl, 2006). Furthermore, BR of bZIPs are positioned about 6

bp N-terminal to and immediately blend into the zipper (Glover and Harrison, 1995; Niu et al., 1999; Wang et al., 2015), while the CYCLOPS CC and NLS are separated by a long stretch of 20 bp harboring two conserved Pro residues, which would disrupt the helical formation (Singh et al., 2014). Despite those differences, the CYCLOPS-BR was just like bZIP BRs unstructured in the crystal, suggesting a helical folding only upon specific DNA-binding (Patel et al., 1990; Weiss et al., 1990).

In agreement with the dimeric conformation of the CYCLOPS-BD, the identified *CYC-REs* are palindromic (Cerri et al., 2017; Pimprikar et al., 2016; Singh et al., 2014). While the *CYC-RE_{RAMI}* has a centre of symmetry, the *CYC-REs* in the *ERN1* and *NIN* promoter harbour a 2 bp overhang in the middle. EMSA experiments confirmed sequence-specific binding of CYCLOPS to the *CYC-REs* (Figure 6 and 7). Although no consensus sequence could be deduced, all sites were enriched in GC-content, one of the most ubiquitously occurring motif in *cis*-regulatory elements (Hapgood et al., 2001). The CYCLOPS-BD revealed a low affinity for the so far identified *CYC-REs*, implying a non-optimal binding site (Figure 11; R. Heermann, unpublished data). In natural promoters many *cis*-regulatory elements deviate from the consensus target sequence, because cooperative interactions with multiple TFs allows dynamic and differential transcriptional responses instead of constant, high-affinity binding (Ramos and Barolo, 2013). Additionally, cooperativity may also expand the repertoire of possible DNA target sequences of CYCLOPS.

The AD is positioned in the central part of CYCLOPS between amino acid 265 and 367 (Figure 3). Characteristic for ADs, the region is evolutionary not well conserved and lacks secondary structure prediction, indicating a folding only open recruitment of the RNA polymerase and mediators to the transcriptional start site (Ptashne and Gann, 1997). The AD contains several serine-rich stretches, which were predicted as putative phosphorylation sites using DIPHOS (Iakoucheva et al., 2004). However, no *in vivo* or *in vitro* phosphorylation sites of CCaMK were identified in this region (Marx et al., 2016; Singh et al., 2014). Interestingly, fusion of the CYCLOPS-AD to the GAL4-BD was sufficient to transactivate via the *upstream activating sequence (UAS)* in *N. benthamiana*, but required a tandem fusion for full activity in *S. cerevisiae* (Figure 3), which demonstrates that recruitment of the transcriptional machinery significantly depends on conformational plasticity and distance between AD and BD. Further studies including mutational analysis of important stretches and putative post-translational modification sites within the AD as well as interaction studies with mediator proteins will be necessary to further characterize the CYCLOPS-AD.

2. The CCaMK/CYCLOPS Complex is a Central Regulator of Symbiotic Development

Analyses of knockout and deregulated versions of CCaMK and CYCLOPS defined the calcium-activatable complex as the master regulator of developmental programming during RNS and AM (Singh et al., 2014; Takeda et al., 2012; Tirichine et al., 2006; Yano et al., 2008). However, activation of the complex by both rhizobial and AM-fungal stimuli raised the question, which mechanisms are in place to ensure encoding of nuclear calcium spiking into appropriate symbiosis-associated gene expression.

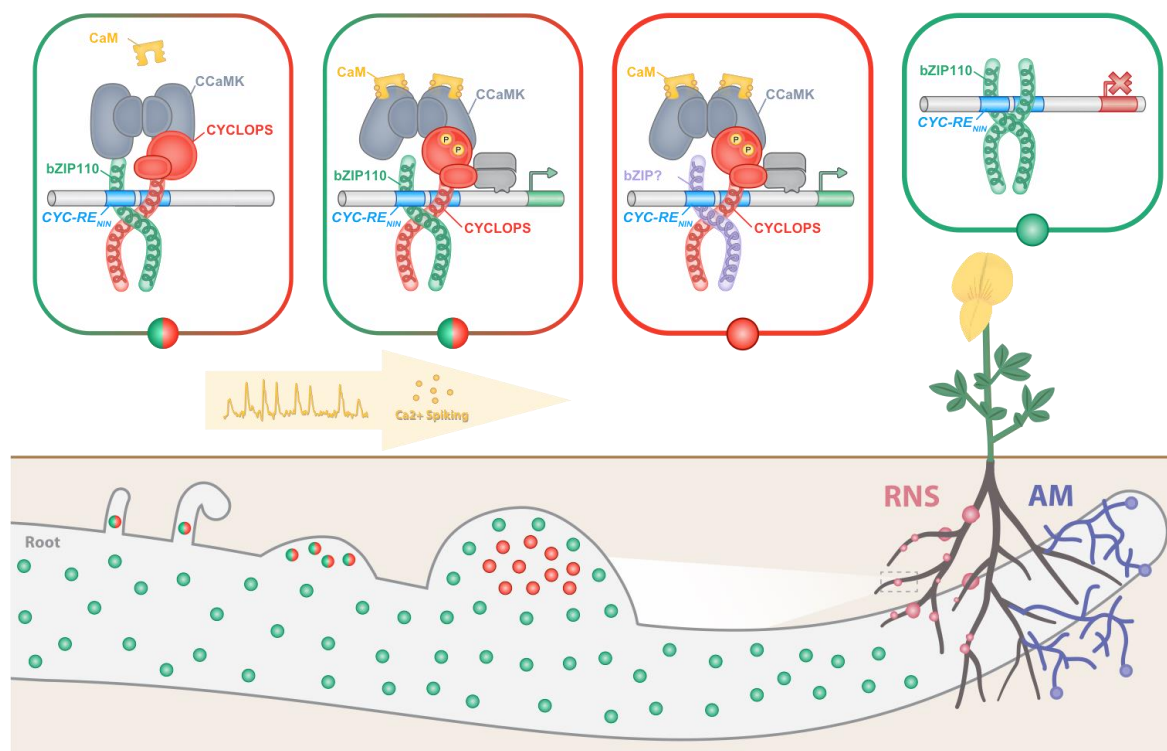


Figure 19. Proposed Function of Heterodimeric CYCLOPS Zipper Complexes in Cell-Specific Development during RNS.

CCaMK/CYCLOPS form a preassembled complex with bZIP110 on a target element in the nodulation-specific *NIN* promoter (*CYC-RE_{NIN}*) (Singh et al., 2014) in nuclei of root hairs. bZIP110 renders the complex inactive and increases DNA-binding affinity to the *CYC-RE_{NIN}*. In response to rhizobial infection, calcium spiking is triggered. CCaMK is activated by binding to calcium/calmodulin (CaM) and phosphorylates CYCLOPS at two critical serines in the N-terminal region, which results in conformational changes and recruitment of the basal transcriptional machinery. *NIN* expression is induced, which reinitiates cell cycle divisions in cortical cells resulting in nodule organogenesis. At later stages of nodule development, bZIP110 and CYCLOPS expression become mutually exclusive. While bZIP110 functions as homodimeric repressor of *NIN* expression in outer nodule cells and the root cortex, CYCLOPS mediates infection processes in the nodule interior, probably by heterodimerization with other zipper-containing proteins. In analogy, heterodimerization of CYCLOPS with AM-related bZIP proteins may regulate cell-specific development during fungal infection. Figure was created by A. Binder.

A model was established, in which specificity-determining factors like bZIP110 were recruited to the CCaMK/CYCLOPS complex (Figure 19). While the CYCLOPS zipper defines assembly of symbiotic regulators, CCaMK controls activity of the complex in response to calcium signaling (Figure 16). In the absence of a symbiotic stimulus, kinase-inactive CCaMK forms a pre-assembled, autoinhibited complex with CYCLOPS and bZIP110 on the *CYC-RE_{NIN}* (Figure 19). In this enclosed conformation, transcriptional activity may be repressed by masking the CYCLOPS-AD inaccessible or by recruiting co-repressors to the complex. Once calcium spiking is triggered, as shown by calcium-independent gain-of function versions of CCaMK, a conformational change is induced, which switches transcriptional inhibition to activation. Though recruitment of the basal transcriptional machinery, the complex may be tethered more stably to DNA and expression of *NIN* can be induced (Figure 19). Similarly, interaction of CYCLOPS with further zipper-containing proteins may mediate cell-specific expression of *ERN1* and *RAM1* and thereby initiate a complex transcriptional network ultimately leading to the main symbiotic programs, nodule organogenesis and bacterial and fungal infection (Figure 20).

Nodule formation requires coordinated reinitiation of cortical cell divisions and involves cytokinin and local auxin signaling (Heckmann et al., 2011; Suzaki et al., 2012; Tirichine et al., 2006). Autoactive CCaMK versions containing the kinase domain only (CCaMK¹⁻³¹⁴) or substitutions at T265 (CCaMK^{T265D/I/A}) and a phosphomimetic version of CYCLOPS (CYCLOPS^{DD}) were sufficient to induce nodule organogenesis in the absence of rhizobia and compensated for the loss of genes involved in calcium-spike generation (Gleason et al., 2006; Madsen et al., 2010; Singh et al., 2014). CCaMK and CYCLOPS act upstream of the *L. japonicus* cytokinin receptor Lotus Histidine Kinase (LHK) 1, as no spontaneous nodules were formed by autoactive CCaMK versions in a loss-of-function *lhk1* mutant, while a gain-of-function LHK1 version was sufficient to activate nodule organogenesis in a *cyclops* mutant background (Madsen et al., 2010). As a direct target of CYCLOPS, *NIN* was identified, which is induced upon cytokinin treatment in the cortex and promotes expression of the *M. truncatula* LHK1 homolog (*CRE1*) (Gonzalez-Rizzo et al., 2006; Heckmann et al., 2011; Singh et al., 2014; Soyano et al., 2013; Vernié et al., 2015). *NIN* regulates expression of two components of the NF-Y complex, *NF-YA1* and *NF-YA2*, which in analogy to their mammalian homologs are believed to trigger entry into the cell division cycle (Laloum et al., 2014; Laloum et al., 2013). In accordance, external application of cytokinin and ectopic expression of either *NF-YA1* and *NF-YB1* or *NIN*

induced the formation of nodule primordia or abnormal lateral root organs, respectively (Gonzalez-Rizzo et al., 2006; Heckmann et al., 2011; Soyano et al., 2013). These results conceptually explain a transcriptional cascade, which is initiated upon CYCLOPS activation, results in *NIN* expression and eventually leads to nodule organogenesis (Figure 20). However, full-sized nodules were not formed by *NIN* overexpression (Soyano et al., 2013), suggesting alternative CYCLOPS target genes beside *NIN*, genetic redundancy at the level of CYCLOPS or parallel transcriptional pathways to regulate nodule organogenesis (Limpens and Bisseling, 2014). These hypotheses are supported by the fact that nodule primordia were formed in *cyclops* mutants upon inoculation with *M. loti* and the finding that CCaMK^{T265D} spontaneously induced nodules in a *cyclops* background (Yano et al., 2008). The GRAS domain TFs NSP1 and NSP2 are required for nodule organogenesis and were genetically positioned downstream of CCaMK in the early NF-signaling pathway (Catoira et al., 2000; Heckmann et al., 2006; Kaló et al., 2005; Murakami et al., 2006; Oldroyd and Long, 2003; Smit et al., 2005). A heterocomplex of both proteins was shown to bind to the *NIN* promoter in close proximity to the CYCLOPS binding site (Hirsch et al., 2009; Jin et al., 2016). While the NSPs were dispensable for CYCLOPS^{DD}-mediated *2xCYC-RENIN:GUS* activation, spontaneous nodules were absent in *nsp* mutants, suggesting a downstream or parallel pathway (Singh et al., 2014). Recently, the GRAS domain protein DELLA was identified as transcriptional activator during RNS, which bridges NSP1/NSP2 to the CCaMK/CYCLOPS complex and may thereby coordinate cooperative binding to the *NIN* promoter (Jin et al., 2016).

Furthermore, CCaMK and CYCLOPS are indispensable for rhizobial infection (Levy et al., 2004; Mitra et al., 2004; Yano et al., 2008). Expression of *SYMREMI*, a scaffolding protein localized to plasma membrane microdomains and involved in IT formation, is dependent on CYCLOPS (Lefebvre et al., 2010; Toth et al., 2012). Also *NIN*, the direct target of CYCLOPS, is involved in transcriptional regulation in the epidermis (Figure 20). *NIN* has been shown to bind and transactivate the *NPL* promoter, an enzyme required for local degradation of plant cell wall pectin during IT formation in root hair cells (Xie et al., 2012), and the *EPR3* promoter, which determines rhizobial compatibility throughout infection (Kawaharada et al., 2015; Kawaharada et al., 2017). Interestingly, the *npl* mutant resembles the *cyclops* phenotype, with the exception that in rare cases aberrantly infected nodules are formed (Xie et al., 2012; Yano et al., 2008).

Also the NIN targets *NF-YA1* and *NF-YA2* are involved in IT formation and progression since *nf-ya1* and *nf-ya2* mutants developed bulbous ITs with thinner cell walls and were severely affected in NF-induced gene expression (Laloum et al., 2014; Laporte et al., 2014). A second *CYC-RE* was identified in the *ERN1* promoter (Cerri et al., 2017). In *M. truncatula*, the double mutant of *ern1* and its closest homolog *ern2* is completely blocked in rhizobial infection and nodule organogenesis, revealing key roles of ERN1/ERN2 at the very early stages of RNS (Cerri et al., 2016). However, not only CYCLOPS tightly regulates the *ERN1* promoter. Using chromatin immunoprecipitation DNA-sequencing (ChIP-seq) analyses, transactivation and EMSAs, also NSP1/NSP2 and NY-A1/NF-YB1 were implicated in the direct activation of *ERN1* (Cerri et al., 2012; Hirsch et al., 2009; Laloum et al., 2014). ERN1 in turn, together with NSP1/NSP2, mediates the expression of *ENOD11*, an early marker gene for NF-induced responses, which is significantly reduced in *cyclops* mutants and encodes a prolin-rich cell wall associated protein (Andriankaja et al., 2007; Boisson-Dernier et al., 2005; Journet et al., 2001). While ERN1 is required for NF-elicited *ENOD11* expression during infection initiation, NSP1/NSP2 regulate *ENOD11* during later stages by binding to a different promoter region than ERN1 (Cerri et al., 2012). NIN was further shown to target the *ENOD11* promoter in proximity to the ERN1/ERN2 recognition sequence, but on the contrary acts as a transcriptional repressor to spatially restrict *ENOD11* expression in the root epidermis (Marsh et al., 2007; Vernié et al., 2015). Therefore, successive activation of *CYCLOPS*, *ERN1*, *NIN* and *NF-YA1* explains a complex transcriptional cascade leading to defined and controlled induction of infection-related genes (Figure 20). Finally, CYCLOPS may also mediate transcriptional responses during rhizobial infection via its interactor DELLA (Jin et al., 2016; Pimprikar et al., 2016). Triple *della* mutants revealed a significantly reduced number of ITs and were reduced in *ERN1*, *NIN* and *Vapyrin* expression (Jin et al., 2016). Recruitment of DELLA to the CCaMK/CYCLOPS may therefore connect the complex to other transcriptional regulators like NSP1/NSP2 and help to fine-tune developmental reprogramming during rhizobial infection.

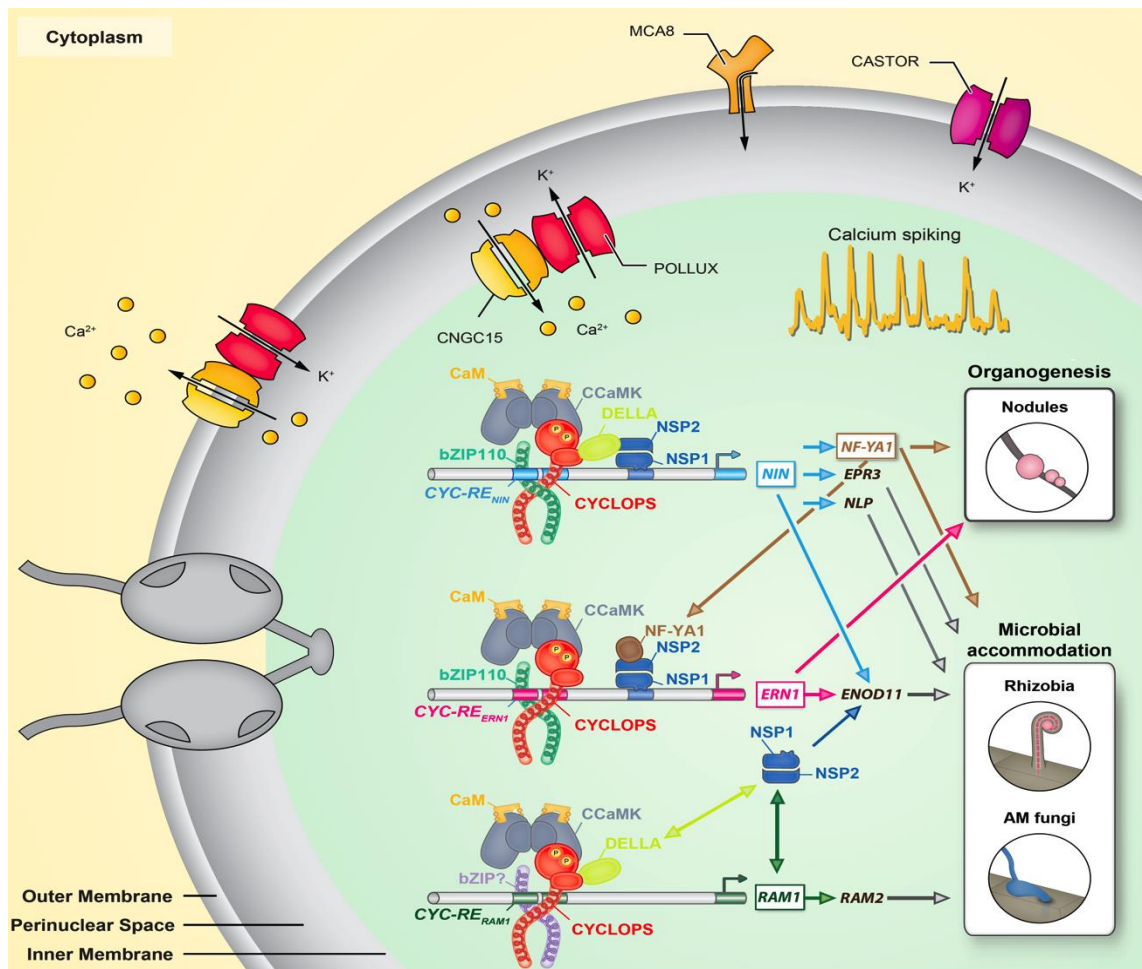


Figure 20. Overview of Transcriptional Networks during Root Symbiotic Development. Perception of rhizobial or AM fungal signals, initiates complex transcriptional networks in nuclei of plant roots, which build on a complex of CCaMK/CYCLOPS as the central regulatory hub in the decision process between both symbiotic developments (Andriankaja et al., 2007; Boisson-Dernier et al., 2005; Bravo et al., 2017; Cerri et al., 2012; Cerri et al., 2016; Gobbato et al., 2012; Gonzalez-Rizzo et al., 2006; Heckmann et al., 2011; Hirsch et al., 2009; Jin et al., 2016; Journet et al., 2001; Kawaharada et al., 2015; Kawaharada et al., 2017; Keymer et al., 2017; Laloum et al., 2014; Liu et al., 2011; Marsh et al., 2007; Pimprikar et al., 2016; Singh et al., 2014; Soyano et al., 2013; Vernié et al., 2015; Xie et al., 2012). The complex is activated after symbiotic calcium spikings in the nucleus generated by calcium (CNGC15 and MCA8) and potassium counter channels (CASTOR and POLLUX) (Binder and Parniske, 2013; Capoen et al., 2011; Charpentier et al., 2016; Venkateshwaran et al., 2012). Binding of CCaMK/CYCLOPS to three target *cis* elements within the *NIN*, *ERN1* and *RAM1* promoter induces important transcriptional cascades eventually leading to nodule organogenesis and microbial accommodation (Cerri et al., 2017; Pimprikar et al., 2016; Singh et al., 2014). Specific and high affinity binding of the complex is mediated by cooperative interactions with zipper-containing transcriptional regulators. Arrow and double arrow indicate transcriptional induction or interaction, respectively. Figure was created by K. Katzer and A. Binder, modified from Singh and Parniske, 2012.

Mutant phenotypes of *ccamk* and *cyclops* also indicate the complex in the transcriptional control during AM development (Perry et al., 2009; Yano et al., 2008). Overexpression of CCaMK¹⁻³¹⁴ initiated expression of AM-related marker genes such as *SbtM1*, *RAM1*, *RAM2* and *Vapyrin* in the absence of AM fungi and calcium spiking and spontaneously induced PPA-like structures in cortical cells (Takeda et al., 2015a; Takeda et al., 2012).

RAM1 was identified as an AM-specific target gene of CYCLOPS (Pimprikar et al., 2016). Accordingly, ectopic expression of *RAM1* could restore arbuscule formation in *cyclops* mutants. *RAM1* interacts with *NSP2* and regulates expression of AM-specific genes including *DWARF27* and *REQUIRED FOR ARBUSCULAR MYCORRHIZATION 2* (*RAM2*), involved in strigolactone, fatty acid and cutin biosynthesis, respectively, and thus explains a transcriptional cascade, in which CYCLOPS acts in a hierarchical succession to initiate AM infection-related processes (Figure 20) (Bravo et al., 2017; Gobbato et al., 2012; Gobbato et al., 2013; Keymer et al., 2017; Liu et al., 2011; Wang et al., 2012). Recently, the CYCLOPS target *NIN* was implicated in AM colonization (Guillotin et al., 2016). Also NF-Ys act as positive regulators of AM and their expression is downregulated during autoregulation of mycorrhization (AOM), a mechanism that regulates the number of fungal infection events via shoot-derived inhibitors similar to AON (Schaarschmidt et al., 2013; Staehelin et al., 2011).

These results suggest that CCaMK/CYCLOPS are part of dynamic and partly overlapping transcriptional cascades, which coordinate appropriate symbiotic development and contribute to root symbiotic specificity (Figure 20). Detailed spatio-temporal information will be important in the future to analyze composition and function of the different signaling complexes in response to calcium spiking in the epidermis and root cortex.

3. Regulation of the CCaMK/CYCLOPS Complex

Size exclusion chromatograms indicated a large complex of CCaMK/CYCLOPS of around 600 kDa, which would account for six CCaMK and CYCLOPS molecules in a 1:1 ratio (V. Gimenez Oya, unpublished data). The stoichiometry is analogous to the CAMKII holoenzyme conformation, where two rings of six CAMKII monomers assemble into a dodecameric structure (Chao et al., 2011), and hints to a similar arrangement for the CCaMK/CYCLOPS complex. This is in agreement with kinetic measurements showing that the amount of autophosphorylation increases exponentially rather than linearly with increasing CCaMK concentrations (Tirichine et al., 2006). Results from several experiments indicated critical conformational changes induced upon calcium spiking, which regulate complex activity and composition. In the following, the influence on differential phosphorylation, interaction with additional complex members and zipper-mediated heterodimerization will be discussed in more detail.

3.1. Phosphorylation

Phosphorylation of CCaMK/CYCLOPS has massive impacts on activity, conformation and composition of the complex and reveals a direct mechanism of nuclear calcium decoding into symbiosis-associated gene expression (Singh et al., 2014). Terminal kinases of signal transduction cascades were shown by ChIP-analyses to form complexes with TFs and components of the chromatin remodeling machinery directly bound to target genes (Edmunds and Mahadevan, 2006; Pokholok et al., 2006). Similarly, CCaMK/CYCLOPS are recruited to *CYC-REs* by specificity-determining factors until calcium-stimulated phosphorylation induces conformational changes with important effects on complex' functioning (Figure 13-16; R. Heermann, unpublished data). CYCLOPS phosphorylation is critical for its DNA-binding and transactivational activity, since WT and phosphoablative CYCLOPS versions were unable to specifically bind to DNA in EMSA experiments (Figure 6) and only weakly transactivated reporter constructs in *N. benthamiana* leaves and *L. japonicus* roots (Pimprikar et al., 2016; Singh et al., 2014). Phosphorylation within ADs and BDs is known to mediate interactions with the transcriptional machinery and to influence sequence-specific DNA-binding (Du and Montminy, 1998; Hunter and Karin, 1992; Li et al., 2011; Smykowski et al., 2015; Szilak et al., 1997). Also heterodimeric preferences between zipper proteins are affected by phosphorylation, thereby controlling target gene specificity (Mair et al., 2015). However, although in total 31 *in vivo* and *in vitro* phosphorylation sites of CYCLOPS were identified (Grimsrud et al., 2010; Marx et al., 2016), none of the sites were located within the CYCLOPS-AD, the C-terminal zipper or the putative BR, which may also be accounted for by weak mass spectrometrical coverage of these regions. Instead two phosphorylation sites in the N-terminal region (S50 and S154) were identified *in vitro* and by large scale phospho-protein analyses in *M. truncatula* (Grimsrud et al., 2010; Marx et al., 2016), which triggered root nodule organogenesis upon phosphomimetic replacement from Ser to Asp (CYCLOPS^{DD}) in the absence of rhizobia and CCaMK (Singh et al., 2014). These findings led to the assumption of an inhibitory conformation, which negatively interferes with the AD and BD of CYCLOPS and keeps the complex in an inactive state (Singh et al., 2014). Accordingly, deletion of the N-terminal domain rendered CYCLOPS autoactive and allowed transactivation of the *2xCYC-RE_{NIN}:GUS* reporter in *N. benthamiana* and *L. japonicus* in the absence of CCaMK or a symbiotic stimulus (Figure 5).

Moreover, phosphorylation at S50 and S154 affected CCaMK/CYCLOPS complex composition. While CYCLOPS^{WT/DD/AA} strongly interacted with CCaMK in FLIM-FRET experiments in *N. benthamiana* (Singh et al., 2014), phosphomimetic replacement increased the interaction with DELLA compared to CYCLOPS^{WT} and CYCLOPS^{AA} in yeast assays (Jin et al., 2016). Besides S50 and S154, there are several indications of further important phosphorylation sites. Expression of CYCLOPS^{DD} in *ccamk* mutant plants was sufficient to restore nodule organogenesis, but did not complement rhizobial infection upon inoculation with *M. loti* (Singh et al., 2014). Moreover, CYCLOPS^{DD} formed a transcriptionally inhibited heterodimer with bZIP110 and required co-expression of deregulated CCaMK versions to terminate repression (Figure 15 and 16; C. Cathebras, unpublished data), indicating that other phosphorylation sites than S50 and S154 were responsible for the release of bZIP110 inhibition.

Interestingly, different patterns of CYCLOPS^{DD} mediated transcriptional activation were observed. While CYCLOPS^{DD} was sufficient to induce expression of the nodulation marker gene *NIN*, it had no activity on the AM-specific *RAMI* promoter (Pimprakar et al., 2016). Furthermore, co-expression of CYCLOPS^{WT} with CCaMK³¹⁴ but not with CCaMK^{T265D} transactivated *RAMI* in *N. benthamiana* leaves, indicating significant differences in symbiotic signal transduction of both CCaMK versions (M.R. Cerri and P. Pimprakar, unpublished data). Indeed, CCaMK³¹⁴ was shown to adopt a conformation with lower, but Ca²⁺/CaM independent phosphorylation activity, and could spontaneously induce nodule organogenesis, PPA-like structures in cortical cells as well as expression of the AM-specific subtilase *SbtMI* (Genre et al., 2008; Gleason et al., 2006; Shimoda et al., 2012; Takeda et al., 2012). However, it only weakly interacted with CYCLOPS and was not sufficient to mediate rhizobial infection (Gleason et al., 2006; Horvath et al., 2011; Shimoda et al., 2012; Takeda et al., 2012). The CCaMK^{T265D} conformation on the other hand had high, but Ca²⁺/CaM dependent phosphorylation activity and interacted strongly with CYCLOPS. It spontaneously induced nodule organogenesis, but still required Ca²⁺/CaM-induced conformational changes and/or further phosphorylation to mediate rhizobial and AM infection (Hayashi et al., 2010; Takeda et al., 2012). These results imply a direct connection between CCaMK activation, differential phosphorylation and specific symbiosis-associated gene expression. Detailed 3D structural information will be inevitable in the future to fully understand and reconstruct the conformational arrangements, which determine signaling specificity at the level of the CCaMK/CYCLOPS complex.

3.2. Additional Complex Components

Reversible protein-protein interactions ensure quick responses to external cues like calcium spiking and can affect localization, activity and functionality of protein complexes. The non-congruent phenotypes of *ccamk* and *cyclops* mutants clearly indicate genetic redundancy at the level of *CYCLOPS* (Levy et al., 2004; Perry et al., 2009; Sathyanarayanan et al., 2000; Yano et al., 2008). While *ccamk* mutants are completely impaired in bacterial infection and nodule formation, *cyclops* mutants still respond with root hair curling around an infection pocket and form nodule primordia (Yano et al., 2008). These findings assume additional factors, which act downstream or parallel to CCaMK and can compensate for the loss of *CYCLOPS*. Several interaction partners of CCaMK and *CYCLOPS* have been identified already:

Binding of Ca^{2+} /CaM to the CaMBD is central for the regulation of CCaMK. It releases the protein from an inhibitory conformation and increases substrate phosphorylation (Gleason et al., 2006; Miller et al., 2013; Tirichine et al., 2006). It may also help in the correct positioning and phosphorylation of downstream targets.

Using the *CYCLOPS* crystal structure in combination with Y2H data of CCaMK, bZIP110 was identified as novel complex component (Figure 12 and 13). Zipper-containing TFs play important roles in many crucial biological processes; however, comprehensive structural and functional characterizations in legumes are limited. ASTRAY/BZF, the HY5 homolog of *L. japonicus* (Nishimura et al., 2002), and *M. truncatula* ATB2 (D'Haeseleer et al., 2010) belonging to the H- and S-group of bZIPs, respectively, show similar phenotypes like *bzip110-1*, indicating bZIP proteins as important transcriptional regulators of root nodule development, but the underlying mechanism remained unknown. In this thesis, bZIP110 was positioned as an early regulator of RNS at a hierarchical level of the CCaMK/*CYCLOPS* complex. Recruitment of bZIP110 to the complex serves two important purposes: assisting in the binding to nodulation-specific target genes and rendering *CYCLOPS* in an inactive conformation until being derepressed upon CCaMK activation (Figure 14 and 16). Besides *CYCLOPS*, bZIP110 may also be involved in the transcriptional regulation, since it was shown for bZIP proteins to engage in diverse interactions with chromatin remodelling factors, co-activators and –repressors (Lively et al., 2004; Miotto and Struhl, 2006). Altogether these unique features classify bZIP110 as an essential complex component to modulate CCaMK/*CYCLOPS* activity during root nodule development.

Binding of CYCLOPS to the GA-inhibitor DELLA integrates hormonal responses with symbiotic signal transduction. DELLA was identified as positive regulator of RNS and AM symbiosis and functions as a bridge protein that connects the CCaMK/CYCLOPS complex with the transcriptional regulators NSP1/NSP2 and NF-YA1 (Floss et al., 2013; Fonouni-Farde et al., 2016; Hirsch et al., 2009; Jin et al., 2016; Maekawa et al., 2009; Pimprikar et al., 2016). The phosphomimetic CYCLOPS^{DD} version revealed an increased interaction with DELLA, suggesting that DELLA recruitment is stimulated by CCaMK phosphorylation (Jin et al., 2016). Likewise, IPD3 (homolog of CYCLOPS in *M. truncatula*) phosphorylation by CCaMK was strongly enhanced in the presence of DELLA (Jin et al., 2016). During RNS, DELLA may be involved in the regulation of *ERN1* and *NIN* expression (Fonouni-Farde et al., 2016; Jin et al., 2016). Since the target sites for CCaMK/CYCLOPS and NSP1/NSP2 in the *ERN1* and *NIN* promoter are in close proximity (Jin et al., 2016; Singh et al., 2014), DELLA mediated bridging of the complexes may have an additive effect on transcriptional activation and promote cooperative binding. This is supported by the findings that NSP1/NSP2- and NF-YA1-induced expression of *ERN1* is enhanced in the presence of DELLA and that induction of spontaneous nodules by a gain-of-function CCaMK version was completely blocked in a *della* double mutant (Fonouni-Farde et al., 2016; Jin et al., 2016). Missing interaction with DELLA and NSP1/NSP2 may also be the reason why a minimal CYCLOPS version lacking the N-terminal domain is sufficient to fully transactivate via the *2xCYC-RE_{NIN}* (Figure 5), but not the full-length *NIN* promoter and did not induce spontaneous nodules in *L. japonicus* (Singh et al., 2014). During arbuscule development, CCaMK/CYCLOPS and DELLA form a complex to regulate *RAM1* expression (Pimprikar et al., 2016). Inhibition of AM formation by GA treatment is therefore caused by degradation of DELLA and subsequent inhibition of *RAM1* expression. Interaction of DELLA with NSP2 (Fonouni-Farde et al., 2016; Jin et al., 2016) may also link NSP1/NSP2 to the transcriptional regulation of *RAM1* and would explain why arbuscule formation was restored by a GA-insensitive DELLA version in the absence of CYCLOPS (Pimprikar et al., 2016).

CCaMK Interacting Protein (CIP) 73, a protein containing a Scythe_N ubiquitin-like domain, was identified as interaction partner of CCaMK in *L. japonicus*, which indicates regulation of CCaMK by ubiquitination (Kang et al., 2011). Ubiquitination plays critical roles in proteasomal degradation, intramolecular autoinhibition and protein trafficking (Betschinger et al., 2005; Jura et al., 2006). CIP73 gets phosphorylated by CCaMK;

however the biological function of this interaction remains to be analyzed.

3.3. Heterodimerization of the CYCLOPS Zipper

Being highly specific and reversible at the same time, the CYCLOPS zipper conformation confers several benefits for the CCaMK/CYCLOPS complex. In contrast to rigid molecules, CCs are intrinsically disordered and get structured upon binding to their complementary partner (Patel et al., 1994; Podust et al., 2001), which enables transient and sequential interactions with multiple TFs. The fast rate of zipper unfolding and re-assembly (Weiss et al., 1990) allows CYCLOPS to rapidly associate with various specificity-determining regulators and thus provides a powerful mechanism to integrate different symbiotic signaling pathways. Distinct spatio-temporal expression pattern of *CYCLOPS* and *bZIP110* were shown to define *NIN* expression during root nodule development (C. Cathebras, unpublished data), thereby preventing tumorous proliferation and uncontrolled infection of root cells caused by unlimited *NIN* levels (Soyano et al., 2013; Yoro et al., 2014). Co-localization of *CYCLOPS* and *bZIP110* in root hairs and inner cortical cells infers a pre-assembled, heterodimeric complex on the *NIN* promoter, which is activated upon rhizobium-induced calcium spikings (Figure 19). Consequently, *NIN* is strongly induced in the epidermis (Radutoiu et al., 2003) and cortical cells of nodule primordia in response to *M. loti* (C. Cathebras, unpublished data). In contrast, expression of homodimeric *bZIP110* in the outer nodule cells and the root cortex inhibits *NIN* expression and thereby confines the number of infected nodule cells and subsequent nodulation events on the root (C. Cathebras, unpublished data). While bZIP110 has a nodulation-specific function (Figure 17 and 18), other zipper-motif containing proteins possibly regulate cell-specific transcriptional reprogramming during AM (Figure 20). Indeed, S-group bZIPs are a large protein family and ubiquitously expressed also in non-leguminous plants (R.E. Andrade, unpublished data). The fact that nodules are formed in a *bzip110-1* mutant background and that *NIN* expression is observed in infected nodule cells in the absence of bZIP110 is likely accounted for by genetically redundant bZIP family members (Figure 17; M.R. Cerri and C. Cathebras, unpublished data).

4. Summary and Outlook

The CCaMK/CYCLOPS complex emerged as the main regulatory hub in the developmental decision process between RNS and AM. With the identification of

CYCLOPS as a novel class of DNA-binding transcriptional regulator, it was possible to link symbiosis-induced calcium signals to specific transcriptional responses.

CCaMK/CYCLOPS form a large oligomeric arrangement, which undergoes significant conformational changes by sensing low or high level of calcium concentrations. Closely connected to these structural changes are differential phosphorylation of CCaMK/CYCLOPS and recruitment or release of additional complex components, which in their entirety create specificity in root symbiotic signaling. In the future, methods like x-ray crystallography and cryo-electron microscopy will provide valuable insights into the 3D structure of the complex and will help to further understand the mechanism of calcium signal transduction.

The CYCLOPS zipper conformation as docking site as well as interactions with bridge proteins like DELLA connect the CCaMK/CYCLOPS complex with other transcriptional regulators and thereby helps to integrate different signaling pathways during root symbiotic development. *In vivo* studies like proximity-dependent biotinylation of proteins (BioID) and co-IP will be useful to find new complex members and analyze complex compositions under varying symbiotic stimuli. Particularly the identification of an AM-induced zipper protein analogous to bZIP110 will increase the current understanding of cell-specific gene expression in response to fungal infection.

So far three *cis* regulatory elements with GC-rich content (*CYC-RE*) were identified in the nodulation-specific *NIN* and *ERN1* and the AM-specific *RAM1* promoter, which underlines the key regulatory role of CYCLOPS in symbiotic programming leading to nodule organogenesis, bacterial and fungal infection. Considering the severity of the *cyclops* phenotype and the continuously increasing number of complex interaction partners, additional targets of CYCLOPS are very likely. Genome-wide identification of regulatory promoter regions in different plant species using techniques like ChIP-Seq will further increase our current knowledge about the transcriptional network that governs specific root symbiotic development. Combined with *in vitro* methods like DNA Immunoprecipitation (DIP) or Systematic Evolution of Ligands by Exponential Enrichment (SELEX) it will be possible to derive a consensus binding sequence for CYCLOPS. This may also facilitate crystallization of the CYCLOPS-BD bound to DNA and help to get structural information of how specific binding is achieved.

VII. References

- Abdel-Lateif, K., Bogusz, D., and Hocher, V.** (2012). The role of flavonoids in the establishment of plant roots endosymbioses with arbuscular mycorrhiza fungi, rhizobia and Frankia bacteria. *Plant Signal Behaviour* 7, 636-641.
- Akiyama, K., Matsuzaki, K., and Hayashi, H.** (2005). Plant sesquiterpenes induce hyphal branching in arbuscular mycorrhizal fungi. *Nature* 435, 824-827.
- Amor, B.B., Shaw, S.L., Oldroyd, G.E., Maillet, F., Penmetsa, R.V., Cook, D., Long, S.R., Denarie, J., and Gough, C.** (2003). The *NFP* locus of *Medicago truncatula* controls an early step of Nod factor signal transduction upstream of a rapid calcium flux and root hair deformation. *Plant Journal* 34, 495-506.
- Andriankaja, A., Boisson-Dernier, A., Frances, L., Sauviac, L., Jauneau, A., Barker, D.G., and de Carvalho-Niebel, F.** (2007). AP2-ERF transcription factors mediate Nod factor dependent *Mt ENOD11* activation in root hairs via a novel *cis*-regulatory motif. *Plant Cell* 19, 2866-2885.
- Antolin-Llovera, M., Ried, M.K., Binder, A., and Parniske, M.** (2012). Receptor kinase signaling pathways in plant-microbe interactions. *Annual Review of Phytopathology* 50, 451-473.
- Antolin-Llovera, M., Ried, M.K., and Parniske, M.** (2014). Cleavage of the SYMBIOSIS RECEPTOR-LIKE KINASE ectodomain promotes complex formation with Nod factor receptor 5. *Current Biology* 24, 422-427.
- Arrighi, J.F., Barre, A., Ben Amor, B., Bersoult, A., Soriano, L.C., Mirabella, R., de Carvalho-Niebel, F., Journet, E.P., Gherardi, M., Huguet, T., et al.** (2006). The *Medicago truncatula* lysin motif-receptor-like kinase gene family includes *NFP* and new nodule-expressed genes. *Plant Physiology* 142, 265-279.
- Bago, B., Pfeffer, P.E., Abubaker, J., Jun, J., Allen, J.W., Brouillette, J., Douds, D.D., Lammers, P.J., and Shachar-Hill, Y.** (2003). Carbon export from arbuscular mycorrhizal roots involves the translocation of carbohydrate as well as lipid. *Plant Physiology* 131, 1496-1507.
- Bapaume, L., and Reinhardt, D.** (2012). How membranes shape plant symbioses: signaling and transport in nodulation and arbuscular mycorrhiza. *Frontiers in Plant Science* 3, 223.
- Besserer, A., Puech-Pagès, V., Kiefer, P., Gomez-Roldan, V., Jauneau, A., Roy, S., Portais, J.-C., Roux, C., Bécard, G., and Séjalon-Delmas, N.** (2006). Strigolactones stimulate arbuscular mycorrhizal fungi by activating mitochondria. *PLOS Biology* 4, e226.
- Betschinger, J., Eisenhaber, F., and Knoblich, J.A.** (2005). Phosphorylation-induced autoinhibition regulates the cytoskeletal protein lethal (2) giant larvae. *Current Biology* 15, 276-282.
- Binder, A., Lambert, J., Morbitzer, R., Popp, C., Ott, T., Lahaye, T., and Parniske, M.** (2014). A modular plasmid assembly kit for multigene expression, gene silencing and silencing rescue in plants. *PLOS ONE* 9, e88218.
- Binder, A., and Parniske, M.** (2013). Analysis of the *Lotus japonicus* nuclear pore NUP107-160 subcomplex reveals pronounced structural plasticity and functional redundancy. *Frontiers in Plant Science* 4, 552.
- Blackwood, E.M., and Eisenman, R.N.** (1991). Max: a helix-loop-helix zipper protein that forms a sequence-specific DNA-binding complex with Myc. *Science* 251, 1211-1217.
- Boisson-Dernier, A., Andriankaja, A., Chabaud, M., Niebel, A., Journet, E.P., Barker, D.G., and de Carvalho-Niebel, F.** (2005). *MtENOD11* gene activation during rhizobial infection and mycorrhizal arbuscule development requires a common AT-rich-containing regulatory sequence. *Molecular Plant-Microbe Interactions* 18, 1269-1276.

- Bonfante, P., and Requena, N.** (2011). Dating in the dark: how roots respond to fungal signals to establish arbuscular mycorrhizal symbiosis. *Current Opinion in Plant Biology* *14*, 451-457.
- Bonvin, C., Etter, B., Udert, K.M., Frossard, E., Nanzer, S., Tamburini, F., and Oberson, A.** (2015). Plant uptake of phosphorus and nitrogen recycled from synthetic source-separated urine. *Ambio* *44*, S217-S227.
- Bravo, A., Brands, M., Wewer, V., Dormann, P., and Harrison, M.J.** (2017). Arbuscular mycorrhiza-specific enzymes FatM and RAM2 fine-tune lipid biosynthesis to promote development of arbuscular mycorrhiza. *New Phytologist* *214*, 1631-1645.
- Broghammer, A., Krusell, L., Blaise, M., Sauer, J., Sullivan, J.T., Maolanon, N., Vinther, M., Lorentzen, A., Madsen, E.B., Jensen, K.J., et al.** (2012). Legume receptors perceive the rhizobial lipochitin oligosaccharide signal molecules by direct binding. *Proceedings of the National Academy of Sciences of the United States of America* *109*, 13859-13864.
- Buendia, L., Wang, T., Girardin, A., and Lefebvre, B.** (2016). The LysM receptor-like kinase SILYK10 regulates the arbuscular mycorrhizal symbiosis in tomato. *New Phytologist* *210*, 184-195.
- Capoen, W., Sun, J., Wysham, D., Otegui, M.S., Venkateshwaran, M., Hirsch, S., Miwa, H., Downie, J.A., Morris, R.J., Ane, J.M., et al.** (2011). Nuclear membranes control symbiotic calcium signaling of legumes. *Proceedings of the National Academy of Sciences of the United States of America* *108*, 14348-14353.
- Cardenas, L., Martinez, A., Sanchez, F., and Quinto, C.** (2008). Fast, transient and specific intracellular ROS changes in living root hair cells responding to Nod factors (NFs). *Plant Journal* *56*, 802-813.
- Carotenuto, G., Chabaud, M., Miyata, K., Capozzi, M., Takeda, N., Kaku, H., Shibuya, N., Nakagawa, T., Barker, D.G., and Genre, A.** (2017). The rice LysM receptor-like kinase *OsCERK1* is required for the perception of short-chain chitin oligomers in arbuscular mycorrhizal signaling. *New Phytologist* *214*, 1440-1446.
- Catoira, R., Galera, C., de Billy, F., Penmetsa, R.V., Journet, E.P., Maillet, F., Rosenberg, C., Cook, D., Gough, C., and Denarie, J.** (2000). Four genes of *Medicago truncatula* controlling components of a nod factor transduction pathway. *Plant Cell* *12*, 1647-1666.
- Cerri, M.R., Frances, L., Kelner, A., Fournier, J., Middleton, P.H., Auriac, M.C., Mysore, K.S., Wen, J., Erard, M., Barker, D.G., et al.** (2016). The symbiosis-related ERN transcription factors act in concert to coordinate rhizobial host root infection. *Plant Physiology* *171*, 1037-1054.
- Cerri, M.R., Frances, L., Laloum, T., Auriac, M.C., Niebel, A., Oldroyd, G.E., Barker, D.G., Fournier, J., and de Carvalho-Niebel, F.** (2012). *Medicago truncatula* ERN transcription factors: regulatory interplay with NSP1/NSP2 GRAS factors and expression dynamics throughout rhizobial infection. *Plant Physiology* *160*, 2155-2172.
- Cerri, M.R., Wang, Q., Stolz, P., Folgmann, J., Frances, L., Katzer, K., Li, X., Heckmann, A.B., Wang, T.L., Downie, J.A., et al.** (2017). The *ERN1* transcription factor gene is a target of the CCaMK/CYCLOPS complex and controls rhizobial infection in *Lotus japonicus*. *New Phytologist* *215*, 323-337.
- Chabaud, M., Genre, A., Sieberer, B.J., Faccio, A., Fournier, J., Novero, M., Barker, D.G., and Bonfante, P.** (2011). Arbuscular mycorrhizal hyphopodia and germinated spore exudates trigger Ca²⁺ spiking in the legume and nonlegume root epidermis. *New Phytologist* *189*, 347-355.

- Chao, L.H., Stratton, M.M., Lee, I.H., Rosenberg, O.S., Levitz, J., Mandell, D.J., Kortemme, T., Groves, J.T., Schulman, H., and Kuriyan, J.** (2011). A mechanism for tunable autoinhibition in the structure of a human Ca²⁺/calmodulin-dependent kinase II holoenzyme. *Cell* 146, 732-745.
- Charpentier, M., Sun, J., Vaz Martins, T., Radhakrishnan, G.V., Findlay, K., Soumpourou, E., Thouin, J., Very, A.A., Sanders, D., Morris, R.J., et al.** (2016). Nuclear-localized cyclic nucleotide-gated channels mediate symbiotic calcium oscillations. *Science* 352, 1102-1105.
- Chen, T., Zhu, H., Ke, D., Cai, K., Wang, C., Gou, H., Hong, Z., and Zhang, Z.** (2012). A MAP kinase kinase interacts with SymRK and regulates nodule organogenesis in *Lotus japonicus*. *Plant Cell* 24, 823-838.
- Choudhury, S.R., and Pandey, S.** (2015). Phosphorylation-dependent regulation of G-protein cycle during nodule formation in soybean. *Plant Cell* 27, 3260-3276.
- Ciaccio, N.A., and Laurence, J.S.** (2009). Effects of disulfide bond formation and protein helicity on the aggregation of activating transcription factor 5. *Molecular Pharmaceutics* 6, 1205-1215.
- Colebatch, G., Desbrosses, G., Ott, T., Krusell, L., Montanari, O., Kloska, S., Kopka, J., and Udvardi, M.K.** (2004). Global changes in transcription orchestrate metabolic differentiation during symbiotic nitrogen fixation in *Lotus japonicus*. *Plant Journal* 39, 487-512.
- Combiér, J.P., Frugier, F., de Billy, F., Boualem, A., El-Yahyaoui, F., Moreau, S., Vernié, T., Ott, T., Gamas, P., Crespi, M., et al.** (2006). *MtHAP2-1* is a key transcriptional regulator of symbiotic nodule development regulated by microRNA169 in *Medicago truncatula*. *Genes & Development* 20, 3084-3088.
- D'Haeseleer, K., De Keyser, A., Goormachtig, S., and Holsters, M.** (2010). Transcription factor *MtATB2*: about nodulation, sucrose and senescence. *Plant and Cell Physiology* 51, 1416-1424.
- De Koninck, P., and Schulman, H.** (1998). Sensitivity of CaM kinase II to the frequency of Ca²⁺ oscillations. *Science* 279, 227-230.
- Deakin, W.J., and Broughton, W.J.** (2009). Symbiotic use of pathogenic strategies: rhizobial protein secretion systems. *Nature Reviews Microbiology* 7, 312-320.
- Delaux, P.M., Becard, G., and Combiér, J.P.** (2013). NSP1 is a component of the Myc signaling pathway. *The New Phytologist* 199, 59-65.
- Delaux, P.M., Radhakrishnan, G.V., Jayaraman, D., Cheema, J., Malbreil, M., Volkening, J.D., Sekimoto, H., Nishiyama, T., Melkonian, M., Pokorný, L., et al.** (2015). Algal ancestor of land plants was preadapted for symbiosis. *Proceedings of the National Academy of Sciences of the United States of America* 112, 13390-13395.
- Delaux, P.M., Varala, K., Edger, P.P., Coruzzi, G.M., Pires, J.C., and Ane, J.M.** (2014). Comparative phylogenomics uncovers the impact of symbiotic associations on host genome evolution. *PLOS Genetics* 10, e1004487.
- Demchenko, K., Winzer, T., Stougaard, J., Parniske, M., and Pawlowski, K.** (2004). Distinct roles of *Lotus japonicus* SYMRK and SYM15 in root colonization and arbuscule formation. *New Phytologist* 163, 381-392.
- Den Herder, G., Yoshida, S., Antolin-Llovera, M., Ried, M.K., and Parniske, M.** (2012). *Lotus japonicus* E3 ligase SEVEN IN ABSENTIA4 destabilizes the symbiosis receptor-like kinase SYMRK and negatively regulates rhizobial infection. *Plant Cell* 24, 1691-1707.
- Denessiouk, K., Permyakov, S., Denesyuk, A., Permyakov, E., and Johnson, M.S.** (2014). Two structural motifs within canonical EF-hand calcium-binding domains identify five different classes of calcium buffers and sensors. *PLOS ONE* 9, e109287.

Díaz, C.L., Grønlund, M., Schlaman, H.R.M., and Spaink, H.P. (2005). Induction of hairy roots for symbiotic gene expression studies. In *Lotus japonicus* Handbook, A.J. Márquez, ed. (Dordrecht: Springer Netherlands), 261-277.

Downie, J.A., and Walker, S.A. (1999). Plant responses to nodulation factors. *Current Opinion in Plant Biology* 2, 483-489.

Doyle, J.J. (2011). Phylogenetic perspectives on the origins of nodulation. *Molecular Plant-Microbe Interactions* 24, 1289-1295.

Du, K.Y., and Montminy, M. (1998). CREB is a regulatory target for the protein kinase Akt/PKB. *Journal of Biological Chemistry* 273, 32377-32379.

Edmunds, J.W., and Mahadevan, L.C. (2006). Protein kinases seek close encounters with active genes. *Science* 313, 449-451.

Ehrhardt, D.W., Wais, R., and Long, S.R. (1996). Calcium spiking in plant root hairs responding to rhizobium nodulation signals. *Cell* 85, 673-681.

Etzler, M.E., Kalsi, G., Ewing, N.N., Roberts, N.J., Day, R.B., and Murphy, J.B. (1999). A nod factor binding lectin with apyrase activity from legume roots. *Proceedings of the National Academy of Sciences of the United States of America* 96, 5856-5861.

Feilotter, H.E., Hannon, G.J., Ruddell, C.J., and Beach, D. (1994). Construction of an improved host strain for two hybrid screening. *Nucleic Acids Research* 22, 1502-1503.

Fitter, A.H., Gilligan, C.A., Hollingworth, K., Kleczkowski, A., Twyman, R.M., Pitchford, J.W., and Programme, N.S.B. (2005). Biodiversity and ecosystem function in soil. *Functional Ecology* 19, 369-377.

Flammer, J.R., Popova, K.N., and Pflum, M.K. (2006). Cyclic AMP response element-binding protein (CREB) and CAAT/enhancer-binding protein beta (C/EBPbeta) bind chimeric DNA sites with high affinity. *Biochemistry* 45, 9615-9623.

Floss, D.S., Gomez, S.K., Park, H.J., MacLean, A.M., Muller, L.M., Bhattarai, K.K., Levesque-Tremblay, V., Maldonado-Mendoza, I.E., and Harrison, M.J. (2017). A transcriptional program for arbuscule degeneration during AM symbiosis is regulated by MYB1. *Current Biology* 27, 1206-1212.

Floss, D.S., Levy, J.G., Levesque-Tremblay, V., Pumplin, N., and Harrison, M.J. (2013). DELLA proteins regulate arbuscule formation in arbuscular mycorrhizal symbiosis. *Proceedings of the National Academy of Sciences of the United States of America* 110, e5025-5034.

Fonouni-Farde, C., Tan, S., Baudin, M., Brault, M., Wen, J., Mysore, K.S., Niebel, A., Frugier, F., and Diet, A. (2016). DELLA-mediated gibberellin signalling regulates Nod factor signalling and rhizobial infection. *Nature Communications* 7, 12636.

Fournier, J., Teillet, A., Chabaud, M., Ivanov, S., Genre, A., Limpens, E., de Carvalho-Niebel, F., and Barker, D.G. (2015). Remodeling of the infection chamber before infection thread formation reveals a two-step mechanism for rhizobial entry into the host legume root hair. *Plant Physiology* 167, 1233-1242.

Fournier, J., Timmers, A.C., Sieberer, B.J., Jauneau, A., Chabaud, M., and Barker, D.G. (2008). Mechanism of infection thread elongation in root hairs of *Medicago truncatula* and dynamic interplay with associated rhizobial colonization. *Plant Physiology* 148, 1985-1995.

Fukai, E., Soyano, T., Umehara, Y., Nakayama, S., Hirakawa, H., Tabata, S., Sato, S., and Hayashi, M. (2012). Establishment of a *Lotus japonicus* gene tagging population using the exon-targeting endogenous retrotransposon LORE1. *Plant Journal* 69, 720-730.

Genre, A., Chabaud, M., Balergue, C., Puech-Pagès, V., Novero, M., Rey, T., Fournier, J., Rochange, S., Bécard, G., and Bonfante, P. (2013). Short-chain chitin oligomers from arbuscular mycorrhizal fungi trigger nuclear Ca²⁺ spiking in *Medicago truncatula* roots and their production is enhanced by strigolactone. *New Phytologist* 198, 190-202.

- Genre, A., Chabaud, M., Faccio, A., Barker, D.G., and Bonfante, P.** (2008). Prepenetration apparatus assembly precedes and predicts the colonization patterns of arbuscular mycorrhizal fungi within the root cortex of both *Medicago truncatula* and *Daucus carota*. *Plant Cell* 20, 1407-1420.
- Genre, A., and Russo, G.** (2016). Does a common pathway transduce symbiotic signals in plant-microbe interactions? *Frontiers in Plant Science* 7, doi: 10.3389/fpls.2016.00096.
- Gianinazzi, S., Gollotte, A., Binet, M.N., van Tuinen, D., Redecker, D., and Wipf, D.** (2010). Agroecology: the key role of arbuscular mycorrhizas in ecosystem services. *Mycorrhiza* 20, 519-530.
- Gleason, C., Chaudhuri, S., Yang, T., Munoz, A., Poovaiah, B.W., and Oldroyd, G.E.** (2006). Nodulation independent of rhizobia induced by a calcium-activated kinase lacking autoinhibition. *Nature* 441, 1149-1152.
- Glover, J.N., and Harrison, S.C.** (1995). Crystal structure of the heterodimeric bZIP transcription factor c-Fos-c-Jun bound to DNA. *Nature* 373, 257-261.
- Gobbato, E., Marsh, J.F., Vernié, T., Wang, E., Maillet, F., Kim, J., Miller, J.B., Sun, J., Bano, S.A., Ratet, P., et al.** (2012). A GRAS-type transcription factor with a specific function in mycorrhizal signaling. *Current Biology* 22, 2236-2241.
- Gobbato, E., Wang, E., Higgins, G., Bano, S.A., Henry, C., Schultze, M., and Oldroyd, G.E.** (2013). *RAM1* and *RAM2* function and expression during arbuscular mycorrhizal symbiosis and *Aphanomyces euteiches* colonization. *Plant Signal Behaviour* 8, doi: 10.4161/psb.26049.
- Gonzalez-Rizzo, S., Crespi, M., and Frugier, F.** (2006). The *Medicago truncatula* CRE1 cytokinin receptor regulates lateral root development and early symbiotic interaction with *Sinorhizobium meliloti*. *Plant Cell* 18, 2680-2693.
- Gough, C., and Cullimore, J.** (2011). Lipo-chitooligosaccharide signaling in endosymbiotic plant-microbe interactions. *Molecular Plant-Microbe Interactions* 24, 867-878.
- Granqvist, E., Sun, J.H., Op den Camp, R., Pujic, P., Hill, L., Normand, P., Morris, R.J., Downie, J.A., Geurts, R., and Oldroyd, G.E.D.** (2015). Bacterial-induced calcium oscillations are common to nitrogen-fixing associations of nodulating legumes and nonlegumes. *New Phytologist* 207, 551-558.
- Grimsrud, P.A., den Os, D., Wenger, C.D., Swaney, D.L., Schwartz, D., Sussman, M.R., Ane, J.M., and Coon, J.J.** (2010). Large-scale phosphoprotein analysis in *Medicago truncatula* roots provides insight into *in vivo* kinase activity in legumes. *Plant Physiology* 152, 19-28.
- Groth, M., Takeda, N., Perry, J., Uchida, H., Draxl, S., Brachmann, A., Sato, S., Tabata, S., Kawaguchi, M., Wang, T.L., et al.** (2010). NENA, a *Lotus japonicus* homolog of Sec13, is required for rhizodermal infection by arbuscular mycorrhiza fungi and rhizobia but dispensable for cortical endosymbiotic development. *Plant Cell* 22, 2509-2526.
- Guillotin, B., Couzigou, J.M., and Combier, J.P.** (2016). NIN is involved in the regulation of arbuscular mycorrhizal symbiosis. *Frontiers in Plant Science* 7, 1704.
- Gust, A.A., Willmann, R., Desaki, Y., Grabherr, H.M., and Nurnberger, T.** (2012). Plant LysM proteins: modules mediating symbiosis and immunity. *Trends in Plant Science* 17, 495-502.
- Gutjahr, C., Novero, M., Guether, M., Montanari, O., Udvardi, M., and Bonfante, P.** (2009). Presymbiotic factors released by the arbuscular mycorrhizal fungus *Gigaspora margarita* induce starch accumulation in *Lotus japonicus* roots. *New Phytologist* 183, 53-61.
- Gutjahr, C., and Parniske, M.** (2013). Cell and developmental biology of arbuscular mycorrhiza symbiosis. *Annual Review of Cell and Developmental Biology* 29, 593-617.

- Gutjahr, C., and Parniske, M.** (2017). Cell biology: control of partner lifetime in a plant-fungus relationship. *Current Biology* 27, R420-R423.
- Gutjahr, C., and Paszkowski, U.** (2013). Multiple control levels of root system remodeling in arbuscular mycorrhizal symbiosis. *Frontiers in Plant Science* 4, 204.
- Handberg, K., and Stougaard, J.** (1992). *Lotus japonicus*, an autogamous, diploid legume species for classical and molecular genetics. *Plant Journal* 2, 487-496.
- Haney, C.H., and Long, S.R.** (2010). Plant flotillins are required for infection by nitrogen-fixing bacteria. *Proceedings of the National Academy of Sciences of the United States of America* 107, 478-483.
- Haney, C.H., Riely, B.K., Tricoli, D.M., Cook, D.R., Ehrhardt, D.W., and Long, S.R.** (2011). Symbiotic rhizobia bacteria trigger a change in localization and dynamics of the *Medicago truncatula* receptor kinase LYK3. *Plant Cell* 23, 2774-2787.
- Hapgood, J.P., Riedemann, J., and Scherer, S.D.** (2001). Regulation of gene expression by GC-rich DNA *cis*-elements. *Cell Biology International* 25, 17-31.
- Harrison, M.J.** (2005). Signaling in the arbuscular mycorrhizal symbiosis. *Annual Review of Microbiology* 59, 19-42.
- Harrison, M.J.** (2012). Cellular programs for arbuscular mycorrhizal symbiosis. *Current Opinion in Plant Biology* 15, 691-698.
- Hayashi, T., Banba, M., Shimoda, Y., Kouchi, H., Hayashi, M., and Imaizumi-Anraku, H.** (2010). A dominant function of CCaMK in intracellular accommodation of bacterial and fungal endosymbionts. *Plant Journal* 63, 141-154.
- Heckmann, A.B., Lombardo, F., Miwa, H., Perry, J.A., Bunnell, S., Parniske, M., Wang, T.L., and Downie, J.A.** (2006). *Lotus japonicus* nodulation requires two GRAS domain regulators, one of which is functionally conserved in a non-legume. *Plant Physiology* 142, 1739-1750.
- Heckmann, A.B., Sandal, N., Bek, A.S., Madsen, L.H., Jurkiewicz, A., Nielsen, M.W., Tirichine, L., and Stougaard, J.** (2011). Cytokinin induction of root nodule primordia in *Lotus japonicus* is regulated by a mechanism operating in the root cortex. *Molecular Plant-Microbe Interactions* 24, 1385-1395.
- Hirsch, S., Kim, J., Munoz, A., Heckmann, A.B., Downie, J.A., and Oldroyd, G.E.** (2009). GRAS proteins form a DNA binding complex to induce gene expression during nodulation signaling in *Medicago truncatula*. *Plant Cell* 21, 545-557.
- Horvath, B., Yeun, L.H., Domonkos, A., Halasz, G., Gobbato, E., Ayaydin, F., Miro, K., Hirsch, S., Sun, J., Tadege, M., et al.** (2011). *Medicago truncatula* IPD3 is a member of the common symbiotic signaling pathway required for rhizobial and mycorrhizal symbioses. *Molecular Plant-Microbe Interactions* 24, 1345-1358.
- Howarth, R.W., and Marino, R.** (2006). Nitrogen as the limiting nutrient for eutrophication in coastal marine ecosystems: Evolving views over three decades. *Limnology and Oceanography* 51, 364-376.
- Howarth, R.W., Swaney, D.P., Boyer, E.W., Marino, R., Jaworski, N., and Goodale, C.** (2006). The influence of climate on average nitrogen export from large watersheds in the Northeastern United States. *Biogeochemistry* 79, 163-186.
- Hrabak, E.M., Chan, C.W., Gribskov, M., Harper, J.F., Choi, J.H., Halford, N., Kudla, J., Luan, S., Nimmo, H.G., Sussman, M.R., et al.** (2003). The *Arabidopsis* CDPK-SnRK superfamily of protein kinases. *Plant Physiology* 132, 666-680.
- Hudmon, A., and Schulman, H.** (2002). Neuronal CA²⁺/calmodulin-dependent protein kinase II: the role of structure and autoregulation in cellular function. *Annual Review of Biochemistry* 71, 473-510.
- Hunter, T., and Karin, M.** (1992). The regulation of transcription by phosphorylation. *Cell* 70, 375-387.

Hwang, J.H., Ellingson, S.R., and Roberts, D.M. (2010). Ammonia permeability of the soybean nodulin 26 channel. *FEBS Letters* 584, 4339-4343.

Iakoucheva, L.M., Radivojac, P., Brown, C.J., O'Connor, T.R., Sikes, J.G., Obradovic, Z., and Dunker, A.K. (2004). The importance of intrinsic disorder for protein phosphorylation. *Nucleic Acids Research* 32, 1037-1049.

Imaizumi-Anraku, H., Takeda, N., Charpentier, M., Perry, J., Miwa, H., Umehara, Y., Kouchi, H., Murakami, Y., Mulder, L., Vickers, K., et al. (2005). Plastid proteins crucial for symbiotic fungal and bacterial entry into plant roots. *Nature* 433, 527-531.

Jakobsen, I., and Rosendahl, L. (1990). Carbon flow into soil and external hyphae from roots of mycorrhizal cucumber plants. *New Phytologist* 115, 77-83.

Jakoby, M., Weisshaar, B., Droge-Laser, W., Vicente-Carbajosa, J., Tiedemann, J., Kroj, T., Parcy, F., and b, Z.I.P.R.G. (2002). bZIP transcription factors in *Arabidopsis*. *Trends in Plant Science* 7, 106-111.

Jarsch, I.K., and Ott, T. (2011). Perspectives on remorin proteins, membrane rafts, and their role during plant-microbe interactions. *Molecular Plant-Microbe Interactions* 24, 7-12.

Javot, H., Penmetsa, R.V., Terzaghi, N., Cook, D.R., and Harrison, M.J. (2007a). A *Medicago truncatula* phosphate transporter indispensable for the arbuscular mycorrhizal symbiosis. *Proceedings of the National Academy of Sciences of the United States of America* 104, 1720-1725.

Javot, H., Pumplin, N., and Harrison, M.J. (2007b). Phosphate in the arbuscular mycorrhizal symbiosis: transport properties and regulatory roles. *Plant, Cell & Environment* 30, 310-322.

Jerabek-Willemsen, M., Wienken, C.J., Braun, D., Baaske, P., and Duhr, S. (2011). Molecular interaction studies using microscale thermophoresis. *Assay and Drug Development Technologies* 9, 342-353.

Jin, Y., Liu, H., Luo, D., Yu, N., Dong, W., Wang, C., Zhang, X., Dai, H., Yang, J., and Wang, E. (2016). DELLA proteins are common components of symbiotic rhizobial and mycorrhizal signalling pathways. *Nature Communications* 7, 12433.

Johnson, P.F., Sterneck, E., and Williams, S.C. (1993). Activation domains of transcriptional regulatory proteins. *Journal of Nutritional Biochemistry* 4, 386-398.

Jones, K.M., Kobayashi, H., Davies, B.W., Taga, M.E., and Walker, G.C. (2007). How rhizobial symbionts invade plants: the *Sinorhizobium-Medicago* model. *Nature Reviews Microbiology* 5, 619-633.

Jones, K.M., Sharopova, N., Lohar, D.P., Zhang, J.Q., VandenBosch, K.A., and Walker, G.C. (2008). Differential response of the plant *Medicago truncatula* to its symbiont *Sinorhizobium meliloti* or an exopolysaccharide-deficient mutant. *Proceedings of the National Academy of Sciences of the United States of America* 105, 704-709.

Journet, E.P., El-Gachtouli, N., Vernoud, V., de Billy, F., Pichon, M., Dedieu, A., Arnould, C., Morandi, D., Barker, D.G., and Gianinazzi-Pearson, V. (2001). *Medicago truncatula* *ENOD11*: a novel RPRP-encoding *early nodulin* gene expressed during mycorrhization in arbuscule-containing cells. *Molecular Plant-Microbe Interactions* 14, 737-748.

Jura, N., Scotto-Lavino, E., Sobczyk, A., and Bar-Sagi, D. (2006). Differential modification of Ras proteins by ubiquitination. *Molecular Cell* 21, 679-687.

Kaló, P., Gleason, C., Edwards, A., Marsh, J., Mitra, R.M., Hirsch, S., Jakab, J., Sims, S., Long, S.R., and Rogers, J. (2005). Nodulation signaling in legumes requires NSP2, a member of the GRAS family of transcriptional regulators. *Science* 308, 1786-1789.

Kanamori, N., Madsen, L.H., Radutoiu, S., Frantescu, M., Quistgaard, E.M., Miwa, H., Downie, J.A., James, E.K., Felle, H.H., Haaning, L.L., et al. (2006). A nucleoporin is required for induction of Ca²⁺ spiking in legume nodule development and essential for rhizobial and fungal symbiosis. *Proceedings of the National Academy of Sciences of the United States of America* *103*, 359-364.

Kang, H., Zhu, H., Chu, X., Yang, Z., Yuan, S., Yu, D., Wang, C., Hong, Z., and Zhang, Z. (2011). A novel interaction between CCaMK and a protein containing the Scythe_N ubiquitin-like domain in *Lotus japonicus*. *Plant Physiology* *155*, 1312-1324.

Kawaharada, Y., Kelly, S., Nielsen, M.W., Hjuler, C.T., Gysel, K., Muszynski, A., Carlson, R.W., Thygesen, M.B., Sandal, N., Asmussen, M.H., et al. (2015). Receptor-mediated exopolysaccharide perception controls bacterial infection. *Nature* *523*, 308-312.

Kawaharada, Y., Nielsen, M.W., Kelly, S., James, E.K., Andersen, K.R., Rasmussen, S.R., Fuchtbauer, W., Madsen, L.H., Heckmann, A.B., Radutoiu, S., et al. (2017). Differential regulation of the Epr3 receptor coordinates membrane-restricted rhizobial colonization of root nodule primordia. *Nature Communications* *8*, 14534.

Ke, D., Fang, Q., Chen, C., Zhu, H., Chen, T., Chang, X., Yuan, S., Kang, H., Ma, L., Hong, Z., et al. (2012). The small GTPase ROP6 interacts with NFR5 and is involved in nodule formation in *Lotus japonicus*. *Plant Physiology* *159*, 131-143.

Kevei, Z., Lougnon, G., Mergaert, P., Horvath, G.V., Kereszt, A., Jayaraman, D., Zaman, N., Marcel, F., Regulski, K., Kiss, G.B., et al. (2007). 3-hydroxy-3-methylglutaryl coenzyme a reductase 1 interacts with NORK and is crucial for nodulation in *Medicago truncatula*. *Plant Cell* *19*, 3974-3989.

Keymer, A., Pimprikar, P., Wewer, V., Huber, C., Brands, M., Bucerius, S., Delaux, P.-M., Klingl, V., von Roepenack-Lahaye, E., Wang, T.L., et al. (2017). Lipid transfer from plants to arbuscular mycorrhiza fungi. *bioRxiv*, doi: <https://doi.org/10.1101/143883>.

Kistner, C., and Parniske, M. (2002). Evolution of signal transduction in intracellular symbiosis. *Trends in Plant Science* *7*, 511-518.

Kistner, C., Winzer, T., Pitzschke, A., Mulder, L., Sato, S., Kaneko, T., Tabata, S., Sandal, N., Stougaard, J., and Webb, K.J. (2005). Seven *Lotus japonicus* genes required for transcriptional reprogramming of the root during fungal and bacterial symbiosis. *Plant Cell Online* *17*, 2217-2229.

Koncz, C., and Schell, J. (1986). The Promoter of TI-DNA gene 5 controls the tissue-specific expression of chimeric genes carried by a novel type of *Agrobacterium* binary vector. *Molecular and General Genetics* *204*, 383-396.

Krusell, L., Krause, K., Ott, T., Desbrosses, G., Kramer, U., Sato, S., Nakamura, Y., Tabata, S., James, E.K., Sandal, N., et al. (2005). The sulfate transporter SST1 is crucial for symbiotic nitrogen fixation in *Lotus japonicus* root nodules. *Plant Cell* *17*, 1625-1636.

Laloum, T., Baudin, M., Frances, L., Lepage, A., Billault-Penneteau, B., Cerri, M.R., Ariel, F., Jardinaud, M.F., Gamas, P., de Carvalho-Niebel, F., et al. (2014). Two CCAAT-box-binding transcription factors redundantly regulate early steps of the legume-rhizobia endosymbiosis. *Plant Journal* *79*, 757-768.

Laloum, T., De Mita, S., Gamas, P., Baudin, M., and Niebel, A. (2013). CCAAT-box binding transcription factors in plants: Y so many? *Trends in Plant Science* *18*, 157-166.

Laporte, P., Lepage, A., Fournier, J., Catrice, O., Moreau, S., Jardinaud, M.F., Mun, J.H., Larrainzar, E., Cook, D.R., Gamas, P., et al. (2014). The CCAAT box-binding transcription factor NF-YA1 controls rhizobial infection. *Journal of Experimental Botany* *65*, 481-494.

Lauressergues, D., Delaux, P.M., Formey, D., Lelandais-Briere, C., Fort, S., Cottaz, S., Becard, G., Niebel, A., Roux, C., and Combier, J.P. (2012). The microRNA miR171h modulates arbuscular mycorrhizal colonization of *Medicago truncatula* by targeting *NSP2*. *Plant Journal* *72*, 512-522.

- Lazo, G.R., Stein, P.A., and Ludwig, R.A.** (1991). A DNA transformation-competent *Arabidopsis* genomic library in *Agrobacterium*. *Biotechnology* 9, 963-967.
- Lefebvre, B., Timmers, T., Mbengue, M., Moreau, S., Herve, C., Toth, K., Bittencourt-Silvestre, J., Klaus, D., Deslandes, L., Godiard, L., et al.** (2010). A remorin protein interacts with symbiotic receptors and regulates bacterial infection. *Proceedings of the National Academy of Sciences of the United States of America* 107, 2343-2348.
- Leong, S.A., Williams, P.H., and Ditta, G.S.** (1985). Analysis of the 5' regulatory region of the gene for delta-aminolevulinic-acid synthetase of *Rhizobium meliloti*. *Nucleic Acids Research* 13, 5965-5976.
- Levy, J., Bres, C., Geurts, R., Chalhoub, B., Kulikova, O., Duc, G., Journet, E.P., Ane, J.M., Lauber, E., Bisseling, T., et al.** (2004). A putative Ca²⁺ and calmodulin-dependent protein kinase required for bacterial and fungal symbioses. *Science* 303, 1361-1364.
- Li, X.Y., Zhan, X.R., Liu, X.M., and Wang, X.C.** (2011). CREB is a regulatory target for the protein kinase Akt/PKB in the differentiation of pancreatic ductal cells into islet beta-cells mediated by hepatocyte growth factor. *Biochemical and Biophysical Research Communications* 404, 711-716.
- Liao, J., Singh, S., Hossain, M.S., Andersen, S.U., Ross, L., Bonetta, D., Zhou, Y., Sato, S., Tabata, S., Stougaard, J., et al.** (2012). Negative regulation of CCaMK is essential for symbiotic infection. *Plant Journal* 72, 572-584.
- Limpens, E., and Bisseling, T.** (2014). CYCLOPS: a new vision on rhizobium-induced nodule organogenesis. *Cell Host & Microbe* 15, 127-129.
- Limpens, E., Franken, C., Smit, P., Willemse, J., Bisseling, T., and Geurts, R.** (2003). LysM domain receptor kinases regulating rhizobial Nod factor-induced infection. *Science* 302, 630-633.
- Liu, J., Blaylock, L.A., Endre, G., Cho, J., Town, C.D., VandenBosch, K.A., and Harrison, M.J.** (2003). Transcript profiling coupled with spatial expression analyses reveals genes involved in distinct developmental stages of an arbuscular mycorrhizal symbiosis. *Plant Cell* 15, 2106-2123.
- Liu, W., Kohlen, W., Lillo, A., Op den Camp, R., Ivanov, S., Hartog, M., Limpens, E., Jamil, M., Smaczniak, C., Kaufmann, K., et al.** (2011). Strigolactone biosynthesis in *Medicago truncatula* and rice requires the symbiotic GRAS-type transcription factors NSP1 and NSP2. *Plant Cell* 23, 3853-3865.
- Lively, T.N., Nguyen, T.N., Galasinski, S.K., and Goodrich, J.A.** (2004). The basic leucine zipper domain of c-Jun functions in transcriptional activation through interaction with the N terminus of human TATA-binding protein-associated factor-1 (human TAF(II)250). *Journal of Biological Chemistry* 279, 26257-26265.
- Lupas, A., Van Dyke, M., and Stock, J.** (1991). Predicting coiled coils from protein sequences. *Science* 252, 1162-1164.
- Ma, F., Lu, R., Liu, H., Shi, B., Zhang, J., Tan, M., Zhang, A., and Jiang, M.** (2012). Nitric oxide-activated calcium/calmodulin-dependent protein kinase regulates the abscisic acid-induced antioxidant defence in maize. *Journal of Experimental Botany* 63, 4835-4847.
- Maathuis, F.J.** (2009). Physiological functions of mineral macronutrients. *Current Opinion in Plant Biology* 12, 250-258.
- Madsen, E.B., Madsen, L.H., Radutoiu, S., Olbryt, M., Rakwalska, M., Szczyglowski, K., Sato, S., Kaneko, T., Tabata, S., Sandal, N., et al.** (2003). A receptor kinase gene of the LysM type is involved in legume perception of rhizobial signals. *Nature* 425, 637-640.

Madsen, L.H., Tirichine, L., Jurkiewicz, A., Sullivan, J.T., Heckmann, A.B., Bek, A.S., Ronson, C.W., James, E.K., and Stougaard, J. (2010). The molecular network governing nodule organogenesis and infection in the model legume *Lotus japonicus*. *Nature Communications* 1, 10.

Maekawa, T., Kusakabe, M., Shimoda, Y., Sato, S., Tabata, S., Murooka, Y., and Hayashi, M. (2008). Polyubiquitin promoter-based binary vectors for overexpression and gene silencing in *Lotus japonicus*. *Molecular Plant-Microbe Interactions* 21, 375-382.

Maekawa, T., Maekawa-Yoshikawa, M., Takeda, N., Imaizumi-Anraku, H., Murooka, Y., and Hayashi, M. (2009). Gibberellin controls the nodulation signaling pathway in *Lotus japonicus*. *Plant Journal* 58, 183-194.

Maillet, F., Poinot, V., André, O., Puech-Pagès, V., Haouy, A., Gueunier, M., Cromer, L., Giraudet, D., Formey, D., and Niebel, A. (2011). Fungal lipochitooligosaccharide symbiotic signals in arbuscular mycorrhiza. *Nature* 469, 58-63.

Mair, A., Pedrotti, L., Wurzinger, B., Anrather, D., Simeunovic, A., Weiste, C., Valerio, C., Dietrich, K., Kirchler, T., Nagele, T., et al. (2015). SnRK1-triggered switch of bZIP63 dimerization mediates the low-energy response in plants. *Elife* 4, doi: 10.7554/eLife.05828.

Mantovani, R. (1999). The molecular biology of the CCAAT-binding factor NF-Y. *Gene* 239, 15-27.

Markmann, K., Giczey, G., and Parniske, M. (2008). Functional adaptation of a plant receptor-kinase paved the way for the evolution of intracellular root symbioses with bacteria. *PLOS Biology* 6, e68.

Marsh, J.F., Rakocevic, A., Mitra, R.M., Brocard, L., Sun, J., Eschstruth, A., Long, S.R., Schultze, M., Ratet, P., and Oldroyd, G.E. (2007). *Medicago truncatula* NIN is essential for rhizobial-independent nodule organogenesis induced by autoactive calcium/calmodulin-dependent protein kinase. *Plant Physiology* 144, 324-335.

Marx, H., Minogue, C.E., Jayaraman, D., Richards, A.L., Kwiecien, N.W., Siahpirani, A.F., Rajasekar, S., Maeda, J., Garcia, K., Del Valle-Echevarria, A.R., et al. (2016). A proteomic atlas of the legume *Medicago truncatula* and its nitrogen-fixing endosymbiont *Sinorhizobium meliloti*. *Nature Biotechnology* 34, 1198-1205.

Masclaux-Daubresse, C., Daniel-Vedele, F., Dechorgnat, J., Chardon, F., Gaufichon, L., and Suzuki, A. (2010). Nitrogen uptake, assimilation and remobilization in plants: challenges for sustainable and productive agriculture. *Annals Botany* 105, 1141-1157.

Mbengue, M., Camut, S., de Carvalho-Niebel, F., Deslandes, L., Froidure, S., Klaus-Heisen, D., Moreau, S., Rivas, S., Timmers, T., Herve, C., et al. (2010). The *Medicago truncatula* E3 ubiquitin ligase PUB1 interacts with the LYK3 symbiotic receptor and negatively regulates infection and nodulation. *Plant Cell* 22, 3474-3488.

Mcgonigle, T.P., Miller, M.H., Evans, D.G., Fairchild, G.L., and Swan, J.A. (1990). A new method which gives an objective-measure of colonization of roots by vesicular arbuscular mycorrhizal fungi. *New Phytologist* 115, 495-501.

Menge, D.N., Hedin, L.O., and Pacala, S.W. (2012). Nitrogen and phosphorus limitation over long-term ecosystem development in terrestrial ecosystems. *PLOS ONE* 7, e42045.

Messinese, E., Mun, J.H., Yeun, L.H., Jayaraman, D., Rouge, P., Barre, A., Lougnon, G., Schornack, S., Bono, J.J., Cook, D.R., et al. (2007). A novel nuclear protein interacts with the symbiotic DMI3 calcium- and calmodulin-dependent protein kinase of *Medicago truncatula*. *Molecular Plant-Microbe Interactions* 20, 912-921.

Middleton, P.H., Jakab, J., Penmetsa, R.V., Starker, C.G., Doll, J., Kaló, P., Prabhu, R., Marsh, J.F., Mitra, R.M., and Kereszt, A. (2007). An ERF transcription factor in *Medicago truncatula* that is essential for Nod factor signal transduction. *Plant Cell Online* 19, 1221-1234.

- Miller, J.B., Pratap, A., Miyahara, A., Zhou, L., Bornemann, S., Morris, R.J., and Oldroyd, G.E.** (2013). Calcium/Calmodulin-dependent protein kinase is negatively and positively regulated by calcium, providing a mechanism for decoding calcium responses during symbiosis signaling. *Plant Cell* 25, 5053-5066.
- Miotto, B., and Struhl, K.** (2006). Differential gene regulation by selective association of transcriptional coactivators and bZIP DNA-binding domains. *Molecular and Cellular Biology* 26, 5969-5982.
- Mitra, R.M., Gleason, C.A., Edwards, A., Hadfield, J., Downie, J.A., Oldroyd, G.E., and Long, S.R.** (2004). A Ca²⁺/calmodulin-dependent protein kinase required for symbiotic nodule development: Gene identification by transcript-based cloning. *Proceedings of the National Academy of Sciences of the United States of America* 101, 4701-4705.
- Miwa, H., Sun, J., Oldroyd, G.E., and Downie, J.A.** (2006a). Analysis of calcium spiking using a cameleon calcium sensor reveals that nodulation gene expression is regulated by calcium spike number and the developmental status of the cell. *Plant Journal* 48, 883-894.
- Miwa, H., Sun, J., Oldroyd, G.E., and Downie, J.A.** (2006b). Analysis of Nod-factor-induced calcium signaling in root hairs of symbiotically defective mutants of *Lotus japonicus*. *Molecular Plant-Microbe Interactions* 19, 914-923.
- Moitra, J., Szilak, L., Krylov, D., and Vinson, C.** (1997). Leucine is the most stabilizing aliphatic amino acid in the d position of a dimeric leucine zipper coiled coil. *Biochemistry* 36, 12567-12573.
- Morieri, G., Martinez, E.A., Jarynowski, A., Driguez, H., Morris, R., Oldroyd, G.E., and Downie, J.A.** (2013). Host-specific Nod-factors associated with *Medicago truncatula* nodule infection differentially induce calcium influx and calcium spiking in root hairs. *New Phytologist* 200, 656-662.
- Murakami, Y., Miwa, H., Imaizumi-Anraku, H., Kouchi, H., Downie, J.A., Kawaguchi, M., and Kawasaki, S.** (2006). Positional cloning identifies *Lotus japonicus* NSP2, a putative transcription factor of the GRAS family, required for *NIN* and *ENOD40* gene expression in nodule initiation. *DNA Research* 13, 255-265.
- Murray, J.D.** (2011). Invasion by invitation: rhizobial infection in legumes. *Molecular Plant-Microbe Interactions* 24, 631-639.
- Murray, J.D., Karas, B.J., Sato, S., Tabata, S., Amyot, L., and Szczygłowski, K.** (2007). A cytokinin perception mutant colonized by rhizobium in the absence of nodule organogenesis. *Science* 315, 101-104.
- Niemietz, C.M., and Tyerman, S.D.** (2000). Channel-mediated permeation of ammonia gas through the peribacteroid membrane of soybean nodules. *FEBS Letters* 465, 110-114.
- Nishimura, R., Ohmori, M., Fujita, H., and Kawaguchi, M.** (2002). A *Lotus* basic leucine zipper protein with a RING-finger motif negatively regulates the developmental program of nodulation. *Proceedings of the National Academy of Sciences of the United States of America* 99, 15206-15210.
- Niu, X., Renshaw-Gegg, L., Miller, L., and Guiltinan, M.J.** (1999). Bipartite determinants of DNA-binding specificity of plant basic leucine zipper proteins. *Plant Molecular Biology* 41, 1-13.
- Offringa, I.A., Melchers, L.S., Regensburgtuink, A.J.G., Costantino, P., Schilperoort, R.A., and Hooykaas, P.J.J.** (1986). Complementation of *Agrobacterium-Tumefaciens* Tumor-Inducing *Aux* Mutants by Genes from the Tr-Region of the Ri Plasmid of *Agrobacterium-Rhizogenes*. *P Natl Acad Sci USA* 83, 6935-6939.
- Oldroyd, G.E.** (2013). Speak, friend, and enter: signalling systems that promote beneficial symbiotic associations in plants. *Nature Reviews Microbiology* 11, 252-263.

- Oldroyd, G.E., and Downie, J.A.** (2008). Coordinating nodule morphogenesis with rhizobial infection in legumes. *Annual Review of Plant Biology* 59, 519-546.
- Oldroyd, G.E., and Long, S.R.** (2003). Identification and characterization of *nodulation-signaling pathway 2*, a gene of *Medicago truncatula* involved in Nod actor signaling. *Plant Physiology* 131, 1027-1032.
- Oldroyd, G.E., Murray, J.D., Poole, P.S., and Downie, J.A.** (2011). The rules of engagement in the legume-rhizobial symbiosis. *Annual Review of Genetics* 45, 119-144.
- Op den Camp, R., Streng, A., De Mita, S., Cao, Q., Polone, E., Liu, W., Ammiraju, J.S., Kudrna, D., Wing, R., Untergasser, A., et al.** (2011). LysM-type mycorrhizal receptor recruited for rhizobium symbiosis in nonlegume *Parasponia*. *Science* 331, 909-912.
- Ortu, G., Balestrini, R., Pereira, P.A., Becker, J.D., Küster, H., and Bonfante, P.** (2012). Plant genes related to gibberellin biosynthesis and signaling are differentially regulated during the early stages of AM fungal interactions. *Molecular Plant*, 951-954.
- Ovchinnikova, E., Journet, E.P., Chabaud, M., Cosson, V., Ratet, P., Duc, G., Fedorova, E., Liu, W., den Camp, R.O., Zhukov, V., et al.** (2011). IPD3 controls the formation of nitrogen-fixing symbiosomes in pea and *Medicago Spp.* *Molecular Plant-Microbe Interactions* 24, 1333-1344.
- Parniske, M.** (2008). Arbuscular mycorrhiza: the mother of plant root endosymbioses. *Nature Reviews Microbiology* 6, 763-775.
- Patel, L., Abate, C., and Curran, T.** (1990). Altered protein conformation on DNA binding by Fos and Jun. *Nature* 347, 572-575.
- Patel, L.R., Curran, T., and Kerppola, T.K.** (1994). Energy transfer analysis of Fos-Jun dimerization and DNA binding. *Proceedings of the National Academy of Sciences of the United States of America* 91, 7360-7364.
- Patil, S., Takezawa, D., and Poovaiah, B.W.** (1995). Chimeric plant calcium/calmodulin-dependent protein kinase gene with a neural visinin-like calcium-binding domain. *Proceedings of the National Academy of Sciences of the United States of America* 92, 4897-4901.
- Pawlowski, K., and Demchenko, K.N.** (2012). The diversity of actinorhizal symbiosis. *Protoplasma* 249, 967-979.
- Peck, M.C., Fisher, R.F., and Long, S.R.** (2006). Diverse flavonoids stimulate NodD1 binding to *nod gene* promoters in *Sinorhizobium meliloti*. *Journal of Bacteriology* 188, 5417-5427.
- Perret, X., Staehelin, C., and Broughton, W.J.** (2000). Molecular basis of symbiotic promiscuity. *Microbiology and Molecular Biology Reviews* 64, 180-201.
- Perry, J., Brachmann, A., Welham, T., Binder, A., Charpentier, M., Groth, M., Haage, K., Markmann, K., Wang, T.L., and Parniske, M.** (2009). TILLING in *Lotus japonicus* identified large allelic series for symbiosis genes and revealed a bias in functionally defective ethyl methanesulfonate alleles toward glycine replacements. *Plant Physiology* 151, 1281-1291.
- Pimprikar, P., Carbonnel, S., Paries, M., Katzer, K., Klingl, V., Bohmer, M.J., Karl, L., Floss, D.S., Harrison, M.J., Parniske, M., et al.** (2016). A CcMK-CYCLOPS-DELLA complex activates transcription of *RAMI* to regulate arbuscule branching. *Current Biology* 26, 1126.
- Podust, L.M., Krezel, A.M., and Kim, Y.** (2001). Crystal structure of the CCAAT box/enhancer-binding protein beta activating transcription factor-4 basic leucine zipper heterodimer in the absence of DNA. *Journal of Biological Chemistry* 276, 505-513.
- Pogenberg, V., Consani Textor, L., Vanhille, L., Holton, S.J., Sieweke, M.H., and Wilmanns, M.** (2014). Design of a bZip transcription factor with homo/heterodimer-induced DNA-binding preference. *Structure* 22, 466-477.

- Pokholok, D.K., Zeitlinger, J., Hannett, N.M., Reynolds, D.B., and Young, R.A.** (2006). Activated signal transduction kinases frequently occupy target genes. *Science* 313, 533-536.
- Prell, J., White, J.P., Bourdes, A., Bunnewell, S., Bongaerts, R.J., and Poole, P.S.** (2009). Legumes regulate rhizobium bacteroid development and persistence by the supply of branched-chain amino acids. *Proceedings of the National Academy of Sciences of the United States of America* 106, 12477-12482.
- Ptashne, M., and Gann, A.** (1997). Transcriptional activation by recruitment. *Nature* 386, 569-577.
- Pumplin, N., and Harrison, M.J.** (2009). Live-cell imaging reveals periarbuscular membrane domains and organelle location in *Medicago truncatula* roots during arbuscular mycorrhizal symbiosis. *Plant Physiology* 151, 809-819.
- Pumplin, N., Mondo, S.J., Topp, S., Starker, C.G., Gantt, J.S., and Harrison, M.J.** (2010). *Medicago truncatula* VAPYRIN is a novel protein required for arbuscular mycorrhizal symbiosis. *Plant Journal* 61, 482-494.
- Qiu, L., Lin, J.S., Xu, J., Sato, S., Parniske, M., Wang, T.L., Downie, J.A., and Xie, F.** (2015). SCARN a novel class of SCAR protein that is required for root-hair infection during legume nodulation. *PLOS Genetics* 11, e1005623.
- Radutoiu, S., Madsen, L.H., Madsen, E.B., Felle, H.H., Umehara, Y., Grønlund, M., Sato, S., Nakamura, Y., Tabata, S., and Sandal, N.** (2003). Plant recognition of symbiotic bacteria requires two LysM receptor-like kinases. *Nature* 425, 585-592.
- Radutoiu, S., Madsen, L.H., Madsen, E.B., Jurkiewicz, A., Fukai, E., Quistgaard, E.M., Albrechtsen, A.S., James, E.K., Thirup, S., and Stougaard, J.** (2007). LysM domains mediate lipochitin-oligosaccharide recognition and *NFR* genes extend the symbiotic host range. *EMBO Journal* 26, 3923-3935.
- Ramos, A.I., and Barolo, S.** (2013). Low-affinity transcription factor binding sites shape morphogen responses and enhancer evolution. *Philosophical Transactions of the Royal Society of London Series B, Biological Sciences* 368, doi: 10.1098/rstb.2013.0018.
- Rasmussen, S.R., Fuchtbauer, W., Novero, M., Volpe, V., Malkov, N., Genre, A., Bonfante, P., Stougaard, J., and Radutoiu, S.** (2016). Intraradical colonization by arbuscular mycorrhizal fungi triggers induction of a lipochitooligosaccharide receptor. *Scientific Reports* 6, 29733.
- Rellos, P., Pike, A.C., Niesen, F.H., Salah, E., Lee, W.H., von Delft, F., and Knapp, S.** (2010). Structure of the CaMKII δ /calmodulin complex reveals the molecular mechanism of CaMKII kinase activation. *PLOS Biology* 8, e1000426.
- Remy, W., Taylor, T.N., Hass, H., and Kerp, H.** (1994). Four hundred-million-year-old vesicular arbuscular mycorrhizae. *Proceedings of the National Academy of Sciences of the United States of America* 91, 11841-11843.
- Riley, L.G., Ralston, G.B., and Weiss, A.S.** (1996). Multimer formation as a consequence of separate homodimerization domains: the human c-Jun leucine zipper is a transplantable dimerization module. *Protein Engineering* 9, 223-230.
- Roberts, N.J., Morieri, G., Kalsi, G., Rose, A., Stiller, J., Edwards, A., Xie, F., Gresshoff, P.M., Oldroyd, G.E., Downie, J.A., et al.** (2013). Rhizobial and mycorrhizal symbioses in *Lotus japonicus* require lectin nucleotide phosphohydrolase, which acts upstream of calcium signaling. *Plant Physiology* 161, 556-567.
- Routray, P., Miller, J.B., Du, L., Oldroyd, G., and Poovaiah, B.W.** (2013). Phosphorylation of S344 in the calmodulin-binding domain negatively affects CCaMK function during bacterial and fungal symbioses. *Plant Journal* 76, 287-296.

Saha, S., Paul, A., Herring, L., Dutta, A., Bhattacharya, A., Samaddar, S., Goshe, M.B., and DasGupta, M. (2016). Gatekeeper tyrosine phosphorylation of SYMRK is essential for synchronizing the epidermal and cortical responses in root nodule symbiosis. *Plant Physiology* *171*, 71-81.

Saito, K., Yoshikawa, M., Yano, K., Miwa, H., Uchida, H., Asamizu, E., Sato, S., Tabata, S., Imaizumi-Anraku, H., Umehara, Y., et al. (2007). NUCLEOPORIN85 is required for calcium spiking, fungal and bacterial symbioses, and seed production in *Lotus japonicus*. *Plant Cell* *19*, 610-624.

Sathyanarayanan, P.V., Cremo, C.R., and Poovaiah, B.W. (2000). Plant chimeric Ca²⁺/Calmodulin-dependent protein kinase. Role of the neural visinin-like domain in regulating autophosphorylation and calmodulin affinity. *Journal of Biological Chemistry* *275*, 30417-30422.

Schaarschmidt, S., Gresshoff, P.M., and Hause, B. (2013). Analyzing the soybean transcriptome during autoregulation of mycorrhization identifies the transcription factors *GmNF-YA1a/b* as positive regulators of arbuscular mycorrhization. *Genome Biology* *14*, R62.

Schachtman, D.P., Reid, R.J., and Ayling, S.M. (1998). Phosphorus uptake by plants: From soil to cell. *Plant Physiology* *116*, 447-453.

Schauser, L., Roussis, A., Stiller, J., and Stougaard, J. (1999). A plant regulator controlling development of symbiotic root nodules. *Nature* *402*, 191-195.

Schoumans, O.F., Bouraoui, F., Kabbe, C., Oenema, O., and van Dijk, K.C. (2015). Phosphorus management in Europe in a changing world. *Ambio* *44*, 180-192.

Schüßler, A., Schwarzott, D., and Walker, C. (2001). A new fungal phylum, the Glomeromycota: phylogeny and evolution. *Mycological Research* *105*, 1413-1421.

Shaw, S.L., and Long, S.R. (2003). Nod factor elicits two separable calcium responses in *Medicago truncatula* root hair cells. *Plant Physiology* *131*, 976-984.

Shi, B., Ni, L., Zhang, A., Cao, J., Zhang, H., Qin, T., Tan, M., Zhang, J., and Jiang, M. (2012). *OsDMI3* is a novel component of abscisic acid signaling in the induction of antioxidant defense in leaves of rice. *Molecular Plant* *5*, 1359-1374.

Shimoda, Y., Han, L., Yamazaki, T., Suzuki, R., Hayashi, M., and Imaizumi-Anraku, H. (2012). Rhizobial and fungal symbioses show different requirements for calmodulin binding to calcium calmodulin-dependent protein kinase in *Lotus japonicus*. *Plant Cell* *24*, 304-321.

Sieberer, B.J., Chabaud, M., Fournier, J., Timmers, A.C., and Barker, D.G. (2012). A switch in Ca²⁺ spiking signature is concomitant with endosymbiotic microbe entry into cortical root cells of *Medicago truncatula*. *Plant Journal* *69*, 822-830.

Singh, S., Katzer, K., Lambert, J., Cerri, M., and Parniske, M. (2014). CYCLOPS, a DNA-binding transcriptional activator, orchestrates symbiotic root nodule development. *Cell Host & Microbe* *15*, 139-152.

Singh, S., and Parniske, M. (2012). Activation of calcium- and calmodulin-dependent protein kinase (CCaMK), the central regulator of plant root endosymbiosis. *Current Opinion in Plant Biology* *15*, 444-453.

Smit, P., Raedts, J., Portyanko, V., Debelle, F., Gough, C., Bisseling, T., and Geurts, R. (2005). NSP1 of the GRAS protein family is essential for rhizobial Nod factor-induced transcription. *Science* *308*, 1789-1791.

Smykowski, A., Fischer, S.M., and Zentgraf, U. (2015). Phosphorylation Affects DNA-Binding of the senescence-regulating bZIP transcription factor GBF1. *Plants* *4*, 691-709.

Soltis, D.E., Soltis, P.S., Chase, M.W., Mort, M.E., Albach, D.C., Zanis, M., Savolainen, V., Hahn, W.H., Hoot, S.B., Fay, M.F., et al. (2000). Angiosperm phylogeny inferred from 18S rDNA, *rbcl*, and *atpB* sequences. *Botanical Journal of the Linnean Society* *133*, 381-461.

Soltis, D.E., Soltis, P.S., Morgan, D.R., Swensen, S.M., Mullin, B.C., Dowd, J.M., and Martin, P.G. (1995). Chloroplast gene sequence data suggest a single origin of the predisposition for symbiotic nitrogen-fixation in angiosperms. *Proceedings of the National Academy of Sciences of the United States of America* 92, 2647-2651.

Soyano, T., Kouchi, H., Hirota, A., and Hayashi, M. (2013). Nodule inception directly targets *NF-Y* subunit genes to regulate essential processes of root nodule development in *Lotus japonicus*. *PLOS Genetics* 9, e1003352.

Soyano, T., Shimoda, Y., and Hayashi, M. (2014). NODULE INCEPTION antagonistically regulates gene expression with nitrate in *Lotus japonicus*. *Plant and Cell Physiology* 56, 368-376.

Sprent, J. (2007a). 60Ma of legume nodulation? What's new? What's changing? *Journal of Experimental Botany* 59, 1081-1084.

Sprent, J.I. (2007b). Evolving ideas of legume evolution and diversity: a taxonomic perspective on the occurrence of nodulation. *New Phytologist* 174, 11-25.

Sprent, J.I., and James, E.K. (2007). Legume evolution: Where do nodules and mycorrhizas fit in? *Plant Physiology* 144, 575-581.

Stahelin, C., Xie, Z.P., Illana, A., and Vierheilig, H. (2011). Long-distance transport of signals during symbiosis: are nodule formation and mycorrhization autoregulated in a similar way? *Plant Signal Behaviour* 6, 372-377.

Stracke, S., Kistner, C., Yoshida, S., Mulder, L., Sato, S., Kaneko, T., Tabata, S., Sandal, N., Stougaard, J., Szczyglowski, K., et al. (2002). A plant receptor-like kinase required for both bacterial and fungal symbiosis. *Nature* 417, 959-962.

Suzaki, T., Yano, K., Ito, M., Umehara, Y., Suganuma, N., and Kawaguchi, M. (2012). Positive and negative regulation of cortical cell division during root nodule development in *Lotus japonicus* is accompanied by auxin response. *Development* 139, 3997-4006.

Szczyglowski, K., Kapranov, P., Hamburger, D., and de Bruijn, F.J. (1998). The *Lotus japonicus* *LjNOD70* nodulin gene encodes a protein with similarities to transporters. *Plant Molecular Biology* 37, 651-661.

Szilak, L., Moitra, J., and Vinson, C. (1997). Design of a leucine zipper coiled coil stabilized 1.4 kcal mol⁻¹ by phosphorylation of a serine in the e position. *Protein Science* 6, 1273-1283.

Takeda, N., Handa, Y., Tsuzuki, S., Kojima, M., Sakakibara, H., and Kawaguchi, M. (2015a). Gibberellin regulates infection and colonization of host roots by arbuscular mycorrhizal fungi. *Plant Signal Behaviour* 10, e1028706.

Takeda, N., Handa, Y., Tsuzuki, S., Kojima, M., Sakakibara, H., and Kawaguchi, M. (2015b). Gibberellins interfere with symbiosis signaling and gene expression and alter colonization by arbuscular mycorrhizal fungi in *Lotus japonicus*. *Plant Physiology* 167, 545-557.

Takeda, N., Maekawa, T., and Hayashi, M. (2012). Nuclear-localized and deregulated calcium- and calmodulin-dependent protein kinase activates rhizobial and mycorrhizal responses in *Lotus japonicus*. *Plant Cell* 24, 810-822.

Takemoto, D., and Hardham, A.R. (2004). The cytoskeleton as a regulator and target of biotic interactions in plants. *Plant Physiology* 136, 3864-3876.

Takezawa, D., Ramachandiran, S., Paranjape, V., and Poovaiah, B.W. (1996). Dual regulation of a chimeric plant serine/threonine kinase by calcium and calcium/calmodulin. *Journal of Biological Chemistry* 271, 8126-8132.

Tirichine, L., Imaizumi-Anraku, H., Yoshida, S., Murakami, Y., Madsen, L.H., Miwa, H., Nakagawa, T., Sandal, N., Albrechtsen, A.S., Kawaguchi, M., et al. (2006). Deregulation of a Ca²⁺/calmodulin-dependent kinase leads to spontaneous nodule development. *Nature* 441, 1153-1156.

- Toth, K., Stratil, T.F., Madsen, E.B., Ye, J., Popp, C., Antolin-Llovera, M., Grossmann, C., Jensen, O.N., Schussler, A., Parniske, M., et al.** (2012). Functional domain analysis of the remorin protein *LjSYMREM1* in *Lotus japonicus*. *PLOS ONE* 7, e30817.
- Triezenberg, S.J.** (1995). Structure and function of transcriptional activation domains. *Current Opinion in Genetics & Development* 5, 190-196.
- Tyerman, S.D., Whitehead, L.F., and Day, D.A.** (1995). A channel-like transporter for NH₄⁺ on the symbiotic interface of N₂-fixing plants. *Nature* 378, 629-632.
- Udvardi, M.K., and Day, D.A.** (1997). Metabolite transport across symbiotic membranes of legume nodules. *Annual Review of Plant Physiology and Plant Molecular Biology* 48, 493-523.
- Van de Velde, W., Zehirov, G., Szatmari, A., Debreczeny, M., Ishihara, H., Kevei, Z., Farkas, A., Mikulass, K., Nagy, A., Tiricz, H., et al.** (2010). Plant peptides govern terminal differentiation of bacteria in symbiosis. *Science* 327, 1122-1126.
- van Rhijn, P., Goldberg, R.B., and Hirsch, A.M.** (1998). *Lotus corniculatus* nodulation specificity is changed by the presence of a soybean lectin gene. *Plant Cell* 10, 1233-1249.
- Vanbrussel, A.A.N., Bakhuizen, R., Vanspronsen, P.C., Spaijk, H.P., Tak, T., Lugtenberg, B.J.J., and Kijne, J.W.** (1992). Induction of preinfection thread structures in the leguminous host Plant by mitogenic lipooligosaccharides of rhizobium. *Science* 257, 70-72.
- Vance, C.P., and Gantt, J.S.** (1992). Control of nitrogen and carbon metabolism in root nodules. *Physiologia Plantarum* 85, 266-274.
- Vance, C.P., Uhde-Stone, C., and Allan, D.L.** (2003). Phosphorus acquisition and use: critical adaptations by plants for securing a nonrenewable resource. *New Phytologist* 157, 423-447.
- Venkateshwaran, M., Cosme, A., Han, L., Banba, M., Satyshur, K.A., Schleiff, E., Parniske, M., Imaizumi-Anraku, H., and Ane, J.M.** (2012). The recent evolution of a symbiotic ion channel in the legume family altered ion conductance and improved functionality in calcium signaling. *Plant Cell* 24, 2528-2545.
- Vernié, T., Kim, J., Frances, L., Ding, Y., Sun, J., Guan, D., Niebel, A., Gifford, M.L., de Carvalho-Niebel, F., and Oldroyd, G.E.** (2015). The NIN transcription factor coordinates diverse nodulation programs in different tissues of the *Medicago truncatula* root. *Plant Cell* 27, 3410-3424.
- Vinson, C., Myakishev, M., Acharya, A., Mir, A.A., Moll, J.R., and Bonovich, M.** (2002). Classification of human b-ZIP proteins based on dimerization properties. *Molecular and Cellular Biology* 22, 6321-6335.
- Walter, M., Chaban, C., Schutze, K., Batistic, O., Weckermann, K., Nake, C., Blazevic, D., Grefen, C., Schumacher, K., Oecking, C., et al.** (2004). Visualization of protein interactions in living plant cells using bimolecular fluorescence complementation. *Plant Journal* 40, 428-438.
- Wang, E., Schornack, S., Marsh, J.F., Gobbato, E., Schwessinger, B., Eastmond, P., Schultze, M., Kamoun, S., and Oldroyd, G.E.** (2012). A common signaling process that promotes mycorrhizal and oomycete colonization of plants. *Current Biology* 22, 2242-2246.
- Wang, L., Huang, C., Yang, M.Q., and Yang, J.Y.** (2010). BindN⁺ for accurate prediction of DNA and RNA-binding residues from protein sequence features. *BMC Systems Biology* 4, S3.
- Wang, Z., Cheng, K., Wan, L., Yan, L., Jiang, H., Liu, S., Lei, Y., and Liao, B.** (2015). Genome-wide analysis of the basic leucine zipper (bZIP) transcription factor gene family in six legume genomes. *BMC Genomics* 16, 1053.

- Weiss, M.A., Ellenberger, T., Wobbe, C.R., Lee, J.P., Harrison, S.C., and Struhl, K. (1990). Folding transition in the DNA-binding domain of GCN4 on specific binding to DNA. *Nature* 347, 575-578.
- Wewer, V., Brands, M., and Dormann, P. (2014). Fatty acid synthesis and lipid metabolism in the obligate biotrophic fungus *Rhizophagus irregularis* during mycorrhization of *Lotus japonicus*. *Plant Journal* 79, 398-412.
- White, J., Prell, J., James, E.K., and Poole, P. (2007). Nutrient sharing between symbionts. *Plant Physiology* 144, 604-614.
- Xie, F., Murray, J.D., Kim, J., Heckmann, A.B., Edwards, A., Oldroyd, G.E., and Downie, J.A. (2012). Legume pectate lyase required for root infection by rhizobia. *Proceedings of the National Academy of Sciences* 109, 633-638.
- Yan, J., Guan, L., Sun, Y., Zhu, Y., Liu, L., Lu, R., Jiang, M., Tan, M., and Zhang, A. (2015). Calcium and *ZmCCaMK* are involved in brassinosteroid-induced antioxidant defense in maize leaves. *Plant and Cell Physiology* 56, 883-896.
- Yang, C., Li, A.L., Zhao, Y.L., Zhang, Z.L., Zhu, Y.F., Tan, X.M., Geng, S.F., Guo, H.Z., Zhang, X.Y., Kang, Z.S., et al. (2011). Overexpression of a wheat *CCaMK* gene reduces ABA sensitivity of *Arabidopsis thaliana* during seed germination and seedling growth. *Plant Molecular Biology Reporter* 29, 681-692.
- Yano, K., Yoshida, S., Müller, J., Singh, S., Banba, M., Vickers, K., Markmann, K., White, C., Schuller, B., and Sato, S. (2008). CYCLOPS, a mediator of symbiotic intracellular accommodation. *Proceedings of the National Academy of Sciences* 105, 20540-20545.
- Yokota, K., Fukai, E., Madsen, L.H., Jurkiewicz, A., Rueda, P., Radutoiu, S., Held, M., Hossain, M.S., Szczyglowski, K., Morieri, G., et al. (2009). Rearrangement of actin cytoskeleton mediates invasion of *Lotus japonicus* roots by *Mesorhizobium loti*. *Plant Cell* 21, 267-284.
- Yoro, E., Suzaki, T., Toyokura, K., Miyazawa, H., Fukaki, H., and Kawaguchi, M. (2014). A positive regulator of nodule organogenesis, NODULE INCEPTION, acts as a negative regulator of rhizobial infection in *Lotus japonicus*. *Plant Physiology* 165, 747-758.
- Yu, N., Luo, D., Zhang, X., Liu, J., Wang, W., Jin, Y., Dong, W., Liu, J., Liu, H., Yang, W., et al. (2014). A DELLA protein complex controls the arbuscular mycorrhizal symbiosis in plants. *Cell Research* 24, 130-133.
- Yuan, S., Zhu, H., Gou, H., Fu, W., Liu, L., Chen, T., Ke, D., Kang, H., Xie, Q., Hong, Z., et al. (2012). A ubiquitin ligase of symbiosis receptor kinase involved in nodule organogenesis. *Plant Physiology* 160, 106-117.
- Zhang, X., Dong, W., Sun, J., Feng, F., Deng, Y., He, Z., Oldroyd, G.E., and Wang, E. (2015). The receptor kinase CERK1 has dual functions in symbiosis and immunity signalling. *Plant Journal* 81, 258-267.
- Zhang, X.C., Wu, X., Findley, S., Wan, J., Libault, M., Nguyen, H.T., Cannon, S.B., and Stacey, G. (2007). Molecular evolution of lysin motif-type receptor-like kinases in plants. *Plant Physiology* 144, 623-636.
- Zhu, H., Chen, T., Zhu, M., Fang, Q., Kang, H., Hong, Z., and Zhang, Z. (2008). A novel ARID DNA-binding protein interacts with SymRK and is expressed during early nodule development in *Lotus japonicus*. *Plant Physiology* 148, 337-347.
- Zhu, Y., Yan, J., Liu, W., Liu, L., Sheng, Y., Sun, Y., Li, Y., Scheller, H.V., Jiang, M., Hou, X., et al. (2016). Phosphorylation of a NAC transcription factor by *ZmCCaMK* regulates abscisic acid-induced antioxidant defense in maize. *Plant Physiology* 3, 1651-1664.
- Zuccaro, A., Lahrman, U., and Langen, G. (2014). Broad compatibility in fungal root symbioses. *Current Opinion in Plant Biology* 20, 135-145.

VIII. List of Figures

Figure 1.	Symbiotic Signal Transduction in Plant Root Cells.	24
Figure 2.	Schematic Overview of CCaMK Activation.....	31
Figure 3.	CYCLOPS is a Transcriptional Regulator with a Modular Structure.....	39
Figure 4.	Alignment of CYCLOPS Amino Acid Sequences.....	39
Figure 5.	A Minimal CYCLOPS Version is Sufficient to Transactivate via <i>2xCYC-RE_{NIN} in planta</i>	40
Figure 6.	CYCLOPS Binds to the <i>CYC-RE_{NIN}</i> in a Sequence-Specific and Phosphorylation-Dependent Manner.....	42
Figure 7.	CYCLOPS Sequence-Specifically Binds to the <i>ERN1</i> and <i>RAM1</i> Promoter.....	43
Figure 8.	Crystal Structure of the CYCLOPS Zipper.....	45
Figure 9.	Comparison of Zipper Interaction Surfaces.	46
Figure 10.	Homo- and Heterodimerization of the CYCLOPS Zipper.....	50
Figure 11.	Homodimerization Analyses of the CYCLOPS Zipper Domain.	52
Figure 12.	Interaction between CYCLOPS and Plant bZIP Transcriptional Regulators.....	55
Figure 13.	bZIP110 Forms a Trimeric Complex with CCaMK/CYCLOPS Bound to DNA.	59
Figure 14.	bZIP110 Preferentially Binds to Nodulation- over AM-Specific Promoter Elements.	61
Figure 15.	bZIP110 Inhibits CYCLOPS ^{DD} -mediated Transactivation in <i>L. japonicus</i> Roots.....	62
Figure 16.	bZIP110-Mediated Repression is Released upon CCaMK Activation.	64
Figure 17.	bZIP110 is a Negative Regulator of Root Nodule Symbiosis but not Arbuscular Mycorrhiza.....	65
Figure 18.	Overexpression of <i>bZIP110</i> Negatively Affects Nodule Development but not AM Colonization.....	67
Figure 19.	Proposed Function of Heterodimeric CYCLOPS Zipper Complexes in Cell-Specific Development during RNS.	87
Figure 20.	Overview of Transcriptional Networks during Root Symbiotic Development.	91

IX. List of Tables

Table 1.	Data Collection and Refinement Statistics.....	48
Table 2.	Growth Phenotype of <i>bzip110-1</i> Mutant Plants.....	66
Table 3.	Segregation of a Stunted Root Phenotype in the Progeny of a Heterozygous <i>bzip110-1</i> Mother Plant.....	66
Table 4.	Complementation Analysis of <i>bzip110-1</i> Mutant Plants.....	68

X. Acknowledgements

I would like to express my gratitude to all the people who supported and helped me during the period of this Ph.D thesis. First of all, my deepest gratitude goes to my Ph.D supervisor, Prof. Dr. Martin Parniske, for giving me the opportunity to graduate in his lab and to work on the fascinating CCaMK/CYCLOPS project. Martin has guided me throughout my thesis with encouragement, outstanding knowledge and support. I greatly appreciate his insightful comments and stimulating suggestions, which were a source of inspiration and motivation for me. I am also very thankful to him for giving me the freedom to pursue my own scientific ideas and for giving me the opportunity to attend several training courses and conferences.

I am very grateful to all the reviewers for giving their precious time and effort to evaluate this thesis.

Many thanks go to Dr. Sylvia Singh, who took me as a Diploma student and continued to guide me through the first years of my Ph.d thesis. She introduced me to my research topic and taught me all the valuable things about CYCLOPS. I want to thank her for the excellent supervision, but also for her friendliness and patience in answering all my questions.

This thesis would not have been possible without the great help of a number of colleagues who collaborated on various projects. I would like to thank Dr. Jérôme Basquin for the structural analysis of the CYCLOPS crystal, Dr. Ralf Heermann for performing SPR assays, Dr. Marion Cerri for qPCR analyses, Dr. Victor Gimenez Oya for helping with the expression and purification of different CCaMK/CYCLOPS complex combinations and Dr. Andreas Binder for creating fantastic Illustrator models and providing a plasmid containing the coding sequence of the *At* bZIP63. Furthermore I want to thank Paul Stolz for phenotyping nodule number of homozygous and heterozygous *bzip110-1* plants, Dr. David Chiasson and Aline Sandré for providing Golden Gate construction plasmids, Prof. Dr. Makoto Hayashi for the *CCaMK³¹⁴-RFP+NLS* (pK7WGR2) plasmid, Prof. Dr. Jens Stougaard for *L. japonicus* LORE1 seeds, Anne Hoffrichter for qRT-PCR primers and José Villaécija Aguilar and Max Griesmann for help with statistical analyses.

Special thanks go to Rosa Elena Andrade and Chloé Cathebras. They not only provided valueable experiments on bZIP phylogeny, Flim-FRET and promoter expression analyses, but were also amazing colleagues and became dear friends. Thank you for all the scientific and personal chats, for your help and support and for the fun times we had in the past years. But above all, I thank you for being true friends.

It was a great pleasure to supervise Gabrielle Wagenstetter, who was an excellent student and great assistance in the lab, but also became a good friend of mine.

I would like to express my heartfelt thanks to all past and present members of the Genetics department in particular the Parniske group, who contributed a lot to the great working environment. Dr. Kinga and Mauricio Sedziewska-Toro became very good friends of mine. Thank you Kinga for your listening, support and all the fun moments we had together. I very much enjoyed going out with Dr. Caroline Gutjahr to share answers and advices about scientific questions, but also life. Many thanks go to my office mates Philipp Bellon, Benjamin Billault-Penneteau and Katy Sollweck for all the cheerful moments and fun we had together. It was a pleasure sharing an office with you.

I am thankful to the groups of Prof. Dr. Thomas Lahaye, Prof. Dr. Thomas Ott, Prof. Dr. Michael Boshart, Prof. Dr. Arthur Schübler, Dr. Caroline Gutjahr, Dr. Andreas Brachmann, Dr. Macarena Marín, the green house and cleaning kitchen staff for continuous help and support in the lab. In particular, I want to thank the people of the repair shop, who always helped me out with technical and mechanical problems.

Finally, I am very grateful to my friends and family, who supported me with their love, motivation and patience. Special warm thanks go to my boyfriend Dragan, who is a wonderful partner and always there for me.

This work was funded by a grant from the German Research Foundation (DFG) to Prof. Dr. Martin Parniske initially within the Research Unit FOR 964 “Calcium signaling via protein phosphorylation in plant model cell types during environmental stress adaptations.” and later within the Research Unit SFB 924 sub-project B11 “Structure and function of the CCaMK/CYCLOPS complex” and by an advanced grant from the European Research Council (ERC) to Prof. Dr. Martin Parniske for project “Molecular inventions underlying the evolution of the nitrogen-fixing root nodule symbiosis.”

XI. Curriculum Vitae

Personal Details

Name: Katja Katzer
Date/Place of Birth: February 20, 1987 in Köthen
Nationality: German
Email: kkatzer87@googlemail.com



Education

From 10/2011 **Ph.D thesis**
 Ludwig-Maximilians-University Munich
 Faculty of Biology, Genetics, Research group Prof. Martin
 Parniske

10/2006 – 09/2011 **Diploma thesis**
 Martin-Luther-University Halle-Wittenberg
 Field of study: Biochemistry
 Final grade: 1.2 (approximate equivalent: A)

08/1999 – 07/2006 **Grammar school**
 Ludwigsgymnasium Köthen
 Final grade: 1.1 (approximate equivalent: A)
 Major: Biology and Chemistry

Work Experience

From 10/2011

Ph.D thesis

Ludwig-Maximilians-University Munich

Faculty of Biology, Genetics, Research group Prof. Dr. Martin Parniske

- Structural and functional characterization of a symbiotic transcription factor
- Protein expression, purification and crystallization
- Protein-protein and protein-DNA interaction analyses
- Supervision of two bachelor and one master student/s
- Primary instructor of the LMU Genetics II practical course 2013-2016
- Tuition associating the LMU Genetics II lectures 2012-2013

10/2010 – 07/2011

Diploma thesis

Ludwig-Maximilians-University Munich (external)

Faculty of Biology, Genetics, Research group Prof. Dr. Martin Parniske

- Identification and engineering of phosphorylation sites of a symbiotic transcription factor
- Agrobacterium-mediated transformation of plants

07/2009 – 09/2009

Leonardo da Vinci Traineeship

VIB University Gent, Belgium

Department of Plant Systems Biology, Research group Prof. Dr. Marcelle Holsters

- CLE-peptid mediated signal transduction during RNS

Additional Qualifications

- 07/2016 **Plant Proteomics Workshop**
University of Wisconsin-Madison, US
- 11/2015 **GMP basis course**
Max-Planck-Institute of Biochemistry, Martinsried
- 04/2014 **Training DNA-Protein-Interaction (DPI)-ELISA**
Eberhard Karls University Tübingen
- 03/2014 **Microscale Thermophoresis User Meeting**
Nanotemper technologies, Munich
Certificate
- 05/2013 **EMBO Practical Course “High throughput Protein**
Production and Crystallization”
Research Complex at Harwell, UK
- 02/2013 – 01/2014 **Educational Tutor Training**
Ludwig-Maximilians-University Munich
Tutor plus certificate

Conferences and Presentations

- 08/2016 **12th European Nitrogen Fixation Congress (ENFC),**
Budapest
Lightening talk “Identification of a novel component of the
CCaMK/CYCLOPS complex“
- 06/2014 **Plant Calcium Signaling (PCS) Meeting, Münster**
Poster prize award

- 09/2013 **International Congress of the German Botanical Society,
Tübingen**
Oral presentation “CYCLOPS, a DNA-binding transcriptional
activator, orchestrates symbiotic root nodule development”
- 09/2012 **10th European Nitrogen Fixation Congress (ENFC), Munich**
- 09/2011 **12th Plant Protein Phosphorylation Symposium, Tübingen**

Languages and Skills

Language Skills:	German	native
	English	fluent
	Croatian	basic
	Portuguese	basic
Computer Skills:	Bioinformatics	CLC Genomics Workbench, Pymol, SigmaPlot
	Image Processing	Photoshop, Illustrator, Biovoxxel, ImageJ
	Microsof Office	Word, Excel, Powerpoint
	Operational Systems	Mac OS, MS Windows

Hobbies and Interests

Member of the Mushroom Association Munich e.V.

XII. Republish Permissions

1. American Society of Plant Biologists

License for “Miller, J.B., Pratap, A., Miyahara, A., Zhou, L., Bornemann, S., Morris, R.J., and Oldroyd, G.E. (2013). Calcium/Calmodulin-dependent protein kinase is negatively and positively regulated by calcium, providing a mechanism for decoding calcium responses during symbiosis signaling. *Plant Cell* 25, 5053-5066”.

This is a License Agreement between LMU Munich, Genetics, Group Prof. Parniske -- Katja Katzer ("You") and American Society of Plant Biologists ("American Society of Plant Biologists") provided by Copyright Clearance Center ("CCC"). The license consists of your order details, the terms and conditions provided by American Society of Plant Biologists, and the payment terms and conditions.

All payments must be made in full to CCC. For payment instructions, please see information listed at the bottom of this form.

License Number	4126521359809
License date	Jun 12, 2017
Licensed content publisher	American Society of Plant Biologists
Licensed content title	The plant cell
Licensed content date	Jan 1, 1989
Type of Use	Thesis/Dissertation
Requestor type	Academic institution
Format	Print, Electronic
Portion	image/photo
Number of images/photos requested	1
Title or numeric reference of the portion(s)	Figure 6
Title of the article or chapter the portion is from	N/A
Editor of portion(s)	N/A
Author of portion(s)	N/A
Volume of serial or monograph.	N/A
Page range of the portion	1
Publication date of portion	Sept 2017
Rights for	Main product
Duration of use	Life of current edition
Creation of copies for the disabled	yes
With minor editing privileges	no
For distribution to	Worldwide
In the following language(s)	Original language of publication
With incidental promotional use	no

The lifetime unit quantity of new product	Up to 499
Made available in the following markets	scientific
The requesting person/organization is:	Katja Katzer, LMU Munich, Genetics, Group Prof. M. Parniske
Order reference number	
Author/Editor	Katja Katzer
The standard identifier of New Work	Katja Katzer
Title of New Work	Structure, Function and Regulation of the CCaMK/CYCLOPS Complex During Root Symbioses.
Publisher of New Work	LMU Munich
Expected publication date	Sep 2017
Estimated size (pages)	150
Customer Tax ID	DE811205325
Total (may include CCC user fee)	0.00 USD

TERMS AND CONDITIONS

The following terms are individual to this publisher:

Permission is granted for the life of the current edition and all future editions, in all languages and in all media.

Other Terms and Conditions:

STANDARD TERMS AND CONDITIONS

1. Description of Service; Defined Terms. This Republication License enables the User to obtain licenses for republication of one or more copyrighted works as described in detail on the relevant Order Confirmation (the "Work(s)"). Copyright Clearance Center, Inc. ("CCC") grants licenses through the Service on behalf of the rightsholder identified on the Order Confirmation (the "Rightsholder"). "Republication", as used herein, generally means the inclusion of a Work, in whole or in part, in a new work or works, also as described on the Order Confirmation. "User", as used herein, means the person or entity making such republication.

2. The terms set forth in the relevant Order Confirmation, and any terms set by the Rightsholder with respect to a particular Work, govern the terms of use of Works in connection with the Service. By using the Service, the person transacting for a republication license on behalf of the User represents and warrants that he/she/it (a) has been duly authorized by the User to accept, and hereby does accept, all such terms and conditions on behalf of User, and (b) shall inform User of all such terms and conditions. In the event such person is a "freelancer" or other third party independent of User and CCC, such party shall be deemed jointly a "User" for purposes of these terms and conditions. In any event, User shall be deemed to have accepted and agreed to all such terms and conditions if User republishes the Work in any fashion.

3. Scope of License; Limitations and Obligations.

3.1 All Works and all rights therein, including copyright rights, remain the sole and exclusive property of the Rightsholder. The license created by the exchange of an Order Confirmation (and/or any invoice) and payment by User of the full amount set forth on that document includes only those rights expressly set forth in the Order Confirmation and in these terms and conditions, and conveys no other rights in the Work(s) to User. All rights not expressly granted are hereby reserved.

3.2 General Payment Terms: You may pay by credit card or through an account with us payable at the end of the month. If you and we agree that you may establish a standing account with CCC, then the following terms apply: Remit Payment to: Copyright Clearance Center, 29118 Network Place, Chicago, IL 60673-1291. Payments Due: Invoices are payable upon their delivery to you (or upon our notice to you that they are available to you for downloading). After 30 days, outstanding amounts will be subject to a service charge of 1-1/2% per month or, if less, the maximum rate allowed by applicable law. Unless otherwise specifically set forth in the Order Confirmation or in a separate written agreement signed by CCC, invoices are due and payable on “net 30” terms. While User may exercise the rights licensed immediately upon issuance of the Order Confirmation, the license is automatically revoked and is null and void, as if it had never been issued, if complete payment for the license is not received on a timely basis either from User directly or through a payment agent, such as a credit card company.

3.3 Unless otherwise provided in the Order Confirmation, any grant of rights to User (i) is “one-time” (including the editions and product family specified in the license), (ii) is non-exclusive and non-transferable and (iii) is subject to any and all limitations and restrictions (such as, but not limited to, limitations on duration of use or circulation) included in the Order Confirmation or invoice and/or in these terms and conditions. Upon completion of the licensed use, User shall either secure a new permission for further use of the Work(s) or immediately cease any new use of the Work(s) and shall render inaccessible (such as by deleting or by removing or severing links or other locators) any further copies of the Work (except for copies printed on paper in accordance with this license and still in User's stock at the end of such period).

3.4 In the event that the material for which a republication license is sought includes third party materials (such as photographs, illustrations, graphs, inserts and similar materials) which are identified in such material as having been used by permission, User is responsible for identifying, and seeking separate licenses (under this Service or otherwise) for, any of such third party materials; without a separate license, such third party materials may not be used.

3.5 Use of proper copyright notice for a Work is required as a condition of any license granted under the Service. Unless otherwise provided in the Order Confirmation, a proper copyright notice will read substantially as follows: “Republished with permission of [Rightsholder’s name], from [Work’s title, author, volume, edition number and year of copyright]; permission conveyed through Copyright Clearance Center, Inc. ” Such notice must be provided in a reasonably legible font size and must be placed either immediately adjacent to the Work as used (for example, as part of a by-line or footnote but not as a separate electronic link) or in the place where substantially all other credits or notices for the new work containing the republished Work are located. Failure to include the required notice results in loss to the Rightsholder and CCC, and the User shall be liable to pay liquidated damages for each such failure equal to twice the use fee specified in the Order Confirmation, in addition to the use fee itself and any other fees and charges specified.

3.6 User may only make alterations to the Work if and as expressly set forth in the Order Confirmation. No Work may be used in any way that is defamatory, violates the rights of third parties (including such third parties' rights of copyright, privacy, publicity, or other tangible or intangible property), or is otherwise illegal, sexually explicit or obscene. In addition, User may not conjoin a Work with any other material that may result in damage to the reputation of the Rightsholder. User agrees to inform CCC if it becomes aware of any infringement of any rights in a Work and to cooperate with any reasonable request of CCC or the Rightsholder in connection therewith.

4. Indemnity. User hereby indemnifies and agrees to defend the Rightsholder and CCC, and their respective employees and directors, against all claims, liability, damages, costs and expenses, including legal fees and expenses, arising out of any use of a Work beyond the scope of the rights granted herein, or any use of a Work which has been altered in any unauthorized way by User, including claims of defamation or infringement of rights of copyright, publicity, privacy or other tangible or intangible property.

5. Limitation of Liability. UNDER NO CIRCUMSTANCES WILL CCC OR THE RIGHTSHOLDER BE LIABLE FOR ANY DIRECT, INDIRECT, CONSEQUENTIAL OR

INCIDENTAL DAMAGES (INCLUDING WITHOUT LIMITATION DAMAGES FOR LOSS OF BUSINESS PROFITS OR INFORMATION, OR FOR BUSINESS INTERRUPTION) ARISING OUT OF THE USE OR INABILITY TO USE A WORK, EVEN IF ONE OF THEM HAS BEEN ADVISED OF THE POSSIBILITY OF SUCH DAMAGES. In any event, the total liability of the Rightsholder and CCC (including their respective employees and directors) shall not exceed the total amount actually paid by User for this license. User assumes full liability for the actions and omissions of its principals, employees, agents, affiliates, successors and assigns.

6. Limited Warranties. THE WORK(S) AND RIGHT(S) ARE PROVIDED "AS IS". CCC HAS THE RIGHT TO GRANT TO USER THE RIGHTS GRANTED IN THE ORDER CONFIRMATION DOCUMENT. CCC AND THE RIGHTSHOLDER DISCLAIM ALL OTHER WARRANTIES RELATING TO THE WORK(S) AND RIGHT(S), EITHER EXPRESS OR IMPLIED, INCLUDING WITHOUT LIMITATION IMPLIED WARRANTIES OF MERCHANTABILITY OR FITNESS FOR A PARTICULAR PURPOSE. ADDITIONAL RIGHTS MAY BE REQUIRED TO USE ILLUSTRATIONS, GRAPHS, PHOTOGRAPHS, ABSTRACTS, INSERTS OR OTHER PORTIONS OF THE WORK (AS OPPOSED TO THE ENTIRE WORK) IN A MANNER CONTEMPLATED BY USER; USER UNDERSTANDS AND AGREES THAT NEITHER CCC NOR THE RIGHTSHOLDER MAY HAVE SUCH ADDITIONAL RIGHTS TO GRANT.

7. Effect of Breach. Any failure by User to pay any amount when due, or any use by User of a Work beyond the scope of the license set forth in the Order Confirmation and/or these terms and conditions, shall be a material breach of the license created by the Order Confirmation and these terms and conditions. Any breach not cured within 30 days of written notice thereof shall result in immediate termination of such license without further notice. Any unauthorized (but licensable) use of a Work that is terminated immediately upon notice thereof may be liquidated by payment of the Rightsholder's ordinary license price therefor; any unauthorized (and unlicensable) use that is not terminated immediately for any reason (including, for example, because materials containing the Work cannot reasonably be recalled) will be subject to all remedies available at law or in equity, but in no event to a payment of less than three times the Rightsholder's ordinary license price for the most closely analogous licensable use plus Rightsholder's and/or CCC's costs and expenses incurred in collecting such payment.

8. Miscellaneous.

8.1 User acknowledges that CCC may, from time to time, make changes or additions to the Service or to these terms and conditions, and CCC reserves the right to send notice to the User by electronic mail or otherwise for the purposes of notifying User of such changes or additions; provided that any such changes or additions shall not apply to permissions already secured and paid for.

8.2 Use of User-related information collected through the Service is governed by CCC's privacy policy, available online here:

<http://www.copyright.com/content/cc3/en/tools/footer/privacypolicy.html>.

8.3 The licensing transaction described in the Order Confirmation is personal to User. Therefore, User may not assign or transfer to any other person (whether a natural person or an organization of any kind) the license created by the Order Confirmation and these terms and conditions or any rights granted hereunder; provided, however, that User may assign such license in its entirety on written notice to CCC in the event of a transfer of all or substantially all of User's rights in the new material which includes the Work(s) licensed under this Service.

8.4 No amendment or waiver of any terms is binding unless set forth in writing and signed by the parties. The Rightsholder and CCC hereby object to any terms contained in any writing prepared by the User or its principals, employees, agents or affiliates and purporting to govern or otherwise relate to the licensing transaction described in the Order Confirmation, which terms are in any way inconsistent with any terms set forth in the Order Confirmation and/or in these terms and conditions or CCC's standard operating procedures, whether such writing is prepared prior to, simultaneously with or subsequent to the Order Confirmation, and whether such writing appears on a copy of the Order Confirmation or in a separate instrument.

8.5 The licensing transaction described in the Order Confirmation document shall be governed by and construed under the law of the State of New York, USA, without regard to the principles thereof of conflicts of law. Any case, controversy, suit, action, or proceeding arising out of, in connection with, or related to such licensing transaction shall be brought, at CCC's sole discretion, in any federal or state court located in the County of New York, State of New York, USA, or in any federal or state court whose geographical jurisdiction covers the location of the Rightsholder set forth in the Order Confirmation. The parties expressly submit to the personal jurisdiction and venue of each such federal or state court. If you have any comments or questions about the Service or Copyright Clearance Center, please contact us at 978-750-8400 or send an e-mail to info@copyright.com.

v1.1

2. Elsevier

License for “CYCLOPS, a DNA-binding transcriptional activator, orchestrates symbiotic root nodule development. *Cell Host & Microbe* 15, 139-152”.

This Agreement between LMU Munich, Genetics, Group Prof. Parniske -- Katja Katzer ("You") and Elsevier ("Elsevier") consists of your license details and the terms and conditions provided by Elsevier and Copyright Clearance Center.

License Number	4123611408725
License date	Jun 07, 2017
Licensed Content Publisher	Elsevier
Licensed Content Publication	Cell Host & Microbe
Licensed Content Title	CYCLOPS, A DNA-Binding Transcriptional Activator, Orchestrates Symbiotic Root Nodule Development
Licensed Content Author	Sylvia Singh, Katja Katzer, Jayne Lambert, Marion Cerri, Martin Parniske
Licensed Content Date	Feb 12, 2014
Licensed Content Volume	15
Licensed Content Issue	2
Licensed Content Pages	14
Start Page	139
End Page	152
Type of Use	reuse in a thesis/dissertation
Portion	full article
Format	both print and electronic
Are you the author of this Elsevier article?	Yes
Will you be translating?	No
Order reference number	
Title of your thesis/dissertation	Structure, function and regulation of the CCaMK/CYCLOPS complex during root

	ymbioses
Expected completion date	Aug 2017
Estimated size (number of pages)	150
Elsevier VAT number	GB 494 6272 12
Requestor Location	LMU Munich, Genetics, Group Prof. Parniske Großhadernerstr. 2-4 Planegg, Bavaria 82152 Germany
Attn:LMU Munich, Genetics, Group Prof. Parniske	
Publisher Tax ID	GB 494 6272 12
Customer VAT ID	DE811205325
Total	0.00 EUR

License for “Singh, S., and Parniske, M. (2012). Activation of calcium- and calmodulin-dependent protein kinase (CCaMK), the central regulator of plant root endosymbiosis. *Current Opinion in Plant Biology* 15, 444-453”.

This Agreement between LMU Munich, Genetics, Group Prof. Parniske -- Katja Katzer ("You") and Elsevier ("Elsevier") consists of your license details and the terms and conditions provided by Elsevier and Copyright Clearance Center.

License Number	4126510895934
License date	Jun 12, 2017
Licensed Content Publisher	Elsevier
Licensed Content Publication	Current Opinion in Plant Biology
Licensed Content Title	Activation of calcium- and calmodulin-dependent protein kinase (CCaMK), the central regulator of plant root endosymbiosis
Licensed Content Author	Sylvia Singh, Martin Parniske
Licensed Content Date	Aug 1, 2012
Licensed Content Volume	15
Licensed Content Issue	4
Licensed Content Pages	10
Start Page	444
End Page	453
Type of Use	reuse in a thesis/dissertation
Portion	figures/tables/illustrations
Number of figures/tables/illustrations	1
Format	both print and electronic
Are you the author of this Elsevier article?	No
Will you be translating?	No
Order reference number	

Original figure numbers	Figure 1
Title of your thesis/dissertation	Structure, function and regulation of the CCaMK/CYCLOPS complex during root symbioses
Expected completion date	Aug 2017
Estimated size (number of pages)	150
Elsevier VAT number	GB 494 6272 12
Requestor Location	LMU Munich, Genetics, Group Prof. Parniske Großhadernerstr. 2-4 Planegg, Bavaria 82152 Germany
Attn: LMU Munich, Genetics, Group Prof. Parniske	
Publisher Tax ID	GB 494 6272 12
Customer VAT ID	DE811205325
Total	0.00 EUR

License for “Pimprikar, P., Carbonnel, S., Paries, M., Katzer, K., Klingl, V., Bohmer, M.J., Karl, L., Floss, D.S., Harrison, M.J., Parniske, M., et al. (2016). A CCaMK-CYCLOPS-DELLA complex activates transcription of *RAM1* to regulate arbuscule branching. *Current Biology* 26, 1126. *Current Biology* 26, 1126”.

This Agreement between LMU Munich, Genetics, Group Prof. Parniske -- Katja Katzer ("You") and Elsevier ("Elsevier") consists of your license details and the terms and conditions provided by Elsevier and Copyright Clearance Center.

License Number	4124331267342
License date	Jun 08, 2017
Licensed Content Publisher	Elsevier
Licensed Content Publication	Current Biology
Licensed Content Title	A CCaMK-CYCLOPS-DELLA Complex Activates Transcription of RAM1 to Regulate Arbuscule Branching
Licensed Content Author	Priya Pimprikar, Samy Carbonnel, Michael Paries, Katja Katzer, Verena Klingl, Monica J. Bohmer, Leonhard Karl, Daniela S. Floss, Maria J. Harrison, Martin Parniske, Caroline Gutjahr
Licensed Content Date	Apr 25, 2016
Licensed Content Volume	26
Licensed Content Issue	8
Licensed Content Pages	12
Start Page	987
End Page	998
Type of Use	reuse in a thesis/dissertation
Portion	figures/tables/illustrations

Number of figures/tables/illustrations	1
Format	both print and electronic
Are you the author of this Elsevier article?	Yes
Will you be translating?	No
Order reference number	
Original figure numbers	7C
Title of your thesis/dissertation	Structure, function and regulation of the CCaMK/CYCLOPS complex during root symbioses
Expected completion date	Aug 2017
Estimated size (number of pages)	150
Elsevier VAT number	GB 494 6272 12
Requestor Location	LMU Munich, Genetics, Group Prof. Parniske Großhadernerstr. 2-4 Planegg, Bavaria 82152 Germany
Attn: LMU Munich, Genetics, Group Prof. Parniske	
Publisher Tax ID	GB 494 6272 12
Customer VAT ID	DE811205325
Total	0.00 EUR

INTRODUCTION

1. The publisher for this copyrighted material is Elsevier. By clicking "accept" in connection with completing this licensing transaction, you agree that the following terms and conditions apply to this transaction (along with the Billing and Payment terms and conditions established by Copyright Clearance Center, Inc. ("CCC"), at the time that you opened your Rightslink account and that are available at any time at <http://myaccount.copyright.com>).

GENERAL TERMS

2. Elsevier hereby grants you permission to reproduce the aforementioned material subject to the terms and conditions indicated.

3. Acknowledgement: If any part of the material to be used (for example, figures) has appeared in our publication with credit or acknowledgement to another source, permission must also be sought from that source. If such permission is not obtained then that material may not be included in your publication/copies. Suitable acknowledgement to the source must be made, either as a footnote or in a reference list at the end of your publication, as follows:

"Reprinted from Publication title, Vol /edition number, Author(s), Title of article / title of chapter, Pages No., Copyright (Year), with permission from Elsevier [OR APPLICABLE SOCIETY COPYRIGHT OWNER]." Also Lancet special credit - "Reprinted from The Lancet, Vol. number, Author(s), Title of article, Pages No., Copyright (Year), with permission from Elsevier."

4. Reproduction of this material is confined to the purpose and/or media for which permission is hereby given.

5. Altering/Modifying Material: Not Permitted. However figures and illustrations may be altered/adapted minimally to serve your work. Any other abbreviations, additions, deletions and/or any other alterations shall be made only with prior written authorization of Elsevier Ltd. (Please

contact Elsevier at permissions@elsevier.com). No modifications can be made to any Lancet figures/tables and they must be reproduced in full.

6. If the permission fee for the requested use of our material is waived in this instance, please be advised that your future requests for Elsevier materials may attract a fee.

7. Reservation of Rights: Publisher reserves all rights not specifically granted in the combination of (i) the license details provided by you and accepted in the course of this licensing transaction, (ii) these terms and conditions and (iii) CCC's Billing and Payment terms and conditions.

8. License Contingent Upon Payment: While you may exercise the rights licensed immediately upon issuance of the license at the end of the licensing process for the transaction, provided that you have disclosed complete and accurate details of your proposed use, no license is finally effective unless and until full payment is received from you (either by publisher or by CCC) as provided in CCC's Billing and Payment terms and conditions. If full payment is not received on a timely basis, then any license preliminarily granted shall be deemed automatically revoked and shall be void as if never granted. Further, in the event that you breach any of these terms and conditions or any of CCC's Billing and Payment terms and conditions, the license is automatically revoked and shall be void as if never granted. Use of materials as described in a revoked license, as well as any use of the materials beyond the scope of an unrevoked license, may constitute copyright infringement and publisher reserves the right to take any and all action to protect its copyright in the materials.

9. Warranties: Publisher makes no representations or warranties with respect to the licensed material.

10. Indemnity: You hereby indemnify and agree to hold harmless publisher and CCC, and their respective officers, directors, employees and agents, from and against any and all claims arising out of your use of the licensed material other than as specifically authorized pursuant to this license.

11. No Transfer of License: This license is personal to you and may not be sublicensed, assigned, or transferred by you to any other person without publisher's written permission.

12. No Amendment Except in Writing: This license may not be amended except in a writing signed by both parties (or, in the case of publisher, by CCC on publisher's behalf).

13. Objection to Contrary Terms: Publisher hereby objects to any terms contained in any purchase order, acknowledgment, check endorsement or other writing prepared by you, which terms are inconsistent with these terms and conditions or CCC's Billing and Payment terms and conditions. These terms and conditions, together with CCC's Billing and Payment terms and conditions (which are incorporated herein), comprise the entire agreement between you and publisher (and CCC) concerning this licensing transaction. In the event of any conflict between your obligations established by these terms and conditions and those established by CCC's Billing and Payment terms and conditions, these terms and conditions shall control.

14. Revocation: Elsevier or Copyright Clearance Center may deny the permissions described in this License at their sole discretion, for any reason or no reason, with a full refund payable to you. Notice of such denial will be made using the contact information provided by you. Failure to receive such notice will not alter or invalidate the denial. In no event will Elsevier or Copyright Clearance Center be responsible or liable for any costs, expenses or damage incurred by you as a result of a denial of your permission request, other than a refund of the amount(s) paid by you to Elsevier and/or Copyright Clearance Center for denied permissions.

LIMITED LICENSE

The following terms and conditions apply only to specific license types:

15. Translation: This permission is granted for non-exclusive world English rights only unless your license was granted for translation rights. If you licensed translation rights you may only translate this content into the languages you requested. A professional translator must perform all translations and reproduce the content word for word preserving the integrity of the article.

16. Posting licensed content on any Website: The following terms and conditions apply as follows: Licensing material from an Elsevier journal: All content posted to the web site must maintain the copyright information line on the bottom of each image; A hyper-text must be included to the Homepage of the journal from which you are licensing at <http://www.sciencedirect.com/science/journal/xxxxx> or the Elsevier homepage for books at <http://www.elsevier.com>; Central Storage: This license does not include permission for a scanned version of the material to be stored in a central repository such as that provided by Heron/XanEdu.

Licensing material from an Elsevier book: A hyper-text link must be included to the Elsevier homepage at <http://www.elsevier.com>. All content posted to the web site must maintain the copyright information line on the bottom of each image.

Posting licensed content on Electronic reserve: In addition to the above the following clauses are applicable: The web site must be password-protected and made available only to bona fide students registered on a relevant course. This permission is granted for 1 year only. You may obtain a new license for future website posting.

17. For journal authors: the following clauses are applicable in addition to the above:

Preprints:

A preprint is an author's own write-up of research results and analysis, it has not been peer-reviewed, nor has it had any other value added to it by a publisher (such as formatting, copyright, technical enhancement etc.).

Authors can share their preprints anywhere at any time. Preprints should not be added to or enhanced in any way in order to appear more like, or to substitute for, the final versions of articles however authors can update their preprints on arXiv or RePEc with their Accepted Author Manuscript (see below).

If accepted for publication, we encourage authors to link from the preprint to their formal publication via its DOI. Millions of researchers have access to the formal publications on ScienceDirect, and so links will help users to find, access, cite and use the best available version. Please note that Cell Press, The Lancet and some society-owned have different preprint policies. Information on these policies is available on the journal homepage.

Accepted Author Manuscripts: An accepted author manuscript is the manuscript of an article that has been accepted for publication and which typically includes author-incorporated changes suggested during submission, peer review and editor-author communications.

Authors can share their accepted author manuscript:

- immediately
 - via their non-commercial person homepage or blog
 - by updating a preprint in arXiv or RePEc with the accepted manuscript
 - via their research institute or institutional repository for internal institutional uses or as part of an invitation-only research collaboration work-group
 - directly by providing copies to their students or to research collaborators for their personal use
 - for private scholarly sharing as part of an invitation-only work group on commercial sites with which Elsevier has an agreement
- After the embargo period
 - via non-commercial hosting platforms such as their institutional repository
 - via commercial sites with which Elsevier has an agreement

In all cases accepted manuscripts should:

- link to the formal publication via its DOI
- bear a CC-BY-NC-ND license - this is easy to do
- if aggregated with other manuscripts, for example in a repository or other site, be shared in alignment with our hosting policy not be added to or enhanced in any way to appear more like, or to substitute for, the published journal article.

Published journal article (JPA): A published journal article (PJA) is the definitive final record of published research that appears or will appear in the journal and embodies all value-adding publishing activities including peer review co-ordination, copy-editing, formatting, (if relevant) pagination and online enrichment.

Policies for sharing publishing journal articles differ for subscription and gold open access articles:

Subscription Articles: If you are an author, please share a link to your article rather than the full-text. Millions of researchers have access to the formal publications on ScienceDirect, and so links will help your users to find, access, cite, and use the best available version.

Theses and dissertations which contain embedded PJAs as part of the formal submission can be posted publicly by the awarding institution with DOI links back to the formal publications on ScienceDirect.

If you are affiliated with a library that subscribes to ScienceDirect you have additional private sharing rights for others' research accessed under that agreement. This includes use for classroom teaching and internal training at the institution (including use in course packs and courseware programs), and inclusion of the article for grant funding purposes.

Gold Open Access Articles: May be shared according to the author-selected end-user license and should contain a CrossMark logo, the end user license, and a DOI link to the formal publication on ScienceDirect.

Please refer to Elsevier's posting policy for further information.

18. For book authors the following clauses are applicable in addition to the above: Authors are permitted to place a brief summary of their work online only. You are not allowed to download and post the published electronic version of your chapter, nor may you scan the printed edition to create an electronic version. Posting to a repository: Authors are permitted to post a summary of their chapter only in their institution's repository.

19. Thesis/Dissertation: If your license is for use in a thesis/dissertation your thesis may be submitted to your institution in either print or electronic form. Should your thesis be published commercially, please reapply for permission. These requirements include permission for the Library and Archives of Canada to supply single copies, on demand, of the complete thesis and include permission for Proquest/UMI to supply single copies, on demand, of the complete thesis. Should your thesis be published commercially, please reapply for permission. Theses and dissertations which contain embedded PJAs as part of the formal submission can be posted publicly by the awarding institution with DOI links back to the formal publications on ScienceDirect.

Elsevier Open Access Terms and Conditions

You can publish open access with Elsevier in hundreds of open access journals or in nearly 2000 established subscription journals that support open access publishing. Permitted third party re-use of these open access articles is defined by the author's choice of Creative Commons user license. See our open access license policy for more information.

Terms & Conditions applicable to all Open Access articles published with Elsevier:

Any reuse of the article must not represent the author as endorsing the adaptation of the article nor should the article be modified in such a way as to damage the author's honour or reputation. If any changes have been made, such changes must be clearly indicated.

The author(s) must be appropriately credited and we ask that you include the end user license and a DOI link to the formal publication on ScienceDirect.

If any part of the material to be used (for example, figures) has appeared in our publication with credit or acknowledgement to another source it is the responsibility of the user to ensure their reuse complies with the terms and conditions determined by the rights holder.

Additional Terms & Conditions applicable to each Creative Commons user license:

CC BY: The CC-BY license allows users to copy, to create extracts, abstracts and new works from the Article, to alter and revise the Article and to make commercial use of the Article (including reuse and/or resale of the Article by commercial entities), provided the user gives appropriate credit (with a link to the formal publication through the relevant DOI), provides a link to the license, indicates if changes were made and the licensor is not represented as endorsing the use made of the work. The full details of the license are available at <http://creativecommons.org/licenses/by/4.0>.

CC BY NC SA: The CC BY-NC-SA license allows users to copy, to create extracts, abstracts and new works from the Article, to alter and revise the Article, provided this is not done for commercial purposes, and that the user gives appropriate credit (with a link to the formal publication through the relevant DOI), provides a link to the license, indicates if changes were made and the licensor is not represented as endorsing the use made of the work. Further, any new works must be made available on the same conditions. The full details of the license are available at <http://creativecommons.org/licenses/by-nc-sa/4.0>.

CC BY NC ND: The CC BY-NC-ND license allows users to copy and distribute the Article, provided this is not done for commercial purposes and further does not permit distribution of the Article if it is changed or edited in any way, and provided the user gives appropriate credit (with a link to the formal publication through the relevant DOI), provides a link to the license, and that the licensor is not represented as endorsing the use made of the work. The full details of the license are available at <http://creativecommons.org/licenses/by-nc-nd/4.0>. Any commercial reuse of Open Access articles published with a CC BY NC SA or CC BY NC ND license requires permission from Elsevier and will be subject to a fee.

Commercial reuse includes:

- Associating advertising with the full text of the Article
- Charging fees for document delivery or access
- Article aggregation
- Systematic distribution via e-mail lists or share buttons

Posting or linking by commercial companies for use by customers of those companies.

20. Other Conditions:

v1.9

3. John Wiley and Sons

License for “Cerri, M.R., Wang, Q., Stolz, P., Folgmann, J., Frances, L., Katzer, K., Li, X., Heckmann, A.B., Wang, T.L., Downie, J.A., et al. (2017). The *ERN1* transcription factor gene is a target of the CCaMK/CYCLOPS complex and controls rhizobial infection in *Lotus japonicus*. *New Phytologist* 215, 323-337”.

This Agreement between LMU Munich, Genetics, Group Prof. Parniske -- Katja Katzer ("You") and John Wiley and Sons ("John Wiley and Sons") consists of your license details and the terms and conditions provided by John Wiley and Sons and Copyright Clearance Center.

License Number	4124340198499
License date	Jun 08, 2017
Licensed Content Publisher	John Wiley and Sons
Licensed Content Publication	New Phytologist
Licensed Content Title	The <i>ERN1</i> transcription factor gene is a target of the CCaMK/CYCLOPS complex and controls rhizobial infection in <i>Lotus japonicus</i>
Licensed Content Author	Marion R. Cerri, Quanhui Wang, Paul Stolz, Jessica Folgmann, Lisa Frances, Katja Katzer, Xiaolin Li, Anne B. Heckmann, Trevor L. Wang, J. Allan Downie, Andreas Klingl, Fernanda Carvalho Niebel, Fang Xie, Martin Parniske
Licensed Content Date	May 15, 2017
Licensed Content Pages	15
Type of use	Dissertation/Thesis
Requestor type	Author of this Wiley article
Format	Print and electronic
Portion	Figure/table
Number of figures/tables	1
Original Wiley figure/table number(s)	Figure 6 A
Will you be translating?	No
Title of your thesis / dissertation	Structure, function and regulation of the CCaMK/CYCLOPS complex during root symbioses
Expected completion date	Aug 2017
Expected size (number of pages)	150
Requestor Location	LMU Munich, Genetics, Group Prof. Parniske Großhadernerstr. 2-4 Planegg, Bavaria 82152 Germany
Attn: LMU Munich, Genetics, Group Prof. Parniske	
Publisher Tax ID	EU826007151
Customer VAT ID	DE811205325
Billing Type	Invoice
Billing Address	LMU Munich, Genetics, Group Prof. Parniske Großhadernerstr. 2-4 Planegg, Germany 82152

Total

0.00 EUR

TERMS AND CONDITIONS

This copyrighted material is owned by or exclusively licensed to John Wiley & Sons, Inc. or one of its group companies (each a "Wiley Company") or handled on behalf of a society with which a Wiley Company has exclusive publishing rights in relation to a particular work (collectively "WILEY"). By clicking "accept" in connection with completing this licensing transaction, you agree that the following terms and conditions apply to this transaction (along with the billing and payment terms and conditions established by the Copyright Clearance Center Inc., ("CCC's Billing and Payment terms and conditions"), at the time that you opened your RightsLink account (these are available at any time at <http://myaccount.copyright.com>).

Terms and Conditions

- The materials you have requested permission to reproduce or reuse (the "Wiley Materials") are protected by copyright.
- You are hereby granted a personal, non-exclusive, non-sub licensable (on a stand-alone basis), non-transferable, worldwide, limited license to reproduce the Wiley Materials for the purpose specified in the licensing process. This license, and any CONTENT (PDF or image file) purchased as part of your order, is for a one-time use only and limited to any maximum distribution number specified in the license. The first instance of republication or reuse granted by this license must be completed within two years of the date of the grant of this license (although copies prepared before the end date may be distributed thereafter). The Wiley Materials shall not be used in any other manner or for any other purpose, beyond what is granted in the license. Permission is granted subject to an appropriate acknowledgement given to the author, title of the material/book/journal and the publisher. You shall also duplicate the copyright notice that appears in the Wiley publication in your use of the Wiley Material. Permission is also granted on the understanding that nowhere in the text is a previously published source acknowledged for all or part of this Wiley Material. Any third party content is expressly excluded from this permission.
- With respect to the Wiley Materials, all rights are reserved. Except as expressly granted by the terms of the license, no part of the Wiley Materials may be copied, modified, adapted (except for minor reformatting required by the new Publication), translated, reproduced, transferred or distributed, in any form or by any means, and no derivative works may be made based on the Wiley Materials without the prior permission of the respective copyright owner. For STM Signatory Publishers clearing permission under the terms of the STM Permissions Guidelines only, the terms of the license are extended to include subsequent editions and for editions in other languages, provided such editions are for the work as a whole in situ and does not involve the separate exploitation of the permitted figures or extracts. You may not alter, remove or suppress in any manner any copyright, trademark or other notices displayed by the Wiley Materials. You may not license, rent, sell, loan, lease, pledge, offer as security, transfer or assign the Wiley Materials on a stand-alone basis, or any of the rights granted to you hereunder to any other person.
- The Wiley Materials and all of the intellectual property rights therein shall at all times remain the exclusive property of John Wiley & Sons Inc, the Wiley Companies, or their respective licensors, and your interest therein is only that of having possession of and the right to reproduce the Wiley Materials pursuant to Section 2 herein during the continuance of this Agreement. You agree that you own no right, title or interest in or to the Wiley Materials or any of the intellectual property rights therein. You shall have no rights hereunder other than the license as provided for above in Section 2. No right, license or interest to any trademark, trade name, service mark or other branding ("Marks") of WILEY or its licensors is granted hereunder, and you agree that you shall not assert any such right, license or interest with respect thereto

- NEITHER WILEY NOR ITS LICENSORS MAKES ANY WARRANTY OR REPRESENTATION OF ANY KIND TO YOU OR ANY THIRD PARTY, EXPRESS, IMPLIED OR STATUTORY, WITH RESPECT TO THE MATERIALS OR THE ACCURACY OF ANY INFORMATION CONTAINED IN THE MATERIALS, INCLUDING, WITHOUT LIMITATION, ANY IMPLIED WARRANTY OF MERCHANTABILITY, ACCURACY, SATISFACTORY QUALITY, FITNESS FOR A PARTICULAR PURPOSE, USABILITY, INTEGRATION OR NON-INFRINGEMENT AND ALL SUCH WARRANTIES ARE HEREBY EXCLUDED BY WILEY AND ITS LICENSORS AND WAIVED BY YOU.
- WILEY shall have the right to terminate this Agreement immediately upon breach of this Agreement by you.
- You shall indemnify, defend and hold harmless WILEY, its Licensors and their respective directors, officers, agents and employees, from and against any actual or threatened claims, demands, causes of action or proceedings arising from any breach of this Agreement by you.
- IN NO EVENT SHALL WILEY OR ITS LICENSORS BE LIABLE TO YOU OR ANY OTHER PARTY OR ANY OTHER PERSON OR ENTITY FOR ANY SPECIAL, CONSEQUENTIAL, INCIDENTAL, INDIRECT, EXEMPLARY OR PUNITIVE DAMAGES, HOWEVER CAUSED, ARISING OUT OF OR IN CONNECTION WITH THE DOWNLOADING, PROVISIONING, VIEWING OR USE OF THE MATERIALS REGARDLESS OF THE FORM OF ACTION, WHETHER FOR BREACH OF CONTRACT, BREACH OF WARRANTY, TORT, NEGLIGENCE, INFRINGEMENT OR OTHERWISE (INCLUDING, WITHOUT LIMITATION, DAMAGES BASED ON LOSS OF PROFITS, DATA, FILES, USE, BUSINESS OPPORTUNITY OR CLAIMS OF THIRD PARTIES), AND WHETHER OR NOT THE PARTY HAS BEEN ADVISED OF THE POSSIBILITY OF SUCH DAMAGES. THIS LIMITATION SHALL APPLY NOTWITHSTANDING ANY FAILURE OF ESSENTIAL PURPOSE OF ANY LIMITED REMEDY PROVIDED HEREIN.
- Should any provision of this Agreement be held by a court of competent jurisdiction to be illegal, invalid, or unenforceable, that provision shall be deemed amended to achieve as nearly as possible the same economic effect as the original provision, and the legality, validity and enforceability of the remaining provisions of this Agreement shall not be affected or impaired thereby.
- The failure of either party to enforce any term or condition of this Agreement shall not constitute a waiver of either party's right to enforce each and every term and condition of this Agreement. No breach under this agreement shall be deemed waived or excused by either party unless such waiver or consent is in writing signed by the party granting such waiver or consent. The waiver by or consent of a party to a breach of any provision of this Agreement shall not operate or be construed as a waiver of or consent to any other or subsequent breach by such other party.
- This Agreement may not be assigned (including by operation of law or otherwise) by you without WILEY's prior written consent.
- Any fee required for this permission shall be non-refundable after thirty (30) days from receipt by the CCC.
- These terms and conditions together with CCC's Billing and Payment terms and conditions (which are incorporated herein) form the entire agreement between you and WILEY concerning this licensing transaction and (in the absence of fraud) supersedes all prior agreements and representations of the parties, oral or written. This Agreement may not be amended except in writing signed by both parties. This Agreement shall be binding upon and inure to the benefit of the parties' successors, legal representatives, and authorized assigns.
- In the event of any conflict between your obligations established by these terms and conditions and those established by CCC's Billing and Payment terms and conditions, these terms and conditions shall prevail.

- WILEY expressly reserves all rights not specifically granted in the combination of (i) the license details provided by you and accepted in the course of this licensing transaction, (ii) these terms and conditions and (iii) CCC's Billing and Payment terms and conditions.
- This Agreement will be void if the Type of Use, Format, Circulation, or Requestor Type was misrepresented during the licensing process.
- This Agreement shall be governed by and construed in accordance with the laws of the State of New York, USA, without regards to such state's conflict of law rules. Any legal action, suit or proceeding arising out of or relating to these Terms and Conditions or the breach thereof shall be instituted in a court of competent jurisdiction in New York County in the State of New York in the United States of America and each party hereby consents and submits to the personal jurisdiction of such court, waives any objection to venue in such court and consents to service of process by registered or certified mail, return receipt requested, at the last known address of such party.

WILEY OPEN ACCESS TERMS AND CONDITIONS

Wiley Publishes Open Access Articles in fully Open Access Journals and in Subscription journals offering Online Open. Although most of the fully Open Access journals publish open access articles under the terms of the Creative Commons Attribution (CC BY) License only, the subscription journals and a few of the Open Access Journals offer a choice of Creative Commons Licenses. The license type is clearly identified on the article.

The Creative Commons Attribution License

The Creative Commons Attribution License (CC-BY) allows users to copy, distribute and transmit an article, adapt the article and make commercial use of the article. The CC-BY license permits commercial and non-

Creative Commons Attribution Non-Commercial License

The Creative Commons Attribution Non-Commercial (CC-BY-NC) License permits use, distribution and reproduction in any medium, provided the original work is properly cited and is not used for commercial purposes.(see below)

Creative Commons Attribution-Non-Commercial-NoDerivs License

The Creative Commons Attribution Non-Commercial-NoDerivs License (CC-BY-NC-ND) permits use, distribution and reproduction in any medium, provided the original work is properly cited, is not used for commercial purposes and no modifications or adaptations are made. (see below)

Use by commercial "for-profit" organizations

Use of Wiley Open Access articles for commercial, promotional, or marketing purposes requires further explicit permission from Wiley and will be subject to a fee.

Further details can be found on Wiley Online

Library <http://olabout.wiley.com/WileyCDA/Section/id-410895.html>

Other Terms and Conditions:

v1.10 Last updated September 2015